Multi-omics and *in vitro* characterisation of cyanobacterial biochemistry

A Thesis

submitted to

Indian Institute of Science Education and Research Pune in partial fulfilment of the requirements for the BS-MS Dual Degree Programme

by

OYINDRILA SAMANTA

Indian Institute of Science Education and Research Pune

Dr. Homi Bhabha Road

Pashan, Pune 411008, India

Date: 27 March, 2025

Under the guidance of

Supervisor: Prof. Dr. Tobias J Erb

Director, Department of Biochemistry and Synthetic Metabolism

Max-Planck-Institut für terrestrische Mikrobiologie

Karl-von-Frisch-Straße 10

D-35043 Marburg, Germany

June 2024 to March 2025

Certificate

This is to certify that this dissertation entitled **'Multi-omics and *in vitro* characterisation of cyanobacteria biochemistry'** towards the partial fulfilment of the BS-MS dual degree programme at the Indian Institute of Science Education and Research, Pune represents work carried out by Oyindrila Samanta at Max Planck Institute for Terrestrial Microbiology under the supervision of Dr. Tobias Erb- Director, Department of Biochemistry and Synthetic Metabolism, during the academic year 2024-2025.

Prof. Dr. Tobias J Erb

(Supervisor)

Dr Gayathri Pananghat

(Expert)

MAX PLANCK INSTITUTE
FOR TERRESTRIAL MICROBIOLOGY

IISER PUNE

Declaration

I hereby declare that the matter embodied in the report entitled **"Multi-omics and *in vitro* characterisation of cyanobacteria biochemistry"** are the results of the work carried out by me at the Department of Biochemistry and Synthetic Metabolism, Max Planck Institute for Terrestrial Microbiology, under the supervision of Prof. Dr. Tobias J Erb, and the same has not been submitted elsewhere for any other degree. Wherever others contribute, every effort is made to indicate this clearly, with due reference to the literature and acknowledgement of collaborative research and discussions.

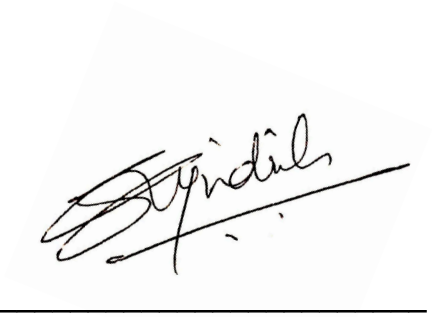

Oyindrila Samanta

(20201037)

This thesis is dedicated to my beloved দাদু (late grandfather)
whose wisdom and resilience will always be the guiding light..

List of Figures

List of Tables

Abbreviations

1. CO_2: Carbon dioxide
2. GOE: Great oxidation event
3. PCC: Pasteur culture collection
4. UTEX: University of Texas Austin (Culture collection of algae)
5. CBB cycle: Calvin-Benson-Bassham cycle
6. RuBisCO: Ribulose-1,5-bisphosphate carboxylase/oxygenase
7. 3PG: 3-phosphoglycerate
8. 2PG: 2-phosphoglycerate
9. PS: Photosystems
10. LHC: Light harvesting complex
11. ETC: Electron transport chain
12. PC: Plastocyanin
13. PQ: Plastoquinone
14. G6P: Glucose-6-phosphate
15. F6P: Fructose-6-phosphate
16. E4P: Erythrose-4-phosphate
17. R5P: Ribulose-5-phosphate
18. NADH/NADPH: Nicotinamide adenine dinucleotide/ phosphate
19. ATP: Adenosine triphosphate
20. CCM: Carbon concentrating mechanisms
21. K_m: Michaelis constant
22. k_{cat}: Turnover number
23. CFPS: Cell-free protein synthesis
24. ROS: Reactive oxygen species

Table of Content

Acknowledgments

I am deeply grateful to everyone who was a part of my journey. Starting with Prof Tobias Erb and MPG-IISER collaboration to provide an opportunity for the thesis. It was one of my best experiences in terms of scientific research, enabling me to learn and grow as a young researcher which has always been my dream. I believe words will not be enough to describe the role of my super knowledgeable and kind mentor Dr Blake Rasor. He has always supported me, guided me and motivated me to become a better version of myself both academically and personally. I truly believe I couldn't have found a better supervisor than him.

I enjoyed my time in the Erb lab, everyone who is and was part of it has always been extremely helpful. I also learnt a lot from the departmental seminars and journal clubs which stimulated scientific discussions. I am grateful to Dr Nicole Paczia for her expertise in metabolomics and helping us with analytical methods, sometimes spending hours on it. I would like to thank Dr Inal Bakhytkyzy for collaborating with us on the project. Special thank you to Dr Andreas Küffner, Dr Owen Jarman, Dr Pascal Pfister, Dr Jan Zarzycki, Dr Tanguy Chotel, Philipp Wichmann, Nitin Bohra, Yuanyang Zhou and all lab members (especially from C.1.15 and 11) for answering all my questions and sharing lab resources. I am grateful to Dr Timo Glatter, Peter Claus and Jörg Kahnt for analytical measurements. I was glad to be a part of the *in vitro* and microbial metabolism (earlier non-model microbes) subgroups which provided a great platform to troubleshoot and discuss different projects. Big thank you to Nelli for always taking care of everything. I thank my expert Dr Gayathri Pananghat, for her scientific inputs and compassion over the years. Cannot miss thanking the cyanobacterias who sacrificed themselves for our science, your contribution will not be forgotten.

My journey was so much more memorable because of my 'gang' with whom I fostered friendships to last a lifetime. Lotte, you have been a blessing, I don't know what I would have done without you! From discussing (complaining) about things, people and everything, I found someone I could talk to about anything. C.1.11 was an amazing lab space where I was also unofficially adopted by my dear friends Nitin and Owen, who have always been by my side (quite literally!). It was really fun to annoy and get annoyed by both of you. My other master's gang including Jogindh,

Tobi, Leo von Bank, Kevin, Titoun, Vaishnav, Karo, Katsu and Arin have always been a delight to talk to, go out with and have fun, I will miss you all. There are many lunchtime conversations which I cannot forget so thank you to everyone who made it the most looked forward time of the day. Special mention to Max- I truly enjoyed our conversations about random things and for also helping me out with applications. I am grateful for having attended the Ringberg retreat, it was a great experience. My roommates- Luisa and Milena deserve a shout-out for being the amazing and kind human they are. These past 10 months is something I will always cherish, mostly because of everyone mentioned here.

At last, of course some of the most important people in my life- my parents, brother and friends. The best part of the day was when I shared everything that happened, from the smallest mundane moments over facetime with my family (yes I know you missed me brother). They have supported me in the most fierce way one could and I am who I am because of them. Yuvraj, thank you for being the protector of my sanity time and again. You have been most patient and loving, while always having my back. Pritha, Akshata and Drishti- my precious trinity who understand, love and cheer me in the most special way. I am the most thankful for hours of call, endless reels and infinite warmth. IISER has been the best journey till now, and I am sincerely grateful for bringing out the best in me in both the highest and lowest points. My dear friends Anish, Vikram, Aparajita and Nisarg, thank you for keeping me entertained with your life updates. Finally, this section would be incomplete without thanking Netflix and Khaled Hosseni.

There is a long list of people I absolutely love and admire, and my heart will always treasure every bit of kindness, friendship and time spent with them.

Contributions

Contributor name	Contributor role
Blake J Rasor, Tobias J Erb, Oyindrila Samanta	Conceptualization Ideas
Blake J Rasor, Oyindrila Samanta	Methodology
Oyindrila Samanta, Blake J Rasor, Nicole Paczia	Software
Oyindrila Samanta	Validation
Oyindrila Samanta, Blake J Rasor, Nicole Paczia, Inal Bakhytkyzy	Formal analysis
Oyindrila Samanta, Blake J Rasor	Investigation
Erb lab, Metabolomics Core, Proteomics Core	Resources
Oyindrila Samanta	Data Curation
Oyindrila Samanta	Writing - original draft preparation
Oyindrila Samanta, Blake J Rasor	Writing - review and editing
Oyindrila Samanta, Blake J Rasor	Visualization
Blake J Rasor, Tobias J Erb	Supervision
Oyindrila Samanta, Blake J Rasor	Project administration
Tobias J Erb	Funding acquisition

This contributor syntax is based on the Journal of Cell Science CRediT Taxonomy[1].

[1] https://journals.biologists.com/jcs/pages/author-contributions

Abstract

Cyanobacteria have been one of the most important organisms in the Earth's biogeochemical cycles. Subject to millions of years of evolution, it is a diverse phylum of photoautotrophs which is responsible for fixing 20-30% of global carbon dioxide. This thesis is an attempt to explore the composition and function of some fast-growing biotechnologically important strains of cyanobacteria in differential growth conditions (ambient, 0.5% or 3% CO_2 in low or high light) using high throughput endometabolomics and proteomic analysis along with *in vitro* assays, to capture the holistic snapshot of metabolism and resource allocation. We focus on proteins related to carbon fixation and light harvesting along with metabolites like sugar phosphates, amino acids and organic acids families. Photosynthetic efficiency with respect to light harvesting and carbon fixation was assessed using cell-free cyanobacterial lysates. The different *in vitro* assays developed here, expand our understanding of the strains and their potential by decoupling metabolism from cell growth and viability constraints. Cyanobacterial lysates show accumulation of 3-phosphoglycerate when supplemented with RuBP as substrate; and glucovanillin via a cascade of enzymatic steps which is then used to understand rates of carbon fixation and gluconeogenesis. Light harvesting capabilities of the cell-free extracts are measured by using the ATP dependent conversion of glucose to glucose-6-phosphate using hexokinase. Together, the compositional and functional datasets will highlight how environmental cues and differential regulation impact CO_2 fixation, light harvesting, and metabolic flux toward precursor molecules of interest to guide subsequent engineering and biosynthesis efforts.

Chapter 1

Introduction

The evolution of life on Earth has been profoundly influenced by shifts in atmospheric composition, especially the rise of molecular oxygen. This transformation, driven by the advent of oxygenic photosynthesis, set the stage for complex biological processes and the emergence of multicellular life. Cyanobacteria played a central role in these events, contributing significantly to Earth's biogeochemical cycles and the evolution of key metabolic pathways. Understanding the past dynamics of oxygen accumulation, the mechanisms underlying photosynthesis, and the evolution of cyanobacterial diversity provides critical insights into modern challenges such as climate change and carbon fixation. Furthermore, advances in synthetic biology and metabolic engineering offer new opportunities to harness cyanobacteria as chassis for sustainable biomanufacturing. This introduction explores the historical context of oxygenic photosynthesis, the current implications of anthropogenic climate change, and future perspectives on engineering cyanobacteria for biotechnological applications.

---

1. Past: Evolution and significance of cyanobacteria

Nature is subject to constant change, and in order to survive, organisms have to adapt and evolve. The biochemical processes we see today have undergone multiple rounds of evolution. Oftentimes understanding the past could lead us to better insights for the future.

1.1 Rise of Oxygen in early Earth

The early Earth environment was anoxic, primarily composed of nitrogen, carbon dioxide, methane and water vapour with minimal free molecular oxygen (O_2) present. It was a different ecosystem that thrived in such conditions where electron donors like hydrogen sulfide and ferrous iron were utilised for energy metabolism. Examples of anoxygenic phototrophs are green sulphur bacteria (*Chlorobaculum tepidum*), and

purple sulphur bacteria (*Chromatium okenii*.) The transition from this anoxic state to an oxygen-rich environment occurred during the Great Oxidation Event (GOE), approximately 2.4 billion years ago (A Bekker et al., 2004; Holland., 2006; Lyons et al., 2014). The GOE was driven by the evolution of oxygenic photosynthesis in cyanobacteria, leading to the progressive accumulation of oxygen in the atmosphere. Geochemical evidence from banded iron formations (BIFs) suggests episodic oxygen production prior to the GOE, but it was only with the widespread rise of cyanobacteria in aquatic environments that sustained oxygenation was achieved; which lead to evolution of aerobic life and higher eukaryotic forms as we see today (Jochen J. Brocks et al., 1999). However, there have been many debates on the exact dates and conditions of early earth and evolution based on insufficient or contradicting fossil evidence (Rasmussen *et al*., 2008, Schirrmeister *et al*., 2016). Oxygenation events also drove the diversification of cyanobacteria, enabling them to spread to new ecological niches and establish themselves as primary producers in marine and freshwater environments (Och & Shields-Zhou, 2012).

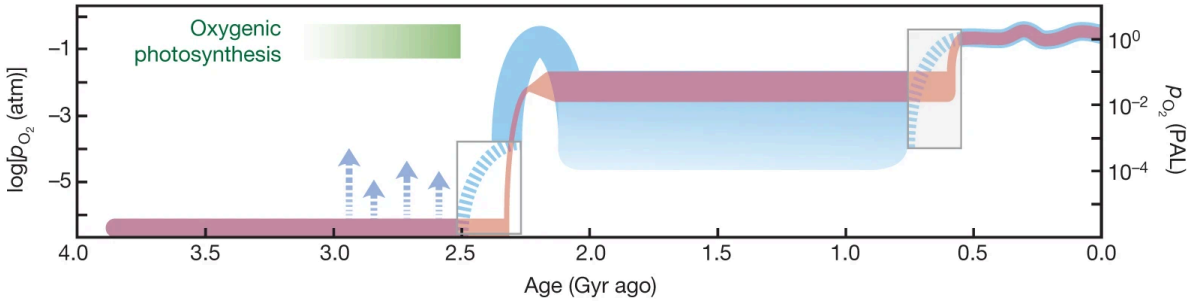

Figure 1.1: The rise of levels of oxygen in the atmosphere over the evolution of Earth from 4 billion years ago to current day. The concentration of O_2 was negligible till around 2.5 billion years ago until the rising O_2 levels marked as the Great oxidation event (GOE) primarily contributed by oxygenic photosynthesis. (Figure adapted from Lyons et al., 2014).

1.2 Phylogeny and evolution

Cyanobacteria represent one of the oldest known photosynthetic lineages thought to have diverged from anoxygenic photoautotrophs. Phylogenetic studies indicate that they share a common ancestor with other bacterial groups, but their divergence led to the development of oxygenic photosynthesis (Shih et al., 2013). Molecular clock analyses suggest that cyanobacteria originated over 2.7 billion years ago, coinciding with the earliest evidence of stromatolite formation and presence of methyl hopanes in Archean shales, which provides the most compelling evidence (though disputed)

of early microbial activity (Jochen J. Brocks et al., 1999; Brasier, M., Green, O., Jephcoat, A. et al., 2002). Over time, cyanobacteria diversified into a range of morphologies and ecological adaptations, from unicellular species to complex filamentous forms capable of nitrogen fixation.

1.3 Photosynthesis

Cyanobacteria are the only prokaryotic organisms capable of performing oxygenic photosynthesis, facilitating the Great Oxidation Event (GOE) and catalyzing the diversification of aerobic life. Photosynthesis in cyanobacteria is a highly coordinated biochemical process involving two distinct photosystems- light-driven electron transport chain (ETC), and the Calvin-Benson-Bassham (CBB) cycle, which governs carbon assimilation.

1.3.1 Photosystem

Cyanobacteria have chlorophyll-containing thylakoid membranes that employ two photosystems- Photosystem I (PSI) and Photosystem II (PSII)- functioning in tandem to capture and convert solar energy. PSII mediates the photolysis of water, generating molecular oxygen, protons, and electrons. These electrons traverse the ETC, which includes plastoquinone (PQ), cytochrome b_6f complex, and plastocyanin (PC), before reaching PSI, which facilitates NADPH production by transferring electrons to ferredoxin and ultimately reducing $NADP^+$.

The structural organization of cyanobacterial photosystems is highly conserved with that of chloroplasts in eukaryotic phototrophs, connecting to their shared evolutionary ancestry . Unlike plants, cyanobacteria employ specialized light-harvesting antennae known as phycobilisomes, which enable efficient photon capture in diverse aquatic environments (Liu et al., 2013). Phylogenetic and structural analyses reveal adaptive modifications in photosystem components across different cyanobacterial taxa, reflecting their ecological and evolutionary adaptations (Raymond et al., 2002, Cardona et al., 2015) .

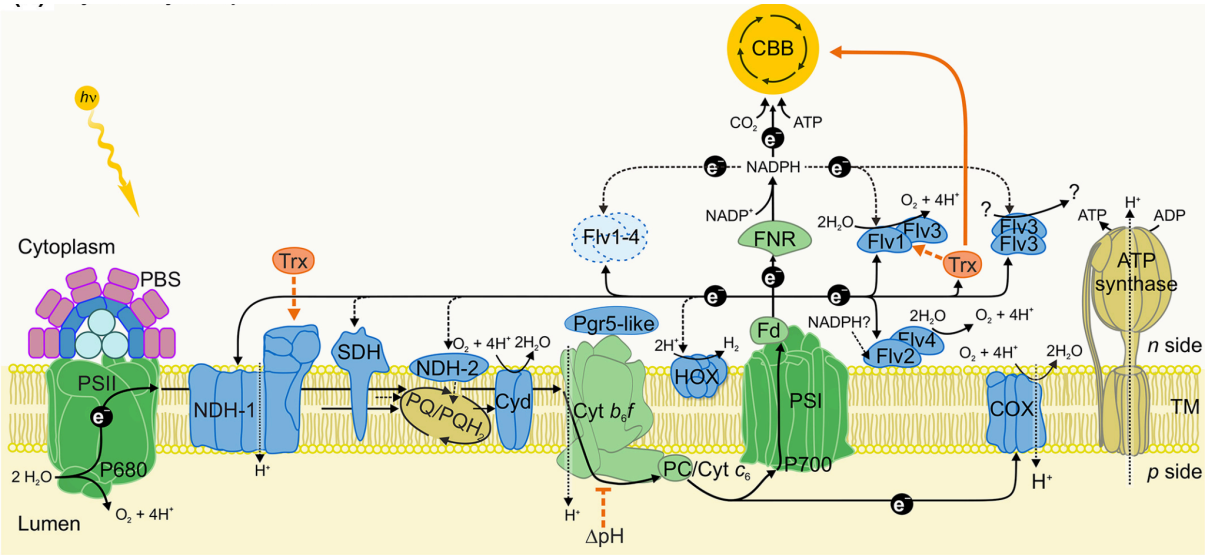

Figure 1.2: The schematics of light harvesting complex and electron transport chain on the thylakoid membrane of cyanobacteria (here PCC 6803). It involves the phycobilisomes (PBS) which harvest the photons from light and excite P_{680} and P_{700} chlorophyll at PSI and PSII respectively. This facilitates electron transfer by splitting water and releasing O_2 as a by-product. The electrons are transferred via plastoquinone, cytochrome b_6f complex and plastocyanin, finally to reach PSI which then reduces $NADP^+$ to NADPH. This transfer of electrons also generates an electrochemical gradient to power the ATP synthase to pump a H^+ outside the membrane (proton motive force) which allows ATP synthesis from ADP and P_i. (Figure adapted from Nikkanen et al., 2021)

1.3.2 Light and dark reactions

Photosynthesis in cyanobacteria comprises two major phases: light-dependent (light) reactions and light-independent (dark) reactions. The light reactions, occurring in the thylakoid membranes, harness solar energy to generate ATP and NADPH while splitting water molecules to release oxygen. Key biochemical steps include:

- **Water oxidation by PSII**: $2H_2O \rightarrow O_2 + 4H^+ + 4e^-$
- **Electron transport and ATP synthesis**: Electrons pass through PQ, cytochrome b_6f, PC, and PSI, driving proton translocation and ATP synthesis via ATP synthase
- **NADPH production**: Electrons from PSI reduce $NADP^+$ to NADPH, providing reducing power for carbon fixation via CBB cycle

The dark reactions, localized in the cytoplasm, encompass the CBB cycle, where ATP and NADPH drive the fixation and assimilation of CO_2 into organic molecules, ultimately contributing to glucose biosynthesis and other metabolic pathways. The

photosynthetic machinery was incorporated by photosynthetic eukaryotes via endosymbiosis (chlorophytes, rhodophytes, and glaucophytes) (Falkowski *et al.*, 2004).

1.3.3 Calvin-Benson-Bassham (CBB) cycle

The Calvin Cycle is the principal pathway for carbon fixation in cyanobacteria and comprises three distinct phases:

- **Carboxylation**: Rubisco catalyzes the fixation of CO_2 with ribulose-1,5-bisphosphate (RuBP), yielding two molecules of 3-phosphoglycerate (3-PGA)
- **Reduction**: ATP and NADPH facilitate the conversion of 3-PGA into glyceraldehyde-3-phosphate (G3P), which serves as a precursor for carbohydrate biosynthesis
- **Regeneration**: ATP-dependent reactions regenerate RuBP, ensuring the continuity of the cycle

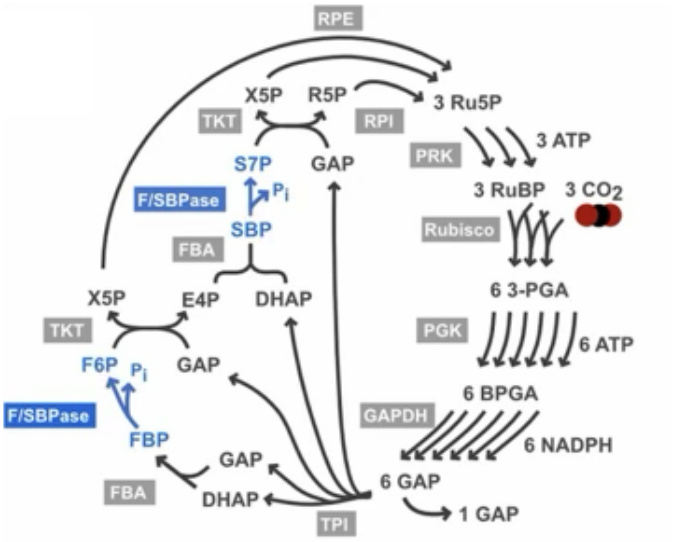

Figure 1.3: The canonical CBB cycle in cyanobacteria with the fluxes of different enzymatic steps. The energy requirements are 9 ATP, 6 NADPH per glyceraldehyde-3-phosphate (GAP) which is quite high (Figure adapted from Hudson, 2024).

1.3.4 RuBisCO

Rubisco is the key enzyme in the CBB cycle that leads to formation of 3-phosphoglycerate from RuBP and CO_2. In nature, there are 4 known Rubisco isoforms- (Form I, II, III and IV) with varying kinetic properties, allowing them to adapt to fluctuating environmental CO_2 concentrations (Tabita et al., 2008). Form I RuBisCO which is most common and found in plants, microalgae & cyanobacteria is a ~530 kDa complex comprising of eight large (RbcL) and eight small (RbcS) subunits forming a multimeric L_8S_8 holoenzyme. Chaperonins GroEL-GroES along with Raf1 and RbcX assist the folding of this large complex of L_8S_8 (Saschenbrecker, S. et al., 2008; Liu, C. et al., 2010; Bracher et al., 2011).

Rubisco is first carbamylated at the ϵ-amino group of a specific lysine residue, with divalent cations bound to adjacent acidic residues stabilizing the carbamate. The carbamylated lysine catalyses proton abstraction from RuBP, thus initiating the catalytic cycle (Cleland et al., 1998). The catalytic efficiency of Rubisco is quite slow for most known autotrophs (~3-12 s^{-1}) and the reaction results in formation of 3-phosphoglycerate (3PG) and 2-phosphoglycerate; as Rubsico is substrate promiscuous towards O_2. 2PG is toxic as it inhibits two central carbon metabolism enzymes- triose phosphate isomerase and phosphofructokinase (Flügel et al., 2017), it needs to be converted to a non-toxic product. This results in energetically costly photorespiration which involves converting 2PG to 3PG that can be then used Cyanobacteria

The evolutionary origins of Rubisco can be traced to ancient anoxygenic phototrophs, which utilized rudimentary carbon fixation pathways before the advent of oxygenic photosynthesis. Molecular phylogenetic analyses indicate that ancestral Rubisco variants exhibited broader substrate specificity and higher tolerance to variable CO_2 and O_2 levels, likely contributing to their early evolutionary success. Integrating ancestral Rubisco into engineered cyanobacterial strains represents a promising approach for mitigating the inefficiencies associated with modern photosynthesis (Schulz et al., 2022).

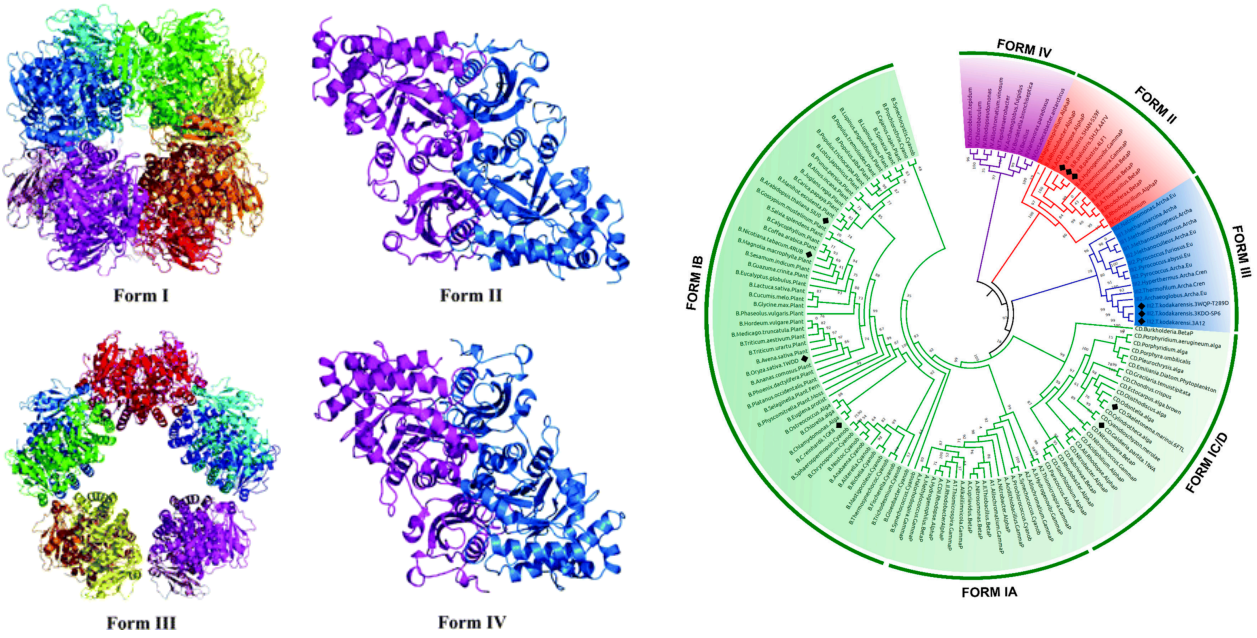

Figure 1.4: A- These are the structures of different forms of Rubisco, all of them consisting of dimers of large subunits. Form I has four dimers of the small sub-unit (SSU) on the top and bottom of the octameric large subunit core. Form I is found in most photosynthetic cyanobacteria. Form II has dimers of the large subunit and can be of the form L_2-L_8. Form III is made of dimers of the large subunit in L_2 or $(L_2)_5$ manner. Form IV (rubisco like protein or RLP) is of L_2 form (Figure adapted from Tabita et al., 2008). B- Maximum likelihood phylogeny of the large subunit family of Rubisco protein rbcL (Figure adapted from Camel & Zolla, 2021).

1.3.5 Carbon concentrating mechanism (CCM)

Cyanobacteria employ carbon-concentrating mechanisms (CCMs) to mitigate CO_2 diffusion limitations and enhance Rubisco efficiency. These mechanisms include the compartmentalization of Rubisco within carboxysomes, microcompartments that facilitate CO_2 accumulation and minimize oxygenase activity, thereby reducing photorespiration.

Cyanobacteria can use multiple transporters to actively acquire CO_2 and bicarbonate (HCO_3^-) from their surroundings. Some examples of such transporters are BicA, SbtA, BCT1 and NDH-1 (Zhang et al., 2020). Other carbon concentrating mechanisms include the carboxysomes- which are polyhedral microcompartments encapsulating and enriching Rubisco concentrations in association with carbonic anhydrase- to convert HCO_3^- into CO_2 inside the carboxysome shell, which is devoid of O_2. The importance of enrichment of CO_2 for Rubisco is evident from the energetics of producing carboxysomes, as it involves many shell proteins CsoS2,

CcmM, CcmN,CcmK, CcaA (Kinnery et al., 2011). The two forms existing in nature are α-carboxysomes (*Halothiobacillus neopolitanus*) and β-carboxysomes (Synechococcus PCC 7942).

Other organisms have different mechanisms for improving carbon fixation efficiency like pyrenoids in the microalgae such as *Chlamydomonas reinhardtii* while plants have devised C4 and Crassulacean Acid Metabolism (CAM) pathways to bypass photorespiratory losses. Hence, these mechanisms serve as interesting engineering targets for improving natural carbon fixation to combat climate change and increase primary productivity.

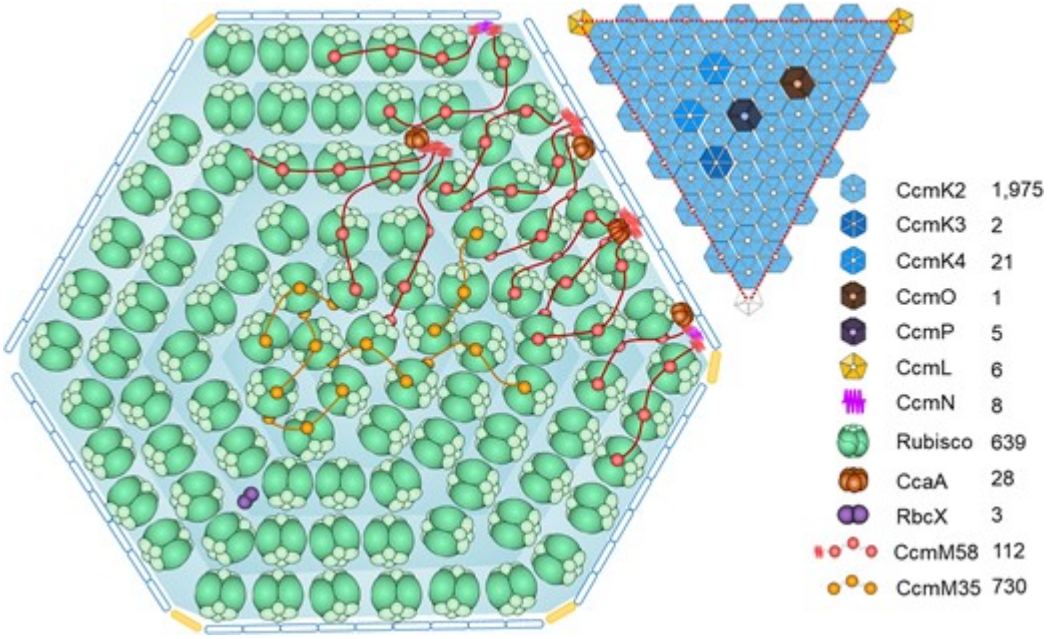

Figure 1.5: This is a schematic of the β-carboxysome structure of PCC 7942. The carboxysome shell is packed with layers of Rubisco. CcmN and CcmM proteins help rubisco binding to the shell complex. CcmK2, CcmK3 and CcmK4 are structural hexameric proteins that form the shell facets. The vertices are capped by CcmL pentameric proteins (Figure adapted from Sun et al., 2024)

2. Present: Studying model cyanobacteria

The climate crisis is one of the most pressing global challenges, with anthropogenic greenhouse gas emissions leading to significant shifts in temperature, precipitation patterns, ocean acidification and more. The Intergovernmental Panel on Climate Change (IPCC) reports that CO_2 levels have increased from pre-industrial levels of 280 ppm to over 415 ppm, resulting in an average global temperature rise of 1.1°C (IPCC, 2021). The consequences of this warming include extreme weather events, declining biodiversity, and disruptions to agricultural productivity. The need of the hour is to explore, engineer and optimise carbon mitigation strategies, including natural and synthetic carbon fixation approaches.

2.1 Carbon Fixation

Carbon fixation is a process in the global carbon cycle, involving the conversion of inorganic carbon (CO_2) into organic compounds. Cyanobacteria, algae and plants play a vital role in natural carbon fixation through photosynthesis, contributing significantly to global carbon sequestration.

Natural carbon fixation occurs via the CBB cycle, and Cyanobacteria, as major contributors to global primary production, are estimated to fix nearly 25% of total atmospheric CO_2 (Falkowski, 2012). Marine cyanobacteria such as *Prochlorococcus* and *Synechococcus* contribute significantly to oceanic carbon cycling, sustaining food webs and influencing global climate patterns.

Recent efforts to improve photosynthetic efficiency have focused on increasing Rubisco specificity towards CO_2, improving catalytic efficiency and reducing photorespiration. These strategies include engineering carbon-concentrating mechanisms (CCMs) to enhance CO_2 availability for Rubisco and modifying light-harvesting complexes to optimize energy capture (Mangan et al., 2016). Some studies also attempt to understand biochemical and structural aspects of ancestral Rubisco evolution and activity to design a more efficient form of the enzyme (Schulz et al., 2022). Synthetic biology approaches, such as incorporating CCM components into higher plants, have resulted in improved crop yield and stress tolerance (Atkinson et al., 2015).

Synthetic carbon fixation involves designing alternative pathways to capture and convert CO_2 into valuable products. Researchers have developed engineered

microbes capable of utilizing non-natural carbon fixation routes, such as the reductive glycine pathway (Claassens et al., 2020). Many synthetic carbon fixation pathways have also been developed *in vitro* like crotonyl-CoA/ethylmalonyl-CoA/hydroxybutyryl-CoA (CETCH) cycle, which can be more energy efficient and use enzymes like crotonyl CoA reductase to fix CO_2, and are not promiscuous to oxygen. (Schwander et al., 2016).

Other approaches of improving carbon fixation is to minimise photorespiration (e.g. C4 and CAM pathways in plants). Other synthetic photorespiratory bypasses like 3-hydroxypropionate bi-cycle (Shih & Zarzycki et al., 2014) and β-hydroxyaspartate cycle (Roell et al., 2021; Chen et al., 2025) are engineered into other organisms like cyanobacteria, *Arabidopsis thaliana* and *Oryza sativa* to improve biomass and agricultural productivity along with carbon fixation.

2.2 Cyanobacterial strains

Identifying and characterising biotechnologically relevant cyanobacteria is necessary to expand the capacities of sustainable biomanufacturing, and some strains serve as interesting candidates. The Pasteur Culture collection of Cyanobacteria (PCC) serves as a repository of around 750 axenic strains of cyanobacteria, which can be shipped around the world for research (Ripkka et al, 1979). Similarly there is a culture collection of algae at University of Texas at Austin (UTEX) which has over 3,000 strains of algae.

2.2.1 PCC 7942

Synechococcus elongatus PCC 7942 is a model freshwater cyanobacterium widely used for genetic and metabolic engineering studies. It possesses a relatively simple genome and has been instrumental in studying circadian rhythms and photosynthetic regulation (Golden et al., 1997). Its adaptability to controlled laboratory conditions makes it a preferred strain for synthetic biology applications. PCC 7942 is robust even in the case of environmental fluctuations, making it a great candidate for industrial applications (e.g. carbon sequestration and biofuel production). Its high photosynthetic efficiency and well-characterized regulatory pathways have made it a primary candidate for metabolic engineering efforts.

2.2.2 UTEX 2973

UTEX 2973 is a close relative of PCC 7942 (differing at only 55 genetic loci), and is known for its remarkably fast growth rate especially in high light compared to other cyanobacteria. The strain exhibits decreased phycobilisome and increased Photosystem I (PSI) cytochrome *f* and plastocyanin concentrations, which result in increased electron flow, in turn producing more ATP and NADPH and enabling faster growth (Ungerer et al., 2018). It emerges as a promising strain for biomanufacturing industrially relevant compounds, encouraging development of toolkits for genetic modifications.

2.2.3 PCC 7002

PCC 7002 is an unicellular marine cyanobacterium known for its high salt tolerance and robust metabolic flexibility (Ludwig & Bryant, 2012). It has been used to study photoprotection mechanisms and carbon fixation under stress conditions, opening up research in biomanufacturing (e.g. Vitamins- Kachel 2020) and bioremediation with the same .

2.2.4 PCC 11901

A relatively recent isolate from Singapore, PCC 11901, is being explored for its high photosynthetic efficiency and resilience in fluctuating environmental conditions. This strain is gaining attention for its rapid biomass generation and subsequently free-fatty acid production capabilities (Wlodarczyk et al., 2020). Like most marine cyanobacteria, it also requires external supplementation of Vitamin B_{12}.

2.2.5 PCC 7120

Also known as *Anabaena* PCC 7120, this filamentous strain forms heterocysts, specialized cells that fix nitrogen under anaerobic conditions. It serves as a model for studying nitrogen metabolism (Muro-Pastor et al., 1999). In the presence of a nitrogen source (ammonium or nitrates), Anabaena forms long filaments of 100 or more identical vegetative cells. Its natural ability to fix atmospheric nitrogen makes it an important candidate for biofertilizer development and sustainable agriculture. Studies have also focused on its role in synergistic relationships with plant roots for enhanced crop productivity (Bocchi & Malgioglio 2010).

2.2.6 PCC 6803

Synechocystis PCC 6803 is one of the most extensively studied cyanobacterial strains, commonly used for genetic manipulation and synthetic biology applications (Kaneko et al., 1996). Its fully sequenced genome and metabolic network are well studied and is an interesting strain to test novel genetic circuits due to its natural competence for DNA uptake (Knoop et al., 2010). Genome editing of 6803 is made possible with the help of CRISPR (Du et al., 2024).

2.2.7 PCC 7345

Arthrospira platensis PCC 7345 is a filamentous cyanobacteria that shows a more diverse gene set for osmotic stress adaptation, including additional transporters and regulatory proteins. PCC 7345 has been proposed as a candidate for space missions due to its resilience in low-temperature environments and has the ability to produce higher titres of total protein, and established safety for human consumption (Jester et al., 2022).

---

3. Future: Enhancing applications of cyanobacteria

3.1 Engineering Cyanobacteria

Modern genetic tools, including CRISPR-Cas systems, recombineering, and transposon-mediated mutagenesis, have enabled genome editing and these techniques facilitate the introduction of heterologous pathways, allowing for the production of biofuels, pharmaceuticals, and biopolymers (Atsumi, 2013). Recent bioengineering efforts have focused on optimizing Rubisco activity through directed evolution, mutagenesis, and the introduction of high-affinity variants from other photosynthetic organisms. Enhancing Rubisco's catalytic performance in cyanobacteria holds significant potential for increasing biomass yield and photosynthetic efficiency, making it a critical target for synthetic biology applications.

Cyanobacteria serve as a promising chassis for biomanufacturing due to their ability to directly capture and convert CO_2 into valuable products using light energy. Engineering cyanobacteria for the production of biofuels, pigments, and other biochemicals presents a sustainable alternative to traditional petrochemical-based manufacturing industries.

- **Biofuels**

  Cyanobacteria have been engineered to produce biofuels such as ethanol, butanol, and biodiesel precursors. Strains like *Synechocystis* PCC 6803 have been modified to enhance lipid biosynthesis, making them an interesting chassis for large-scale biofuel production. Advances in metabolic engineering have focused on increasing carbon flux towards fuel precursors while minimizing tradeoff with growth (Machado & Atsumi, 2019).

- **Pigments and Dyes**

  Cyanobacteria produce a range of natural pigments, including phycocyanin, chlorophyll, and carotenoids. These pigments have applications in the food, cosmetic, and pharmaceutical industries (Pagels et al., 2019). Engineering cyanobacteria for enhanced pigment production offers a sustainable alternative to synthetic dyes, reducing environmental impact and improving product quality.

3.1.2 Cell-Free Systems

Cell-free systems provide an alternative approach for utilizing cyanobacterial metabolism without relying on live cells. These systems harness crude or purified enzyme extracts to carry out biochemical reactions *in vitro*, offering advantages in scalability, bioprocess control without competing with one's own growth and metabolism (Hunt & Rasor et al., 2024).

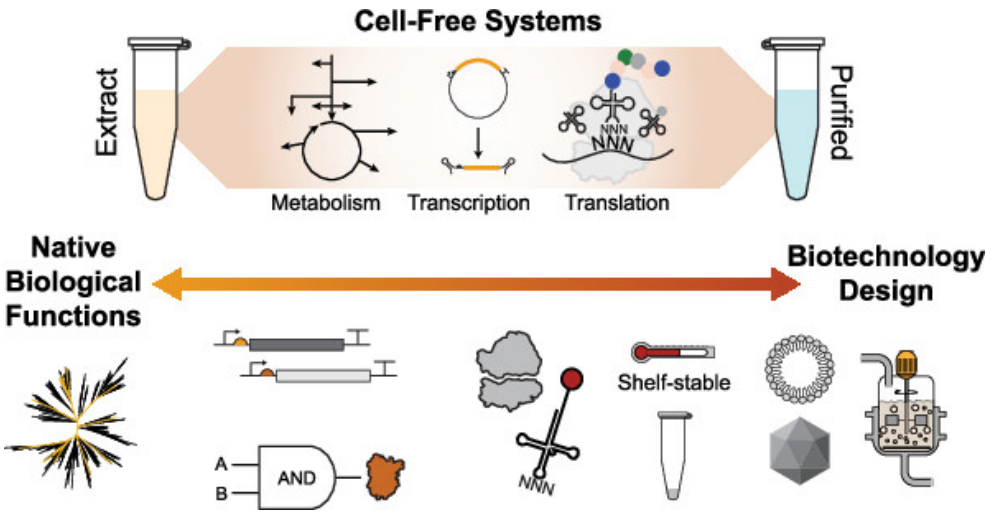

Figure 1.6: Cell-free systems provide a wide range of functional space with precision. It can comprise crude lysate or purified systems which are no longer dependent on the growth constraints of a living cellular system. (Figure adapted from Hunt & Rasor et al., 2024).

Cell-free protein synthesis (CFPS) is an emerging tool that enables rapid protein production without the constraints of cell growth. CFPS systems derived from cyanobacteria could offer unique advantages, including direct incorporation of photosynthetically fixed carbon into target proteins with future optimizations (Liu et al., 2019).

Objectives of the study

The study of cyanobacteria, from their ancient role in Earth's oxygenation to their modern applications in biotechnology, highlights their immense scientific and industrial potential. Understanding their composition and optimizing their photosynthetic capabilities is essential to pave the way for sustainable biomanufacturing.

Despite being one of the most important groups of organisms in the past, present and future; cyanobacteria suffer from lack of characterisation, standardization of protocols and genetic tools, holding them back from being used to their fullest potential (Schmelling & Bross, 2024).

This study sought to:

- Grow diverse cyanobacteria in a matrix of light and CO_2 conditions to characterise their growth rates in different cultivation environments
- Capture differences in global composition of the metabolic and proteomic profile between different strains and conditions using high throughput -omics techniques
- Develop functional in vitro assays to study photosynthetic output with respect to energy production and carbon fixation

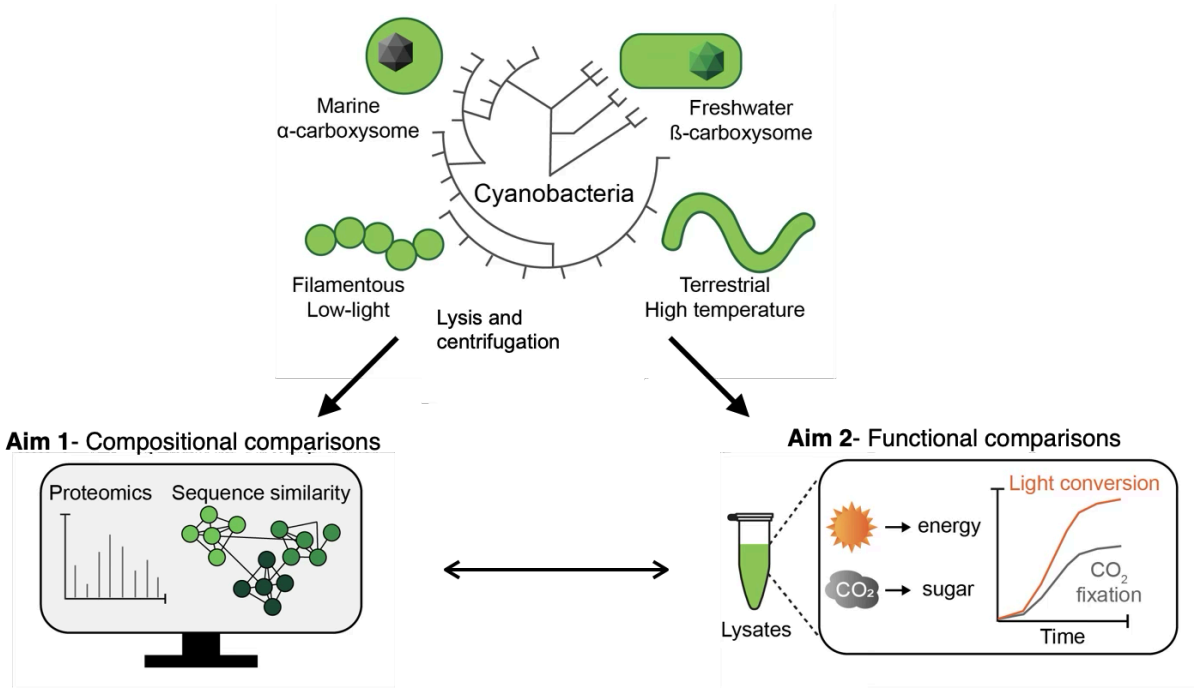

Figure 1.7: Overview of the scope of this study with the main objectives of carrying out compositional and functional comparisons of different cyanobacterial strains. (Figure adapted from Dr Blake Rasor).

Chapter 2

Materials and Methods

---

1. Culturing cyanobacteria

1.1 Media recipes

1.1.1 BG11 (freshwater cyanobacteria)

Stock B1 (100x): Na_2Mg EDTA (0.1 g/L), Ferric ammonium citrate (0.6 g/L), $CaCl_2.2H_2O$ (3.6 g/L), Citric acid (0.6 g/L)

Stock B2 (100x): $MgSO_4.7H_2O$ (7.5 g/L)

Stock 3 (100x): K_2HPO_4 (3.05 g/L) or $K_2HPO_4.3H_2O$ (4 g/L)

Microelements (1000x): H_3BO_3 (2.88 g/L), $MnCl_2.4H_2O$ (1.81g/L), $ZnSO_4.7H_2O$ (0.222 g/L), $CuSO_4.5H_2O$ (0.079 g/L), $CoCl_2.6H_2O$ (0.05 g/L), $NaMoO_4$ (0.391 g/L)

For making 1 Liter of 1x BG-11 medium, 800 mL of deionized or distilled water was added first, followed by 1.5 g of $NaNO_3$ per liter of medium. Then added 10mL stock solutions in order and microelements and 20mL of 1 M HEPES/NaOH buffer (pH 8.0) stock to a final concentration of 20 mM. Fill up with water to 1 Liter, titrate to pH 7.5 and autoclave (some iron may precipitate).

1.1.2 Media A+ (marine cyanobacteria)

20x stock solution: $NaNO_3$ (20g/L), KCl (12 g/L), KH_2PO_4 (1 g/L), Na_2 EDTA.$2H_2O$ (0.6 g/L), Tris/HCl (20 g/L), $MgSO_4.7H_2O$ (100 g/L), $CaCl_2.2H_2O$ (7.04 g/L)

Made separate 20x stocks of $MgSO_4.7H_2O$ and $CaCl_2.2H_2O$, autoclaved each before adding them separately to the 1x media after cooling down.

Trace metals mix (1000x): Ferric ammonium citrate (3.81 g/L), H_3BO_3 (34.4 g/L), $MnCl_2.4H_20$ (4.3 g/L), $ZnCl_2$ (0.315 g/L), MoO_3 (0.03 g/L), $CuSO_4.5H_20$ (0.003 g/L), $CoCl_2$ (0.006 g/L), $NiSO_4.6H_20$ (0.26 g/L)

For 1 L of 1x Medium A, in 750 mL of deionized or distilled water, add 18 g of NaCl followed by 50 mL of 1 M HEPES/NaOH (pH 8), 50 mL of 20x stock solution, 50 mL of 20x $MgSO_4.7H_2O$ stock, 50 mL of 20x $CaCl_2.2H_2O$ stock in order while stirring. Added 1 mL of 1000x trace metals mix and 1 mL of 1000x Vitamin B_{12} and sterile filtered into a sterile bottle. Add sterile filter Vitamin B_{12} after the solution has cooled down in case of autoclaving the media as it is heat and light sensitive (Ludwig M and Bryant DA, 2011).

1.1.3 SOT media for Spirulina

For making 1 L of SOT, 800 mL deionized or distilled water was used, to which $NaHCO_3$ (16.8 g/L), K_2HPO_4 (0.5 g/L), $NaNO_3$ (2.5 g/L), K_2SO_4 (1 g/L), NaCl (1 g/L), $MgSO_4.7H_2O$ (0.2 g/L), $CaCl_2.2H_2O$ (0.04 g/L), $FeSO_4.7H_2O$ (0.01 g/L), Na_2 EDTA.$7H_2O$ (0.01g/L), Trace metal mix B6 (1 mL) and Trace metal mix A5 (1 mL) was added and titrated to final pH 9.

Trace metal mix (A5): H_3BO_3 (2.86 g/L), $MnCl_2.4H_2O$ (1.81 g/L), $ZnSO_4.7H_2O$ (0.222 g/L), $NaMoO_4.2H_2O$ (0.39 g/L), $CuSO_4.5H_2O$ (0.079 g/L), $Co(NO_3)_2.6H_2O$ (49.4 mg/L)

Trace metals mix (B6): NH_4NO_3 (0.23 g/L), $K_2Cr_2(SO_4)_2.24H_2O$ (96 mg/L), $NiSO_4.7H_2O$ (47.8 mg/L), $Na_2WO_4.2H_2O$ (17.9 mg/L), Ti_2O_3 (14.9 mg/L)

1.1.4 Solid media for plates

2x of respective media mix and 2.4% agar in distilled water was prepared separately and autoclaved. 2x media and 2.4% agar was added in 1:1 ratio to make solid media for plates. Add sterile filtered Vitamin B_{12} after the Media A with agar mix has cooled down.

1.1.5 Auto-induction media

To make 1 L of 10x auto-induction media, KH_2PO_4 (68.043 g) or K_2HPO_4 (87.1 g), NH_4SO_4 (33.03 g), glycerol (50 mL), glucose (5 g), lactose monohydrate (20 g) and arabinose (10 g) were used. Starting with 500 mL distilled water and stirring while adding the components and fill to the final volume of 1 L. Sterile filtered the final mix.

100 mL of 10x autoinduction media was added to TB (Terrific Broth- 12 g/L tryptone, 24 g/L yeast extract and 4mL/L glycerol) before use.

1.2 Growth conditions

Strain	Genus	Medium	Temperature (℃)	Doubling time
PCC 7942	*Synechococcus*	BG11 (freshwater)	37	4.9
UTEX 2973	*Synechococcus*	BG11 (freshwater)	37	1.5
PCC 7002	*Synechococcus*	Medium A (Marine)	37	4.3
PCC 11901	*Synechococcus*	Medium A (Marine)	37	2.5
PCC 6803	*Synechocystis*	BG11 (freshwater)	30	2.1
PCC 7120	*Anabaena*	BG11 (freshwater)	30	14
PCC 7345	*Arthrospira*	SOT (freshwater)	30	-

Table 1: List of cyanobacteria used with their genus, environmental conditions and doubling times from literature with most optimised conditions and media for each.

Culture flasks of 100 mL (without baffles) were rinsed twice with deionized water, and autoclaved with Milli-Q water to eliminate any residual detergent. Instead of aluminium foil, SILICOSEN sterile silicone stoppers were used to ensure uniform air permeability and prevent contamination. All cultures were grown in 50 mL media in respective optimal growth conditions in INFORS HT Minitron incubator shaker at 110 RPM. OD_{750} was measured every 24 hours using Polystyrene Semi-micro cuvette 45 x 12 mm, path length 10 mm.

1.3 Cryo stock and revival

Freezing: 100 ml liquid culture is grown to at least an OD_{750} of 1, centrifuged at 6,000 x g for 10 min and resuspended in 4 mL medium. 1 mL aliquots were made into vials with 80 µL of filtered DMSO as an osmoprotectant (mixed gently but quickly). Freeze immediately as DMSO is toxic at room temperature.

Reviving: Thawed the vial quickly. Streaked out onto the plate using an inoculation loop. Wrap the plates and flasks with Kimwipes (to diffuse the light penetration) and incubate for 1-3 days at appropriate temperature without shaking before removing the Kimwipes and beginning to shake the flask. After sustained incubation in low light, green colonies will appear on the plate which can be used for liquid cultures.

2. Protein purification

ArcticExpress (DE3) chemically competent cells from Agilent were used to express all heterologous proteins. The gene fragments were ordered from Twist Biosciences, expressed under T7 promoter in pET29b plasmid with Kanamycin resistance and with Strep-tag II (NdeI-XhoI as insertion sites). Manufacturer's protocol was followed for successful transformants, stored in DMSO at -80°C .

For protein expression, streaked out the transformants on LB (Lysogeny Broth) plates with Kanamycin (50 µg/mL) and Gentamycin (20 µg/mL) and incubated at 30°C overnight. Picked one colony for pre-culture in a 50 mL flask with 25 mL LB with the same antibiotics and grew at 30°C overnight until it reached OD_{600} of 1. Incoculated 1 mL of pre-culture into 100 mL auto-induction media with the same concentration of Kanamycin and Gentamycin at 30°C for 4-6 hours and then at 16°C overnight for production of heterologous protein at 110 RPM.

IBA Strep-tactin was used for purification of the expressed proteins and the manufacturer's protocol was used, followed by estimation of protein content using Bradford assay. SDS PAGE was done to confirm the protein band at desired size.

3. *In vitro* assays

3.1 Making cell-free lysates

The frozen pellets were resuspended in 10 mL of vesicle buffer (50 mM HEPES at pH 7.5, 10 mM MgCl2 and 10 mM K2HPO4 in distilled water) per 1g of biomass. Using the Avestin Emulsiflex B15 homogenizer at 24,000 psi pressure, cyanobacterial extracts were lyzed. Due to this high pressure, most cells are ruptured without damaging the proteins. The lysates can be stored for a few months without losing activity at -80°C after flash-freezing the aliquots in liquid nitrogen.

3.1.1 Concentrating membrane vesicles

To concentrate the membrane vesicles, the lysed cells were centrifuged at 10,000 RPM for 10 mins. The supernatant is transferred and spun at 100,000 g in the Sorvall™ WX+ Ultracentrifuge using a fixed angle rotor for 1 hour at 4°C. The pellet was resuspended in the vesicle buffer (50 mM HEPES at pH 7.5, 10 mM MgCl2 and 10 mM K2HPO4 in distilled water). The concentrated vesicles were flash frozen in liquid nitrogen and stored at -80°C.

3.2 Estimation of chlorophyll content

The chlorophyll content in µg/mL was calculated by measuring the OD at 646, 663 and 700 nm using Polystyrene Semi-micro cuvette 45 x 12 mm, path length 10 mm in 80% acetone at pH 7.8. The formula used is [Chl a+b] = 17.76($E^{646.6}$) + 7.34($E^{663.6}$) where $E^{646.6}$= OD_{646}-OD_{700} and $E^{663.6}$=OD_{663}-OD_{700}. The formula was derived from calculations and corrections to previously accepted Arnon's equations published by Porra, 2001.

3.3 ^{13}C labelling

HEPES pH 7.3 (50 mM), MgCl2 (10 mM), K2PO4 (50 mM), NADP+ (2 mM), ADP (2 mM), Na-L-Ascorbate (10 mM), ATP (1 mM), sorbitol (450 mM), bicarbonate (100 mM), RuBP (500 µM), SOD (Bovine liver) (75 U/mL), Catalase (Bovine liver) (75 U/mL) were used. The reactions were performed in triplicates (30 µL each) in 1.5 eppendorf tubes and are quenched with 10% concentrated formic acid. The reactions were centrifuged at 20,000 rpm at 4˚C for 10 mins and transferred to HPLC vials and stored at -20°C until analysis.

3.4 ATP bioluminescence assay

HEPES pH 7.3 (50 mM), $MgCl_2$ (10 mM), K_2PO_4 (50 mM), NADP+ (2 mM), ADP (2 mM), ADK Inhibitor- DMAPP (500 µM) were always used in the assay while changing other variables as mentioned in Chapter 3. Cyanobacteria extracts/concentrated membrane vesicles were normalized to 25 µg/mL of chlorophyll (a+b).

The reactions were performed in triplicates (30 µL each) in 1.5 eppendorf tubes and are quenched with 10% concentrated formic acid, then transferred to a chilled aluminium rack. 45 µL of triplicates of each sample is aliquoted into a white 384-well flat-bottom luminescence plate (Thermo Fischer Scientific), followed by addition of 5 µL of the luciferase reagent from the ATP Bioluminescence Assay Kit CLS II (Roche). Luminescence at 580 ± 80 nm was measured in an Infinite M Plex microplate reader (Tecan). ATP concentrations were calculated by comparing to a standard curve of samples with known concentrations.

3.5 *In vitro* transcription assay

Rosalind buffer, Tris-HCl (40 mM), DTT (10 mM), NaCl (20 mM), Spermidine (2 mM), $MgCl_2$ (8 mM), K_2PO_4 (10 mM), NEB RNase Inhibitor (1 U/µL), ADK Inhibitor-DMAPP (Sigma) (500 µM), rNTPs (0.75 mM), T7 RNA Polymerase (Takara Bio) (5 U/µL), DFHBI dye (0.2 mM), 3WJdB plasmid (30 nM) were added to the lysed extracts. Fluorescence at an emission wavelength of 509 nm was recorded using an Infinite M Plex microplate reader (Tecan) 384 well plate.

3.6 Hexokinase assay

HEPES pH 7.3 (50 mM), $MgCl_2$ (10 mM), K_2PO_4 (50 mM), NADP+ (2 mM), ADP (2 mM), Glucose (10 mM), hexokinase enzyme (10 µg/mL) were used. Cyanobacteria extracts/concentrated membrane vesicles were normalized to 25 µg/mL of Chlorophyll (a+b). The reactions were performed in triplicates (20 µL each) in 1.5 mL eppendorf tubes and were quenched with 10% concentrated formic acid. The reactions were centrifuged at 20,000 rpm at 4˚C for 10 mins and transferred to HPLC vials and stored at -20°C until analysis.

3.7 Sugar assays

3.7.1 Glucovanillin assay

Reagents used included vanillin (100 µM), RuBP (varied conc. in µM), bicarbonate (varied conc. in µM), G1P (100 µM), UTP, ATP (500 µM), MgCl2 (1mM), enzymes- UGPase and UGT (1 µM). Cyanobacteria extracts were normalized to 25 µg/mL of Chlorophyll (a+b). The reactions were performed in triplicates (20 µL each) and are quenched with 10% conc. formic acid. The reactions were centrifuged at 20,000 rpm at 4˚C for 10 mins and transferred to HPLC vials and stored at -20°C until analysis.

3.7.2 3PG assay

Substrates used included ADP-glu (100 µM), RuBP (varied conc. in µM), bicarbonate (varied conc. in µM), 3PG (200 µM), MgCl2 (1mM), enzymes- GPS1 and 2 (1 µM). Cyanobacteria extracts are normalized to 25 µg/mL of Chlorophyll (a+b). The reactions were performed in triplicates (20 µL each) and are quenched with 10%

conc. formic acid. The reactions were centrifuged at 20,000 rpm at 4˚C for 10 mins and transferred to HPLC vials and stored at -20°C until analysis.

4. Endometabolomics

4.1 Extraction for endometabolomics

Prepared 70% MeOH (v/v) and aliquoted in 2 ml Eppendorf tubes (1 mL in each). Stored the tubes at -80°C (48 hours prior) and an aluminium rack at -20°C.

Extraction fluid: 1:1 of MeOH (LC-MS grade) with TE-buffer at pH 7.0 (10 mM TRIZMA, 1 mM EDTA), stored at -20°C (12 hours before extraction). Store Chloroform in a glass bottle 48 hours prior to extraction

For sampling, cooled down the centrifuge to -9°C. and added 1 mL of culture sample to the pre-cooled quenching solution: 70% MeOH (v/v) and mixed by turning the tube once. Separated the cells by centrifuging at 20,000 rpm for 10 minutes at -9°C. Removed the supernatant with the help of a syringe and stored the pellets at -80°C until extraction.

For extraction of the metabolites, calculate the volume of extraction fluid for each sample. Extraction volume= 50 µL x (OD_{750}). Pellets from -80°C were kept in a pre-cooled aluminium rack as the pellets should not be at room temperature at all. Added 1:1 amount of extraction fluid and chloroform in order and resuspend by vortexing at short intervals. Incubated in a shaker for 2 hours at 700 rpm at 0°C in a cold room. Separated the phases by centrifuging at -9°C for 10 minutes at 20,000 rpm in a fixed angle rotor. Extracted the upper phase (containing the metabolites) with a syringe and needle, turning it upside down to avoid loss of sample. Replaced the needle with Sartorius Minisart SRP 4 PTFE membrane filter and slowly added the extracted sample into a pre-labelled 1.5 mL eppendorf tube placed on a cold aluminium rack. Transferred the samples from the eppendorf into labelled HPLC vials for analysis. Stored the vials at -80°C until measurement.

4.2 Measurement using LC-MS

4.2.1 Quantitative determination of Organic acids

The chromatographic separation was performed on an Agilent Infinity II 1290 HPLC system using a Kinetex EVO C18 column (150 × 2.1 mm, 3 µm particle size, 100 Å

pore size, Phenomenex) connected to a guard column of similar specificity (20 × 2.1 mm, 3 µm particle size, Phenomoenex) at a constant flow rate of 0.2 mL/min with mobile phase A being 0.1 % formic acid in water and phase B being 0.1 % formic acid in methanol (Honeywell, Morristown, New Jersey, USA) at 25 °C.

The injection volume was 1 µL.

The profile of the mobile phase consisted of the following steps and linear gradients: 0 – 4 min constant at 0 % B; 4 – 6 min from 0 % to 100% B; 6 – 7 min constant at 100 % B; 7 – 7.1 min from 100 % to 0% B; 7.1 – 12 min constant at 0 % B.

An Agilent 6495 mass spectrometer was used in negative mode with an electrospray ionization source and the following conditions: ESI spray voltage 2000 V, nozzle voltage 500 V, sheath gas 300 °C at 11 L/min, nebulizer pressure 50 psig and drying gas 80 °C at 16 L/min.

Compounds were identified based on their mass transition and retention time compared to standards. Chromatograms were integrated using MassHunter software (Agilent, Santa Clara, CA, USA). Absolute concentrations were determined based on an external Standard curve.

Mass transitions, collision energies, Cell accelerator voltages, and Dwell times have been optimized using chemically pure standards. The parameter settings of all targets are given in **Table 2**.

Compound	Precursor Ion	Product Ion	Collision energy [V]	Fragmentor Voltage [V]	Cell Accelerator Voltage [V]	Dwell time [msec]	Polarity
Citrate	191	111.1	11	380	5	50	Negative
		85.1	14	380	5	50	
Alpha-ketoglutarate	145.1	101.1	5	380	5	50	Negative
		57.2	8	380	5	50	
Malate	133.1	115.1	8	380	5	50	Negative
		71.2	12	380	5	50	

Succinate	117.2	73.2 55.1	9 15	380 380	5 5	50 50	Negative
Fumarate	115.1	71.2 27.3	4 9	380 380	5 5	50 50	Negative
Lactate	89.2	89.2 71.3	0 10	380 380	5 5	50 50	Negative
Pyruvate	87.1	87.1 43.1	0 4	380 380	5 5	50 50	Negative
Glycolate	75.2	75.2 47.2	0 6	380 380	5 5	50 50	Negative
Glyoxylate	73.2	73.2 45.2	0 7	380 380	5 5	50 50	Negative

Table 2: List of organic acids measured with their precursor ion and product ion masses, collision energy (V), fragmentor energy (V), cell accelerator voltage, dwell time (msec) and polarity

4.2.2 Quantitative determination of Amino acids

Performed using a LC-MS/MS. The chromatographic separation was performed on an Agilent Infinity II 1290 HPLC system using a ZicHILIC SeQuant column (150 × 2.1 mm, 3.5 µm particle size, 100 Å pore size) connected to a ZicHILIC guard column (20 × 2.1 mm, 5 µm particle size) (Merck KgAA) a constant flow rate of 0.3 ml/min with mobile phase A being 0.1 % Formic acid in 99:1 water:acetonitrile (Honeywell, Morristown, New Jersey, USA) and phase B being 0.1 % formic acid 99:1 acetonitrile:water (Honeywell, Morristown, New Jersey, USA) at 25° C.

The injection volume was 1 µl.

The mobile phase profile consisted of the following steps and linear gradients: 0 – 8 min from 80 to 60 % B; 8 – 10 min from 60 to 10 % B; 10 – 12 min constant at 10 % B; 12 – 12.1 min from 10 to 80 % B; 12 to 15 min constant at 80 % B.

An Agilent 6470 mass spectrometer was used in positive mode with an electrospray ionization source and the following conditions: ESI spray voltage 4500 V, nozzle voltage 1500 V, sheath gas 300° C at 12 l/min, nebulizer pressure 30 psig and drying gas 250° C at 11 l/min.

Compounds were identified based on their mass transition and retention time compared to standards.

Chromatograms were integrated using MassHunter software (Agilent, Santa Clara, CA, USA). Relative abundance was determined based on the peak area. Absolute concentrations were determined based on an external Standard curve.

Mass transitions, collision energies, Cell accelerator voltages and Dwell times have been optimized using chemically pure standards. Parameter settings of all targets are given in **Table 3.**

Compound	Precursor	Product	Collision Energy [V]	Fragmentor Voltage [V]	Cell Accelerator Voltage [V]	Dwell time [msec]	Polarity
Tryptophane	205	188	7	90	5	20	Positive
		146	17	90	5	20	Positive
Tyrosine	182.1	165	6	100	5	20	Positive
		136	12	100	5	20	Positive
Arginine	175	116	12	100	5	20	Positive
		70.2	28	100	5	20	Positive
Phenylalanine	166	120.1	14	90	5	20	Positive
		103.1	30	90	5	20	Positive
Histidine	156	110.1	14	120	5	20	Positive
		83.1	28	120	5	20	Positive
Methionine	150	133	7	90	5	20	Positive
		104	7	90	5	20	Positive

Glutamate	148.1	84.1 56.1	17 34	80 80	5 5	20 20	Positive Positive
Glutamine	147	130 84.1	7 17	80 80	5 5	20 20	Positive Positive
Lysine	147.1	130.1 84.1	7 16	80 80	5 5	20 20	Positive Positive
Aspartate	134.1	88 74	9 14	80 80	5 5	20 20	Positive Positive
Asparagine	133.1	87.1 74	17 16	80 80	5 5	20 20	Positive Positive
Isoleucine	132.1	86.2 69.1	8 18	90 90	5 5	20 20	Positive Positive
Leucine	132.1	86.2 30.3	7 18	90 90	5 5	20 20	Positive Positive
Threonine	120.2	74.1 55.9	8 18	90 90	5 5	20 20	Positive Positive
Valine	118.1	72 55.1	9 23	90 90	5 5	20 20	Positive Positive
Proline	116	70.2 43.3	16 35	90 90	5 5	20 20	Positive Positive
Serine	106.1	60.2 41.2	12 11	90 90	5 5	20 20	Positive Positive
Alanine	90	44.1	12	80	5	20	Positive
Glycine	76.1	30.3	32	80	5	20	Positive

		28.3	32	80	5	20	Positive

Table 3: List of amino acids measured with their precursor ion and product ion masses, collision energy (V), fragmentor energy (V), cell accelerator voltage, dwell time (msec) and polarity

4.2.3 Quantitative determination of sugar phosphates

Performed using a LC-MS/MS. The chromatographic separation was performed on an Agilent Infinity II 1290 HPLC system using a SeQuant ZIC-pHILIC column (150 × 2.1 mm, 5 µm particle size, peek coated, Merck) connected to a guard column of similar specificity (20 × 2.1 mm, 5 µm particle size, Phenomoenex) a constant flow rate of 0.1 ml/min with mobile phase A with mobile phase comprised of 10 mM ammonium acetate in water, pH 9, supplemented with medronic acid to a final concentration of 5 µM (A) and 10 mM ammonium acetate in 90:10 acetonitrile to water, pH 9, supplemented with medronic acid to a final concentration of 5 µM (B) at 40° C .

The injection volume was 2 µl.

The mobile phase profile consisted of the following steps and linear gradients: 0 – 1 min constant at 75 % B; 1 – 6 min from 75 to 40 % B; 6 to 9 min constant at 40 % B; 9 – 9.1 min from 40 to 75 % B; 9.1 to 20 min constant at 75 % B. An Agilent 6495 ion funnel mass spectrometer was used in negative and positive ionisation mode with an electrospray ionization source and the following conditions: ESI spray voltage 3500 V, nozzle voltage 1000 V, sheath gas 300° C at 9 l/min, nebulizer pressure 20 psig and drying gas 100° C at 11 l/min. Compounds were identified based on their mass transition and retention time compared to standards. Chromatograms were integrated using MassHunter software (Agilent, Santa Clara, CA, USA). Absolute concentrations were determined based on an external Standard curve.

Mass transitions, collision energies, Cell accelerator voltages, and Dwell times have been optimized using chemically pure standards. Parameter settings of all targets are given in **Table 4.**

Compound	Precursor Ion	Product Ion	Collision energy [V]	Fragmentor Voltage [V]	Cell Accelerator Voltage [V]	Dwell time [msec]	Polarity
Fructose-6-Phosphate/Glucose-6-Phosphate	259	97 79	15 45	380	5	400	Negative
RuBP	309.09	97 79	17 59	380	5	110	Negative
3PG	185.06	185.06 97 79	0 13 32	380	5	110	Negative
2PG	155	155 97 79	0 19 33	380	5	110	Negative

Table 4: List of sugar phosphates measured with their precursor ion and product ion masses, collision energy (V), fragmentor energy (V), cell accelerator voltage, dwell time (msec) and polarity

4.2.4 Untargeted metabolomics

Exometabolite analysis using LC-MS/MS- Untargeted metabolic profiling was performed by using HRES-LC-MS/MS. The chromatographic separation was performed on a Vanquish LC chromatograph (Thermo Scientific), injecting 1 µl of sample per run, and applying four different types of chromatography, as described in detail below.

RP chromatography at low pH was performed using using a Luna Omega PS C18 column (100 × 2.1 mm, 1.6 µm particle size, 100 Å pore size, Phenomenex) connected to a guard column of similar specificity (20 × 2.1 mm, 3 µm particle size, Phenomoenex) at a constant flow rate of 0.25 mL/min with mobile phase A being 0.1 % formic acid in water and phase B being 0.1 % formic acid in acetonitrile (Honeywell, Morristown, New Jersey, USA) at 40 °C.

The profile of the mobile phase consisted of the following steps and linear gradients: 0 – 1 min constant at 30 % B; 1 – 10 min from 30 % to 100% B; 10 – 12 min constant at 100 % B; 12 – 12.1 min from 100 % to 30% B; 12.1 – 17 min constant at 30 % B.

In each case, a Thermo Scientific ID-X Orbitrap mass spectrometer was used in positive and negative ionization mode (separate analytical runs). Ionization was performed using a high-temperature electrospray ion source, with a static spray voltage of 3400 V in positive mode and 2400 V in negative mode. Sheath gas was set to 50 arbitrary units (Arb), auxiliary gas to 10 Arb, with the ion transfer tube and vaporizer temperatures set to 325°C and 350°C, respectively.

Data-dependent MS/MS measurements were conducted at an Orbitrap mass resolution of 120K, using quadrupole isolation within a mass range of 100–1000 m/z, combined with high-energy collision dissociation (HCD). HCD was performed with a cycle time of 1 seconds, targeting the most abundant ions with a relative collision energy of 30%. Fragments were detected using the Orbitrap mass analyzer at a predefined resolution of 30K. To increase coverage, dynamic exclusion was applied with an exclusion duration of 2.5 seconds after one scan, using a mass tolerance of 10 ppm.

Data analysis- Peak annotation was conducted using Compound Discoverer 3.3.1.111. The Compound Discoverer workflow included the following nodes: Peak Detection, Alignment, Fill Gaps, Background Marking, Area Normalization (default normalization method: Constant Mean/Sum), mzCloud Spectra Library Search, Composition Prediction, Mass Matching with online libraries (ChemSpider), in-silico fragmentation, MS/MS spectra matching, and Compound Annotation. (Method adapted from Kueffner et al., 2024)

The output table from each measurement was filtered based on peak rating. We set a peak rating threshold of 5 or higher for all replicates within each biological group. After filtering, the data were exported and consolidated into a single table.

5. Proteomics

5.1 Extraction for proteomics

Culture volume corresponding to 1 mL at OD_{750}= 3 of the culture was added to 1.5 mL eppendorf tube and centrifuged at 20,000 rpm for 10 minutes at low (0-4°C)

temperature. The supernatant was removed using a syringe and needle, and the cell pellet was stored at -80°C. Cell pellets were lysed by adding 500 µL of Tris-HCl with protease inhibitors and 0.5 µg/µL lysozyme (Sigma-Aldrich), incubating at 25°C for 1 hour. 200 µL of 2% sodium deoxycholate (SDC) with 10 mM dithiothreitol (DTT) was added, followed by sonication for at least 30 seconds using a vial tweeter to shear the DNA. The lysates are heated at 90°C for 30 mins followed by centrifugation at 14,000 rpm for 5 minutes at 4°C to clear lysate from debris. The clear supernatant was mixed with 6 volumes of cold (-20°C) acetone and 1 volume of chilled methanol, and mixed well by vortexing and allowing precipitation followed by overnight incubation at -20°C. After centrifugation at 20,000 rpm for 10 minutes at 4°C, the supernatant was discarded. The pellet was washed twice with 200 µL cold methanol, dried, and reconstituted in 100 µL of 0.5% SDC and incubated at 90°C for 10 mins. Protein concentration was determined using BCA and pre-diluted BSA (Pierce BCA, Thermo Fischer Scientific) following the manufacturer's protocol. 5 µL TCEP (40x dilution) was added, vortexed and incubated at 90°C for 15 mins and then allowed the samples to cool down and do a quick spin. Added 5 µL of iodoacetamide solution (74 mg/mL), vortexed and kept at 25°C for 20 minutes in the dark as iodoacetamide is light sensitive. Based on BCA results, volume corresponding to 50 µg of total protein was added into a new tube and trypsin to a final enzyme:protein ratio of 1:50 and digest at 30°C overnight. Following digestion and centrifugation, Trifluoroacetic acid (TFA) was added to a final concentration of 1.5% (pH<2). Samples were centrifuged at 15,000 rpm for 10 mins at 4°C and the supernatant was for solid-phase extraction. Beads were separated and peptides containing supernatant were collected, purified and desalted by C18-solid phase extraction using Chromabound spin columns (Macherey-Nagel). Cartridges were prepared by adding acetonitrile, followed by equilibration with 0.1% TFA. Acidified peptides were loaded on equilibrated cartridges, washed with 5% ACN and 0.1% TFA containing buffer and finally eluted with 50% ACN and 0.1% TFA (Method adapted from Inckemann & Chotel, 2025).

5.2 Measurement using LC-MS and analysis

Peptides were reconstituted in 0.1% TFA and then analyzed using liquid chromatography-mass spectrometry using Exploris 480 instrument connected to an Ultimate 3000 RSLC nano and a nanospray flex ion source (Thermo Scientific). Peptide separation was done on a reverse phase HPLC column (75 µm x 42 cm)

packed in with C18 resin (2.4 µm). The separating gradient used is: 94% solvent A (0.15% formic acid) and 6% solvent B (99.85% acetonitrile, 0.15% formic acid) to 25% solvent B over 97 min., and an additional increase of solvent B to 35% for 35 min. at a 670 flow rate of 300 nl/min. MS raw data was acquired on an Exploris 480 (Thermo Scientific) in data independent acquisition (DIA) mode. Peptides were ionized at a spray voltage of 2.3 kV, 672 ion transfer tube temperature set at 275 °C. The data was analysed using MaxQuant and Perseus proteomics software.

6. Purification of carboxysomes

PCC 7942 pellet stored at -80°C was resuspended in 5 mL /1g of biomass TEMB buffer (10 mM Tris-HCl, 1 mM EDTA at pH8, 10 mM $MgCl_2$, 20 mM $NaHCO_3$). The re-suspended biomass was lysed twice using Avestin Emulsiflex B15 homogenizer at 24,000 psi pressure. The lysate was centrifuged at 6,000 g for 10 mins. 1 mg Lipase (Sigma) and 1 mg DNase (Sigma) were added followed by 1 hour of incubation at 30°C. 1% TritonX was added and incubated again for 1 hour at 30°C. The lysate was centrifuged at 10,000 g.

Sucrose gradient was prepared by various concentrations of sucrose in milliQ water- 20,40 and 60%. The gradients were carefully prepared in an ultracentrifuge tube (8 mL) in the order of 20, 40 and 60 (2mL each) using a long needle going to the bottom of the tube and pushing the layers on top of each other based on density.

1 mL of the supernatant was loaded onto the gradient and centrifuged for 45 minutes at 80,000 to 100,000 g in the Sorvall™ WX+ Ultracentrifuge using a swinging bucket rotor to keep the gradients in order. The interface between 40/60 layer was collected and centrifuged again at 80,000 to 100,000 g. The tube was washed with TEMB and the pellet was resuspended in 6 mL of the buffer followed by centrifugation at 80,000 g for 30 mins. The pellets were resuspended in 500 µL TEMB.

Chapter 3

Results and Discussion

Cyanobacteriota is a diverse phylum with thousands of known as well as unknown species. With the potential to be biotechnologically used for various purposes, it is first useful to understand the biochemistry and metabolism of fast growing cyanobacteria. The strains as mentioned in **Table 1** were used for the study in different capacities.

1. Growth characterisation

The cyanobacteria were grown in a matrix of different light and CO_2 concentrations. Being photoautotrophic organisms, these are the most important factors for its growth. Different conditions with various strains were tested to commit to a final set of growth parameters, with two light settings- 100 and 300 µE in three CO_2 concentrations- 0.04% (Ambient), 0.5% and 3%.

Synechococcus strains of 7942, 2973, 7002 and 11901 are fast growing and have the capacity to accumulate more biomass in the optimal environmental conditions. These are the four main strains used in this study.

OD_{750} was measured every 24 hours. At 750 nm wavelength, the absorption of light by the pigments (chlorophyll and carotenoids) is avoided while only measuring the light scattering. The strains chosen are fast growing with relatively short doubling times, hence interesting for biotechnological applications.

The other parameters measured here are doubling time and biomass (mg/mL). The key takeaways from the growth measurements as shown in **Figure 3.1** for four different strains of cyanobacteria are- 1) Most strains used in the study (7942, 2973, 7002 and 11901) have similar growth trends in higher CO_2 conditions (3% and 0.5%) as compared to ambient (0.04%) conditions. 2) The strains grow faster and accumulate more biomass in the excess of available CO_2. 3) Marine cyanobacteria strains of 7002 and 11901 have higher accumulation of biomass as compared to freshwater strains of 7942 and 2973, and also have a tendency to retain more water. It is also observed that the concentration of CO_2 has a greater effect on biomass

accumulation while the difference in light intensity is not that prominent. An interesting observation from **3.1.A** is that 7942 performs worse in 300 µE light at ambient CO_2 condition. A plausible reason could be excess ROS in higher light

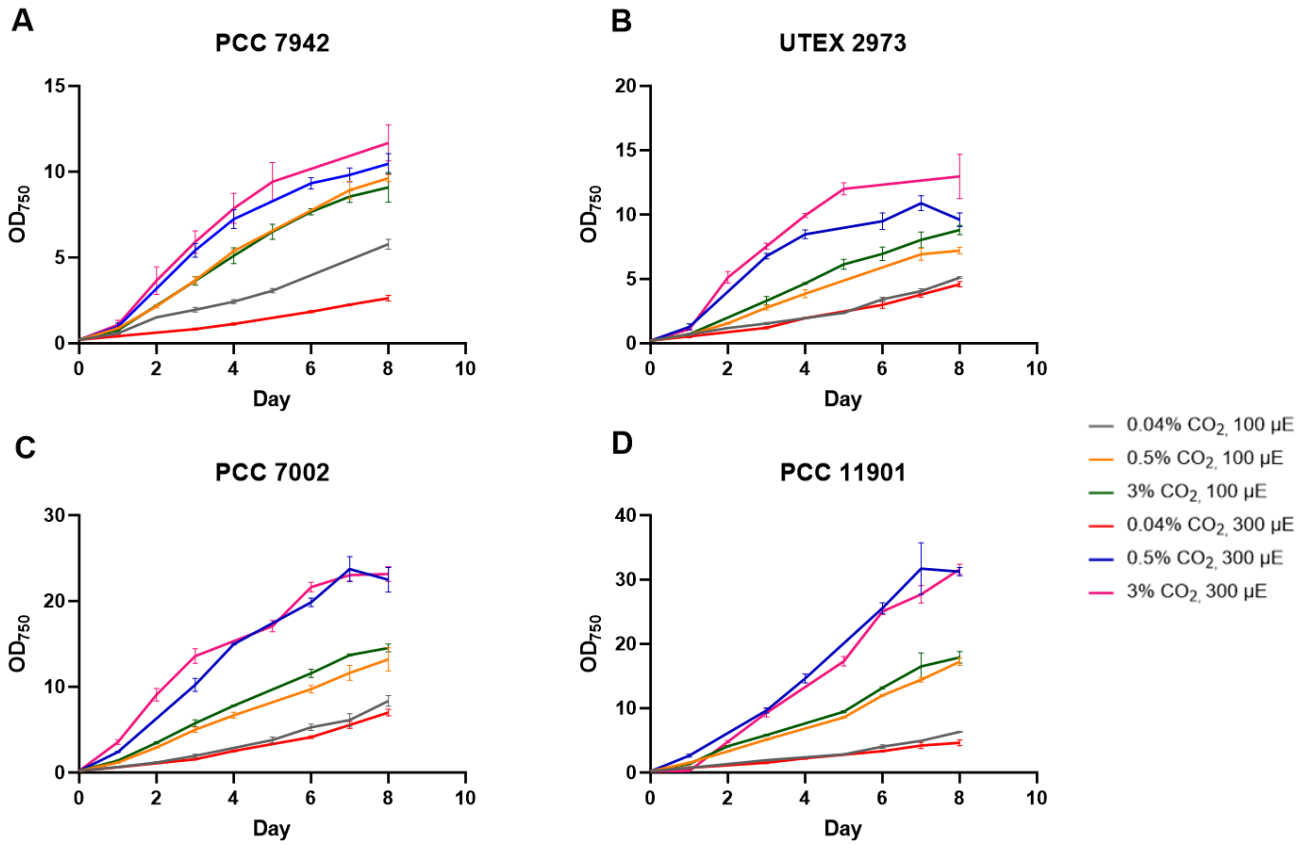

Figure 3.1: Growth curves for PCC 7942, UTEX 2973, PCC 7002, PCC 11901. OD_{750} was measured every 24 hours. Each condition had 3 replicates for measurement. As seen in C and D, marine strains tend to accumulate much higher amounts of biomass as compared to freshwater strains in A and B for almost every varying condition of light intensity and CO_2 concentration. Y-axes are presented with variable scales for clearer visualization within each panel rather than comparisons between panels.

and upregulation of proteins and metabolites involved in stress response as later seen in section 2 and 3. When the cultures have achieved a dense biomass and is in the state of resource limitations, the colour of the cultures turn more yellowish indicating nitrogen starvation (Sauer et al., 2001) and this is particularly seen in strains of 7002 and 11901 at higher CO_2 conditions.

2. Endometabolomics

To understand the output and fluxes of important metabolic processes in different combinations of light and CO_2 in a high throughput fashion, endometabolomics was used. It provides us with a global snapshot of all the metabolites at the same phase of the growth. The samples were quenched when OD_{750} reached 5, which is in the mid-log phase of growth.

The objective is to check the endometabolite profile of different strains (7942 and UTEX) in different conditions with respect to central carbon metabolism by measuring sugar phosphates (G6P, F6P etc), amino acids and organic acids (glycolate, citrate etc)

Figure 3.2 represents the key metabolites analysed and the fold change with respect to control condition of 75 µE light and 3% CO_2. In **Figure 3.2.A**, both strains are grown in 150 µE light and 3% CO_2, making light as the variable factor. When grown in higher light, we see enrichment of some metabolites like citrate in UTEX 2973 while slight decrease in PCC 7942, which could be linked to Tricarboxylic acid cycle (TCA). UTEX 2973 is known to accumulate higher biomass in higher light conditions while PCC 7942 is more light sensitive explaining the differences in citrate and glycolate levels. Proline is in increased concentrations in both the strains which can be explained as it behaves as a stress regulator by trying to maintain redox homeostasis in many different organisms. **Figure 3.2.B** records the differences in important metabolites when there is less availability of CO_2 as compared to control (6 times lesser). We see multi-fold changes in important carbon metabolites like 3PG, Phosphoenolpyruvate (PEP), glycolate and pyruvate in both PCC 7942 and UTEX 2973. These compounds are important and necessary for biomass accumulation as well as meeting energy requirements of the organism. It is interesting to see such large changes despite having similar rates of growth between 3% and 0.5% CO_2 as seen from growth measurements in **Figure 3.1**, as both the CO_2 concentrations are much higher than ambient levels.

There are significant differences in the metabolite profile in the varied conditions as well as between the two strains. Further analysis revealed that the metabolome remains fairly stable over time and different phases of growth within each condition and strain.

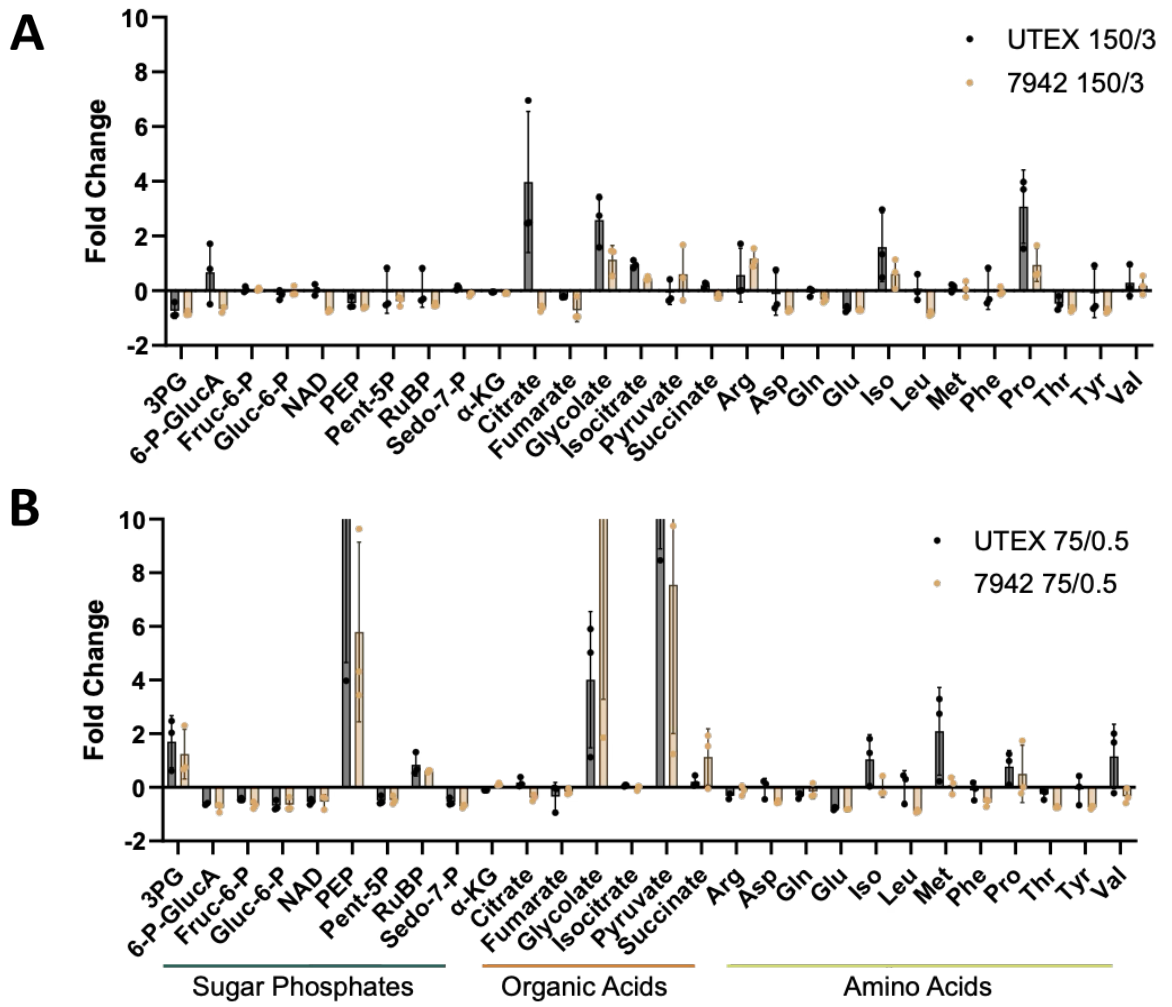

Figure 3.2: Targeted analysis of sugar phosphates, organic acids and amino acids using LC-MS. A- Fold change of respective compounds in 7942 and 2973 in 150 µE light and 3% CO_2 as compared to control 7942 and 2973 in 75 µE light and 3% CO_2, hence shows changes in metabolite concentrations in higher light. B- Fold change of respective compounds in 7942 and 2973 in 75 µE light and 0.5% CO_2 as compared to control 7942 and 2973 in 75 µE light and 3% CO_2, hence shows changes in metabolite concentrations in lower CO_2.

2.1 Untargeted metabolomics

Having observed interesting differences in the metabolic profile, it was worthwhile to explore the global differences using untargeted metabolomics. PCC 7942 grown in 0.5% (low) and 3% CO_2 (high) in 150 µE light was measured in both positive and negative ionization modes. A few important differences that appeared from the analysis was upregulation of stress molecules involved in glutathione production and some amino acids. However there was no clear conclusion derived from the dataset.

3. Proteomics

In a given environment, maximization of fitness requires microbial cells to regulate their proteome to balance the cost and benefit of proteins (Jahn, Michael et al, 2018). The aim is to investigate how different proteins (or classes of proteins e.g. membrane proteins, transcription factors) are regulated with respect to different conditions between different strains. As cyanobacteria are photoautotrophs and can be limited by resources like light and/CO_2, the landscape of the proteome coupled with information about the metabolites can lead to better understanding of resource allocation.

Initial protocol for extraction was based on *E.coli,* leading to broader variations and a large fraction of proteins missing. Subsequently, the extraction protocol was optimised based on *Chlamydomonas reinhardtii* for better resolution from Inckemann & Chotel et al., 2024 due to similarities with membrane and pigment components.

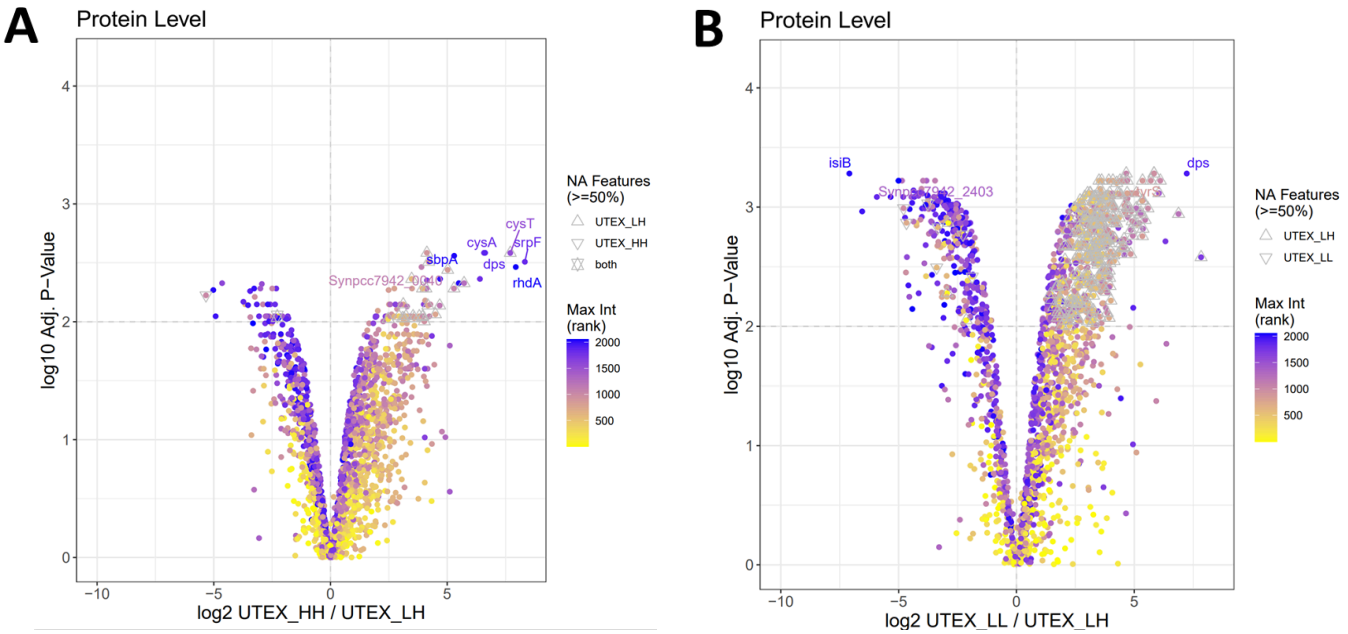

Figure 3.3: Change in total proteome content measured with respect to UTEX 2973 (75 µE light at 3% CO_2) using Log_{10} values. A- Shows all proteins measured for 2973 at higher light (150 µE). B- Shows all proteins measured for 2973 at lower CO_2 (0.5%).

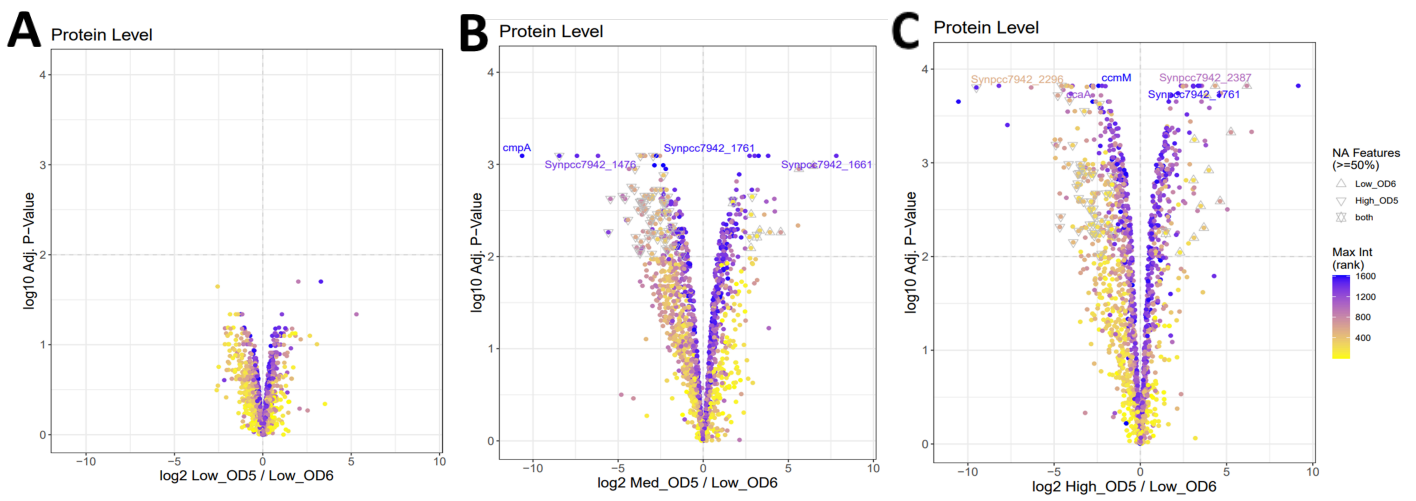

Figure 3.4: Change in total proteome content measured in different CO_2 concentrations with respect to PCC 7942 at OD_{750}= 6 (75 µE light at 0.04% CO_2) using Log_{10} values. A- Shows all proteins measured for 7942 grown in ambient CO_2 at OD_{750}= 5. B- Shows all proteins measured for 7942 grown in medium CO_2 (0.5%) at OD_{750}= 5. C- Shows all proteins measured for 7942 grown in high CO_2 (3%) at OD_{750}= 5. The light intensity was the same for all cultures at 75 µE.

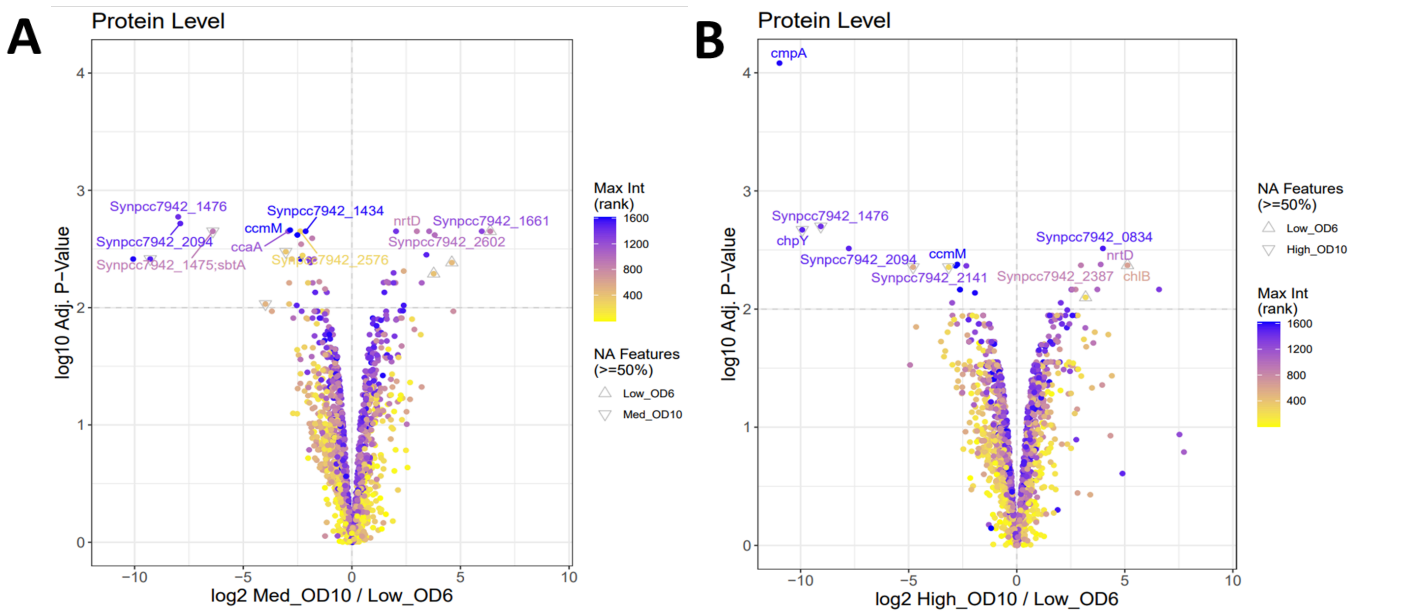

Figure 3.5: Change in total proteome content measured at higher OD_{750} in different CO_2 concentrations with respect to PCC 7942 at OD_{750}= 6 (75 µE light at 0.04% CO_2) using Log_{10} values. A- Shows all proteins measured for 7942 grown in medium CO_2 (0.5%) at OD_{750}= 10. B- Shows all proteins measured for 7942 grown in high CO_2 (3%) at OD_{750}= 10. The light intensity was the same for all cultures at 75 µE

Figure 3.3.A represents volcano plots for total protein content of UTEX 2973 in higher light- HH (150 µE) and **Figure 3.3.B** lower CO_2 conditions- LL (0.5%) with respect to control- LH (75 µE light and 3% CO2). From **Figure 3.3.A** we see a

change in only 10% of the total proteome with upregulation of stress response proteins like glutathione reductase and synthetase (as glutathione metabolism is associated with ROS and stressed environment), proteins involved in DNA protection (dps) and sulfate transport (sbpA, cysT), while downregulation of ribosome associated proteins. We do not observe any significant changes in the light harvesting complex proteins which seem a plausible association with higher light. **Figure 3.3.B** represents a 25% change in the proteome when there is lesser CO_2 available and most proteins that were upregulated were associated with central carbon metabolism like Rubisco related proteins (rbcL, PEP synthase, NAD kinases) and carbon concentrating mechanism (carbonic anhydrase and carboxysome shell proteins like ccmN). This shows that despite 0.5% and 3% CO_2 being much higher than ambient levels, it has a much drastic effect on resource allocation of cyanobacteria.

As interpreted from proteomics in **Figure 3.2** and **3.3**, CO_2 concentration has more impact, leading us to test the correlation in PCC 7942 strain which shares 99% of its genome with UTEX 2973 (Ungerer et al., 2018). **Figure 3.4.A** represents the volcano plots for total protein content of PCC 7942 at OD_{750}=5 in low CO_2 (0.04% which is ambient concentration), **Figure 3.4.B**-medium CO_2 (0.5%) and **Figure 3.4.C** high CO_2 (3%) with respect to control at OD_{750}=6 at ambient CO_2 concentration (0.04%). We see no significant difference in protein content between OD_{750}=5 and OD_{750}=6 at ambient CO_2, which is intuitive as they also lie in the same growth phase. The differences in proteins increase with the increase in CO_2 concentrations. In **Figure 3.4.B**, some major upregulated proteins are uncharacterised proteins, but there is an increase in Acetyl-CoA synthetase suggesting higher flux of central carbon metabolites with CO_2 availability. Some obvious down regulated proteins are related to carbon concentration and fixation due to abundance in CO_2 like carbonic anhydrase, Rubisco and carboxysome shell proteins.

In **Figure 3.5**, the change in protein content with respect to a different phase of growth is observed. OD_{750}=6 is around mid-log phase while OD_{750}=10 is in early stationary phase. Taking control as PCC 7942 at OD_{750}=6 grown in ambient CO_2 to generate volcano plots. From 5.A, we notice upregulation of certain proteins related to nitrogen import (nrtD) and dnaJ like Heat shock protein suggesting stress due to resource limitation. We also observe high levels of downregulation of proteins related to carbon concentration like bicarbonate binding protein (cmpA), CO_2 hydration

protein and carboxysome shell proteins. From **Figure 3.5.B**, we see downregulation of similar proteins as of **Figure 3.5.A**, including carbonic anhydrase and ccmM while upregulation of proteins related to glutathione metabolism and sulfate transport, indicating high stress as also mentioned in previous discussion.

3.1 Global proteome profile of PCC 7942 in 3 conditions

Ultimate objective of proteomic comparison is to understand the trends in protein classes with respect to different conditions. **Figure 3.6** represents 7942 proteomap for decreased CO_2 and increased light conditions with respect to reference of 75 µE light and 3% CO_2. 200 main proteins of interest (which is 10% of the total proteome) were plotted using an online software Bionic visualisation. Certain trends emerged like increase in proteins associated with carbon metabolism and photosynthesis (like rbcL, psaA and B) in decreased CO_2 whereas there was upregulation of proteins associated with stress response (groEL, dnaK) in higher light condition, also consistent with the fact that 7942 cannot handle higher light intensities. However, we expected to observe an increase in light harvesting complex proteins in increased light but there was no significant difference, suggesting the difference in the intensity was not large enough (between 150 and 75 µE).

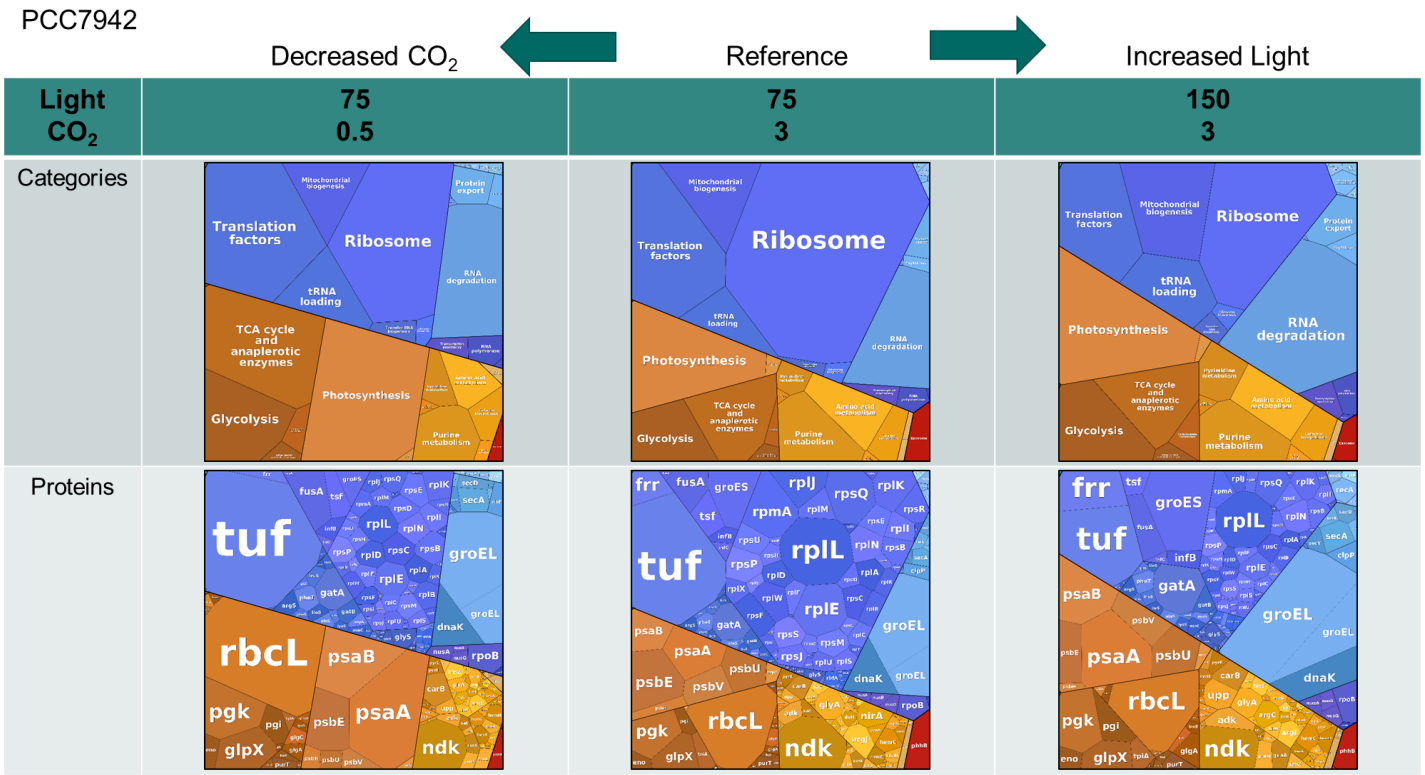

Figure 3.6: Proteomap for PCC 7942 in decreased CO_2 (0.5%) and increased light intensity (150 µE) with respect to control of 3% CO_2 and 75 µE light intensity. First the protein classes are represented and then individual proteins. Trends in major proteins are observed using this method of visualization.

4. *In vitro* assays

Cyanobacteria are slow and inefficient with respect to genetic modifications and hence understanding important metabolic reactions in an *in vitro* setting could be faster and useful to study a subset of reactions at a time without worrying about the entire network of interlinked processes. The objective of the multifaceted *in vitro* experimentation plan is to quantitate and compare the different strains grown in varied conditions on their ability of both CO_2 fixation ATP generation.

4.1 Carbon fixation

Calvin-Benson-Bassham (CBB) cycle as elaborated in chapter (1) 2.2 can fix CO_2 and the enzyme that facilitates the reaction is rubisco. It is almost impossible to accurately determine the rates of CO_2 *in vivo* as there is a continuous flux of the products in both directions, hence this section describes *in vitro* methods to separate global metabolism in a crude cell and focus on specific processes that allows for determining rates of CO_2 fixation between the different cultures grown in different conditions followed by lysis.

4.1.1 ^{13}C labelling to check enrichment in CBB cycle intermediates

The objective of this experiment was to check if the ^{13}C as provided in the form of labelled sodium bicarbonate was getting incorporated into the CBB cycle products and intermediates (glucose-6-phosphate, erythrose-6-phosphate, sedoheptulose-6-phosphate) which would have in turn helped in determining the rate of turnover of the cycle.

There was no difference between the labeled and unlabelled experiments as the majority distribution is of the M+0 fragment and almost negligible M+n (n=1,2,3,4) which indicate the number of heavy carbon incorporations as shown in **Figure 3.7** for glucose-6-phosphate. Erythrose-4-phosphate and ribulose-5-phosphate data shown in **S.1.**

^{13}C wasn't taken up by the extracts and the possible reason could be that the heavier carbon dioxide isotope (added in form of bicarbonate) gets exchanged with the atmospheric carbon dioxide. To enable the extracts to be able to take up ^{13}C, we $^{13}CO_2$ would have to be constantly supplied in a secured chamber. This increases the complexity of the experimental set-up, hence the approach was to move towards simple *in vitro* assays.

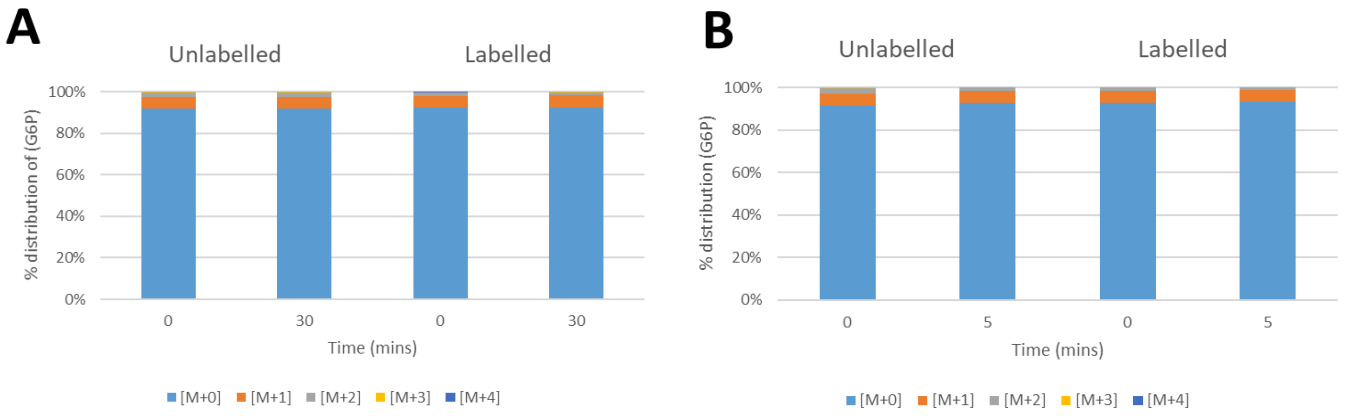

Figure 3.7: ^{13}C labelling was done to check intermediates of CBB cycle. However, no incorporation of heavy carbon isotope was seen in any of the compounds (here glucose-6-phosphate) in both 30 minute and 5 minute incubation.

4.1.2 Sugar assay enzymes to check for Calvin cycle activity

The first objective of this set of *in vitro* assays is to check whether the Calvin cycle enzymes are active in the extracts. The two most important products from the CBB cycle are glucose-6-phosphate and 3-phosphoglycerate. However, both of these compounds are taken into other metabolic cycles, hence the principle is to convert these into a form that is not easily metabolized (absence of native cyanobacterial enzymes to degrade). The following scheme elaborates the reactions used for the various in vitro assays.

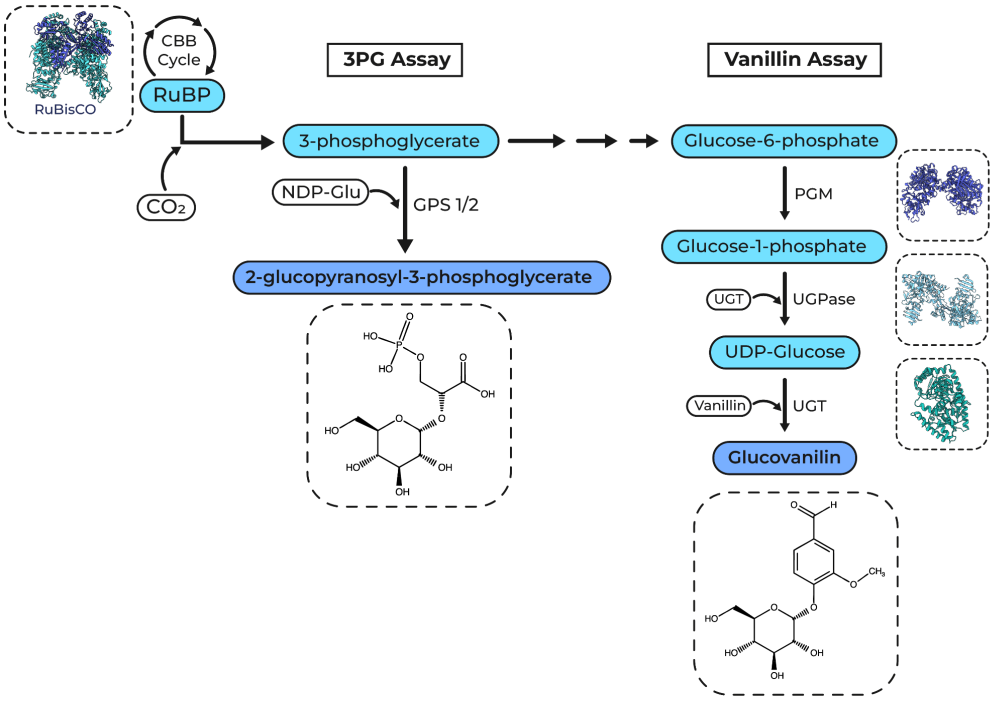

The enzymes used are:

Phosphoglucomutase (pgm- 24.36 kDa) from *E. coli*- Isomerises β-D-glucose-1-phosphate (G1P) to β-D-glucose 6-phosphate (G6P) with a K_{cat}= 21 s^{-1}. It can also do the reverse reaction but with a much slower K_{cat}= 0.5 s^{-1}.

UTP-glucose-1-phosphate uridylyltransferase (UGPase- 34.74 kDa) from *E.coli* can catalyse the transfer of α-D-glucose from α-D-glucose-1-phosphate (G1P) onto UTP producing UDP-glucose and PPi.

UDP-glycosyltransferase 72E2 (UGT72E2- 54.79 kDa) is found in *Arabidopsis thaliana* which has the capability of O-glucosylation of monolignols (alcohol monomers of lignin e.g. vanillin, coumarate etc). Here we are using this enzyme to glycosylate vanillin to glucovanillin using UDP-glucose.

Glucosyl-3-phosphoglycerate synthase (GSP1- 49.69 kDa from Synechococcus PCC7002) and (GSP2- 46.6 kDa from Prochlorococcus marinus SS120) can transfer a glucose moiety from NDP-glucose, here 3PG to 2-glucopyranosyl-3-phosphoglycerate.

4.1.3 Purification of heterologous enzymes for sugar assays

The enzymes mentioned in the sugar assay schemes were all expressed heterologously using the ArcticExpress (DE3) strain of *E.coli*. The strain lacks Lon protease which can degrade recombinant proteins and has consecutive expression of two chaperonins Cpn10 and Cpn60 to facilitate protein folding. The sequences are mentioned in **S2.** Proteins were expressed and purified according to manufacturer's protocols mentioned in chapter 3 section 2.

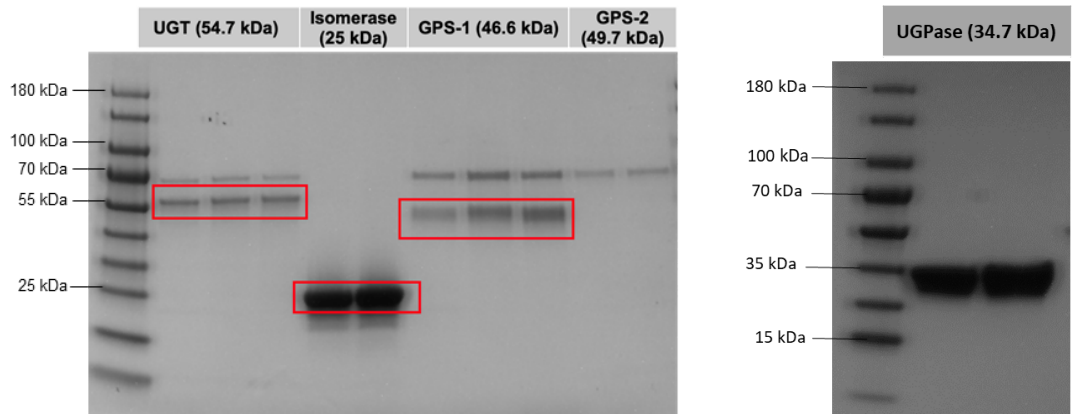

Figure 3.8: Successful purification of UGT, UGPase, PGM, GSP1 which are used for sugar assay schemes

4.1.4 3PG assay

The immediate product of Rubisco catalysed reaction between CO_2 and RuBP is 3-phosphoglycerate. The objective of the assay is to check the accumulation of 3PG over time and to determine the differences between different strains of cyanobacteria with respect to carbon fixation rates. For initial proof of concept testing, UTEX 2973 and PCC 7942 lysates were used by normalising at the same concentration (25 µg/mL of chlorophyll content). It was observed that when the lysates are pre-incubated by addition of carbonic anhydrase (CA) and sodium bicarbonate for an hour prior to addition of RuBP, there is higher accumulation of 3PG as compared to samples that were not pre-incubated. It can be attributed to the activation of Rubisco and higher availability of CO_2 due to the presence of CA (Faisal et al., 2024). From **Figure 3.9**, 7942 showed higher accumulation of 3PG (~200 µM) compared to 2973 (150 µM) over a period of 2 hours.

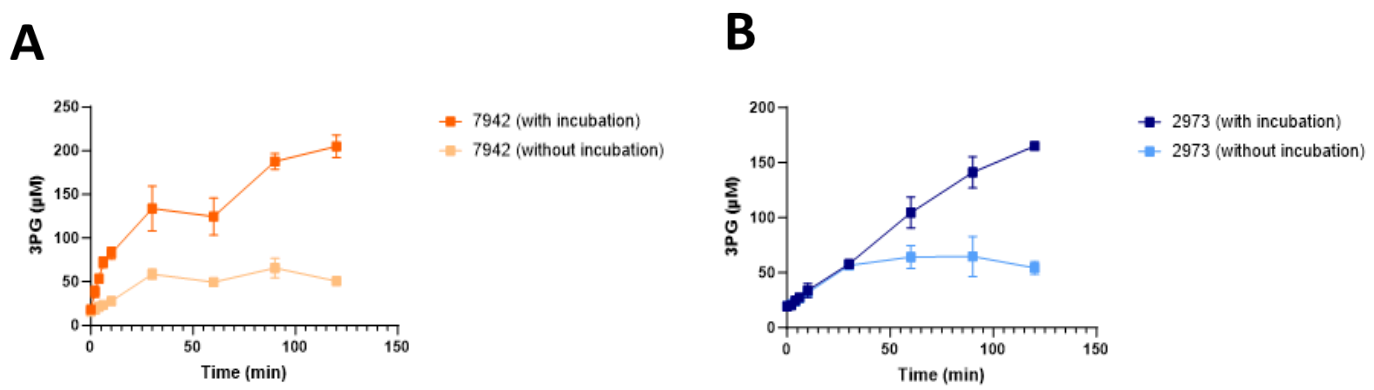

Figure 3.9: A- Accumulation of 3PG in 7942 with and without incubation over 120 mins, B- Accumulation of 3PG in 2973 with and without incubation over 120 mins

Another assay with the dynamics of 3PG was tested **(Figure 3.10)** where it was glycosylated by addition of an external enzyme to form 2-glucopyranosyl-3-phosphoglycerate with the help of externally added enzyme GSP1/2 (Glucosyl-3-phosphoglycerate synthase). The aim was to observe depletion of 3PG over time coupled with accumulation of the glycosylated product. However, the caveat of the assay is the quantification of 2-glucopyranosyl-3-phosphoglycerate due to lack of commercially available standard. Depletion of 3PG was seen over a period of 3 hours for 3 out of 4 reaction conditions.

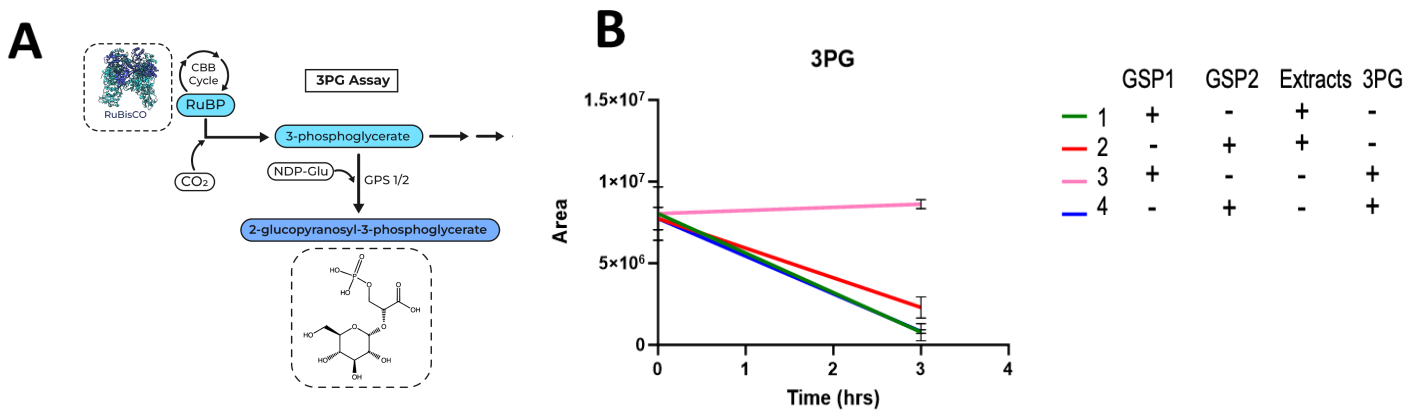

Figure 3.10: A-Schematic of the depletion of 3PG, B- Integrated area of LC-MS peak of 3PG over 3 hours in different reaction set-ups with either GSP1/2 enzyme.

4.1.5 Glucovanillin assay to measure gluconeogenesis

The vanillin assay is to understand the rate of gluconeogenesis and Calvin cycle. Glucose-6-phosphate is isomerized to glucose-1-phosphate (G1P) which glycosylates UTP with the help of UDP-glucose pyrophosphorylase (UGPase) to form UDP-glucose. Now UDP-glucose in turn is used to add a glucose moiety to vanillin producing glucovanillin using UDP-glucosyl transferase (UGT).

Both vanillin and glucovanillin are quantified using LC-MS/MS and commercial standards as shown in **Figure 3.11.A.** Glucovanillin is detected over a time of 4 hours in reactions where all the enzymes (pgm, UGPase and UGT) along with cyanobacterial lysate, which is even higher when there is pure substrate added (G1P) and a further increase in the integrated area of glucovanillin is seen when lysates are spiked with G1P as shown in **Figure 3.11.B**. We see no glucovanillin production in absence of external enzymes needed for the reaction scheme and cyanobacteria don't have native pathways to produce the same. We proceed to test the correlation between the concentrations (0,50 and 100 µM each) of RuBP and bicarbonate (which are substrates for carbon fixation by rubisco). The objective was to determine the rate of carbon fixation, and through a series of steps-gluconeogenesis which could be modulated by varying the substrate concentrations (RuBP and CO_2 from bicarbonate). However, we do not observe any strong association from **Figure 3.11.C and D.** Over 24 hours, we measure 10%

conversion of substrate vanillin into glucovanillin via our enzymatic scheme. The assay is working in principle but it needs more optimization.

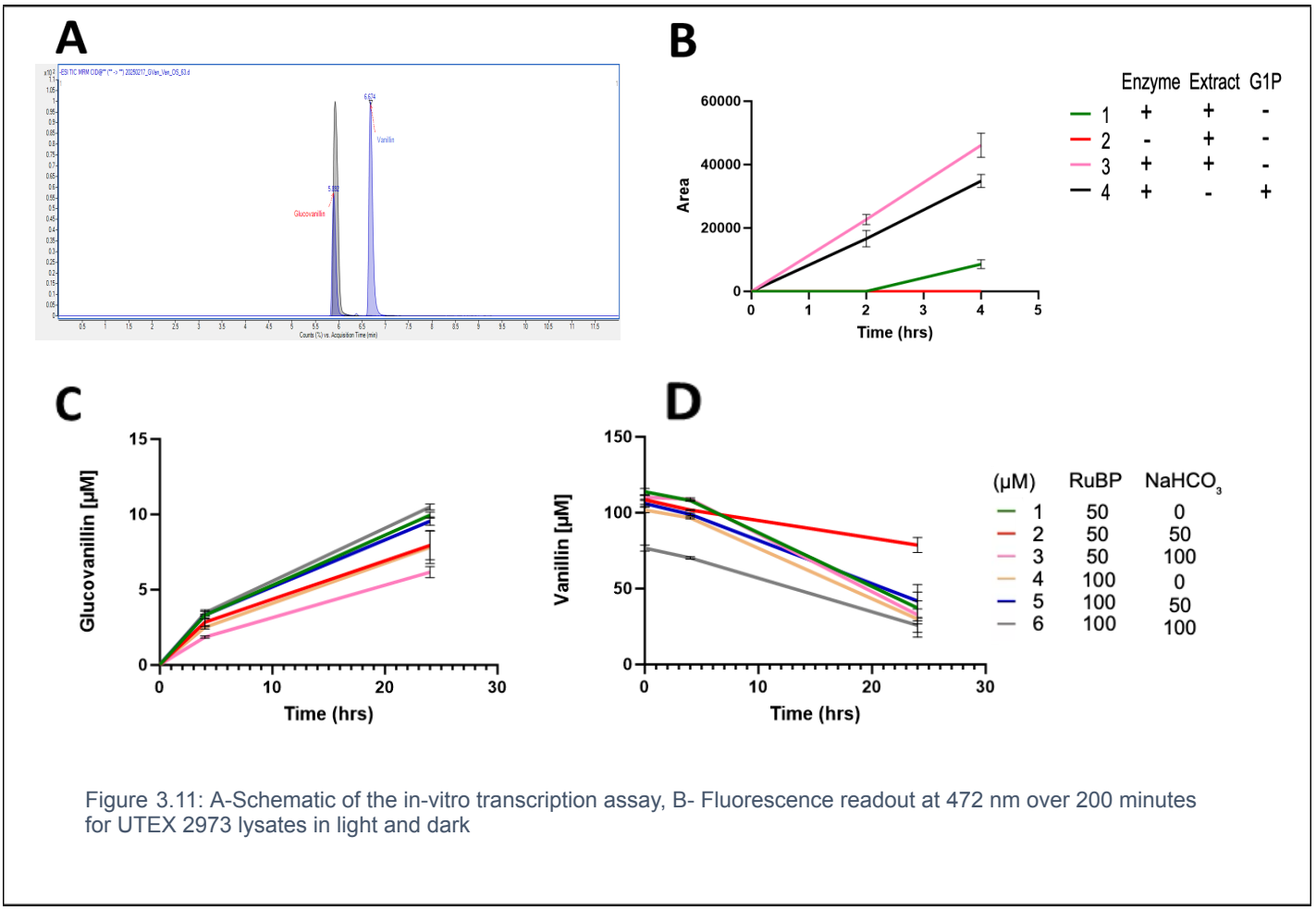

Figure 3.11: A-Schematic of the in-vitro transcription assay, B- Fluorescence readout at 472 nm over 200 minutes for UTEX 2973 lysates in light and dark

4.2 Light driven ATP synthesis

Being photoautotrophic, cyanobacteria have the ability to use atmospheric CO_2 and utilize solar energy to make their own food and energy for growth. To achieve this, cyanobacteria have photosystems and light harvesting complexes (LHCs) to capture and convert the energy of photons through a series of steps of electron transfer via redox chemistry that eventually generates a chemiosmotic gradient allowing for ADP to be phosphorylated to ATP, which can be then used to power various reactions and possibly used for cell-free protein synthesis (CFPS) in future. To validate whether the cell-free extracts are capable of producing ATP in a light dependent manner, three different experimental set-ups were used.

4.2.1 Transcription assay using fluorescent readout

The rationale behind this assay is to power transcription (using T7 RNA polymerase) of the 3WJdB gene (for Broccoli aptamer) with the production of light generated ATP. The aptamer binds to the fluorogenic dye DFHBI-1T and thereby stabilizes its fluorescent confirmation in which DFHBI-1T emits light in the green spectra upon excitation at 472 nm (Luo, Shanshan et al, 2023).

The fluorescence readout was identical for UTEX 2973 lysates at different OD_{750} in both light and dark conditions as shown in **Figure 3.12.B**. It suggests that the NTPs present in the cell-free extracts are driving the *in vitro* transcription of the Broccoli aptamer in the given time frame of the reaction. Due to the background signal, this assay was inconclusive.

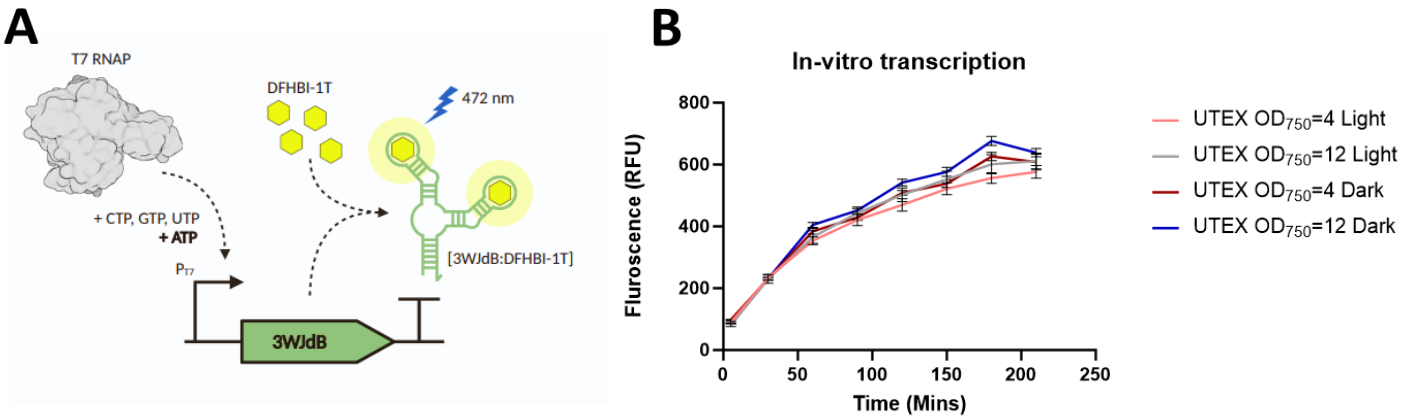

Figure 3.12: A-Schematic of the in-vitro transcription assay, B- Fluorescence readout at 472 nm over 200 minutes for UTEX 2973 lysates in light and dark

4.2.2 ATP bioluminescence assay

To quantitatively measure the differences in ATP generation in cell-free lysates exposed to both light and dark respectively, the principle of oxidation of luciferin to give a fluorescence readout at 595 nm.

Initially, large error bars were obtained, there seemed to be no coherent trend or increase in ATP production with time- **Figure 3.13 A.** Different time intervals and concentrations were tested, addition of antioxidants (Vitamin C, Superoxide dismutase-SOD and catalase), electron carriers like ferredoxin (crFdx from *Chlamydomonas reinhardtii,* and purified membranes were all tried out. An oscillating pattern emerged in many reaction sets, however the concentrations fluctuated and

there was no clear take-away from the various attempts of the assay. It was uncertain whether light dependent ATP production was active or all of the results were background levels of residual metabolism. It was also important to keep in mind that the Luciferase assay is not the most accurate method to determine light dependent energy production as ATP is very unstable and gets hydrolysed easily.

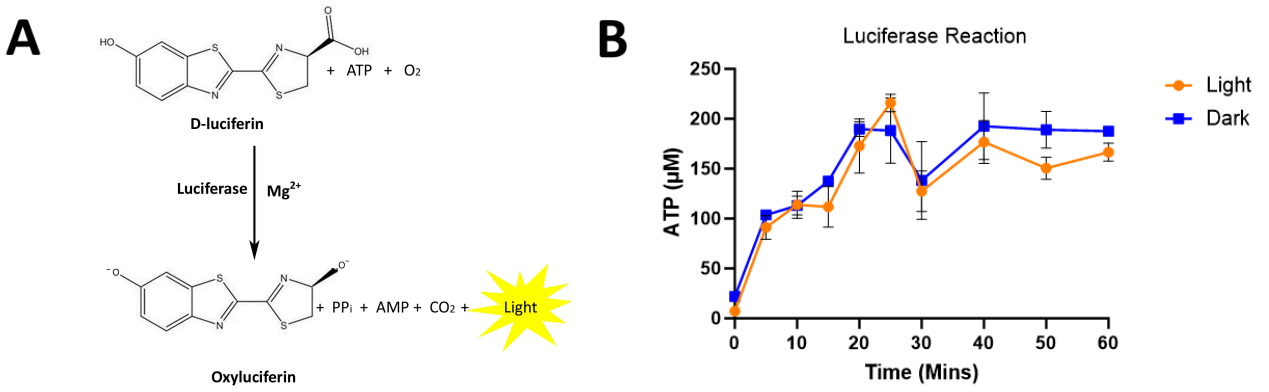

Figure 3.13: A-Schematic of Luciferase assay quantifying ATP, B- ATP (µM) quantified using standards for both light and dark conditions using purified membrane vesicles from UTEX 2973.

4.2.3 Hexokinase assay to measure accumulation of G6P

Given the unclear results of *in vitro* transcription and luciferase assay, it was necessary to try a different approach with a more stable product that could be more precisely measured using LC-MS for better resolution. Hexokinase is an enzyme that converts glucose to glucose-6-phosphate via phosphorylation and this reaction uses one ATP molecule. The objective of this assay is to observe a notable increase in the amount of glucose-6-phosphate over time in the samples that are exposed to light as compared to samples kept in darkness, due to light dependent ATP generation.

Preliminary assays were showing little accumulation of G6P over 3 hours which suggested that the time frames we were looking at from the previous assay were not the most optimal as light dependent ATP generation needs a few hours to stabilize and show differences. First objective was to test the assay with both lysate and concentrated membrane vesicles. It was observed that lysates are better as they accumulate G6P while vesicles do not. The reason might be because vesicles lack or have broken machinery required for light harvesting. It was also important to be sure that the ATP generated is only because of functional photosystems from the

lysates and not due to interconversion of adenosine phosphates using adenosine kinase (ADK) enzymes. This was tested by adding varied concentrations (100 and 500 µM) of ADK inhibitor (DMAPP) enzymes. Total inhibition of ATP was seen at 500 µM ADKi while 100 µM removed background conversion to ATP (**Figure 3.14. A and B**). There was a clear difference in accumulation of G6P in light and dark conditions as seen in **Figure 3.14.B**. We also see that when exposed to higher light (135 µE) as compared to low (25 µE), the UTEX 2973 lysates produce more ATP (related to G6P concentrations) suggesting light dependent ATP production. The concentrations seem to be in a range where the lysates can potentially power CFPS. As observed from **Figure 3.14. C and D**, high amounts of G6P was detected over 24 hours and it increases further over 48 hours, however the rate slows down. UTEX 2973 and PCC 7942 exposed to no light (dark), 30 µE, 75 µE and 300 µE of light over 48 hours, where UTEX 2973 produced almost double the amount of G6P at same concentration, which can be explained from the strains tolerance to higher light intensities as compared to PCC 7942 which is light sensitive. We also see that lower light intensities (30 and 75 µE) do better than 300 µE, due to photobleaching at high light (reaction lysates become clear by 24 hours indicating bleaching and generation of potential ROS).

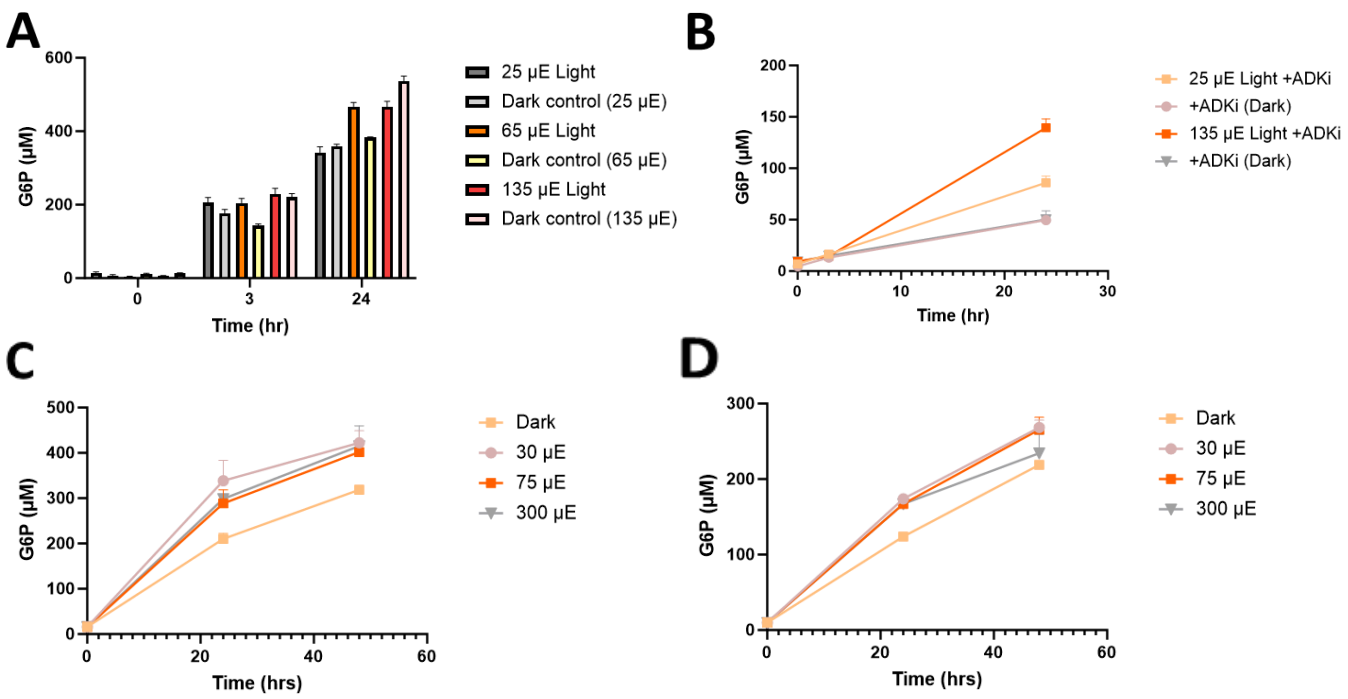

Figure 3.14: All the figures here show accumulation of glucose-6-phosphate (G6P). A- Tests the difference between dark and different light intensities without addition of ADKi. B- Differences between dark and light intensities (when ADKi added) over 3 and 24 hours show a correlation with increasing light. C- Accumulation of G6P in UTEX 2973 lysates with 100 µM ADKi. D- Accumulation of G6P in PCC 7942 extracts with 100 µM ADKi.

5. Carboxysome purification

The final objective of the project is to optimize and improve carbon fixation ability of cyanobacterial lysate systems for *in vitro* engineering. This can be achieved by heterologous addition of proteins, enzymes, pigments or even purified carboxysomes. As PCC 7942 is one of the main strains of the study, purification of their β-carboxysomes was attempted. The purification protocol is adapted from Sun et al., 2022 which was for α-carboxysomes. Using sucrose gradients, the lysates are centrifuged as described in chapter 3, section 6. The gel shown in **Figure 3.15.B** is an attempt to optimize the protocol to obtain the highest concentrations of purified carboxysomes (detected by the band at 55 kDa for large subunit of rubisco- rbcL).

As an attempt to get cleaner bands, an additional 1% TritonX treatment was done for 1 hour at 30°C to the 40/60 interface (wells B-E in **Figure 3.15.B**). These purified carboxysomes can later be used for *in vitro* assay to check and quantify for enhanced rates of carbon fixation in the cell-free extracts.

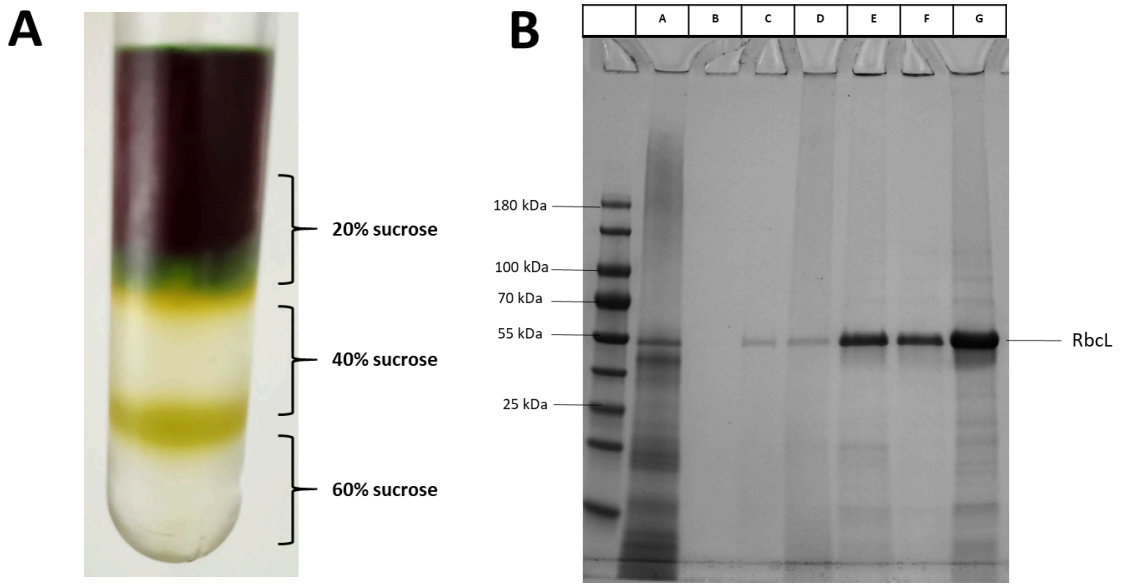

Figure 3.15: A- Representative image of one of the sucrose gradients with the different layers and interfaces. B- SDS PAGE gel of purification of carboxysomes from different fractions of the sucrose gradient. The wells are A- Digested lysate from 7942, B- supernatant from 40/60 interface, C- supernatant from 20/40 interface, D-pellet from 40/60 interface, E- pellet from 20/40 interface, F- 40/60 carboxysome interface without extra Triton X treatment, G- pellet from prep without extra TritonX treatment.

Conclusion

The main four cyanobacterial strains focused in the study- PCC 7942, UTEX 2973, PCC 7002 and PCC 11901 have been all grown in three different CO2 conditions- ambient, 0.5% and 3% CO_2 in low and high light. The growth rates have been measured and compared, the cultures were all quenched and extracted for compositional analysis using metabolomics and proteomics, and are under analytical measurement. The results discussed in this thesis is a small subset of the entire dataset, however these were crucial in understanding and evaluating the conditions, as well as optimising the analysis pipeline. The growth trends help us evaluate the biomass accumulation capabilities, in which PCC 7002 and PCC 11901 clearly have an advantage. It emerged that CO_2 concentrations played a larger role in bulk comparisons. Diving deeper into the metabolic and proteomic landscape, we saw the same trend, of CO_2 concentration (both increase or decrease) being more profound than changes in light intensity, especially with regards to central carbon metabolites and proteins associated with carbon capture and fixation. Light intensity changes resulted mostly in regulation of stress response proteins. This serves as an important takeaway of the study that our selected strains can thrive even under lower light without growth trade-offs which is helpful for photobioreactor design. Usually light is one of the limiting factors for scalability of photobioreactors; and metabolite profiling helps in optimising the growth conditions and reducing operational costs. All four strains mentioned are robust and have immense potential to serve as important biotechnologically relevant chassis for sustainable biosynthesis of industrially relevant metabolites or precursors. Understanding the metabolic flux and resource allocation of the protein landscape will guide in strain selection; and serve as frameworks to develop metabolic flux models and genetic modification tools as well. This thesis is not only useful from an industrial point of view but also gives insights into the biochemistry of one of the most important organisms on this planet. With the emerging popularity of cell-free systems, it was interesting to try to build a cyanobacterial lysate-based system which can be used to study and engineer photosynthesis. Initial assays with fluorescent and bioluminescent readouts failed to provide any significant takeaways for light derived ATP production. Hexokinase assay was a novel way to measure glucose-6-phosphate as a proxy of ATP

generation that finally gave us a clear correlation between light intensity and glucose-6-phosphate accumulation over 24-48 hours. The results enlightened us of the time scale for light powered ATP generation, paving the way for cell-free protein synthesis. To measure CBB cycle activity, initial ^{13}C labelling assays didn't show incorporation of heavy carbon in the intermediates and the follow-up experiment was gassing in heavy CO_2 making it an expensive set-up. Following the cell-free path, the cyanobacterial lysates were used to test if the carbon fixation machinery was active by measuring the concentrations of the first product of CBB cycle, 3-phosphoglycerate. Over a testing period of 2 hours, 3PG concentrations increased when the extracts were pre-incubated with bicarbonate. However, 3PG being a metabolite with rapid turnover rates for various reactions, a cascade of enzymatic steps to convert it into a detectable non-metabolized form (providing a sink) with adding heterologously expressed and purified enzymes was conceptualized and tested. The final product of the assay was glucovanillin which is not naturally produced by cyanobacteria was shown to be produced when all enzymes for the reaction scheme were added to the lysates. A maximum of 10% conversion rate over 24 hours was observed suggesting further optimization of assay for better read-out. The various *in vitro* assays developed can serve as a quick platform to compare and measure photosynthetic capabilities with respect to light harvesting and carbon fixation of a large number of cyanobacterial lysates at once, saving time and effort to study the same *in vivo* using genetic modifications. The goal was to gain a systems-level overview about the physiological state of cyanobacterial extracts and explore their potential use for *in vitro* applications.

However, there are some limitations of the study that are important to keep in mind while moving forward. The cultures were all grown in small flasks which might not be the most uniform and suitable system due to self-shading of cyanobacterial cultures. As the cultures are green, after reaching a certain density, there is a differential light penetration. This could lead to non-uniformities in -omics data. The self-shading phenomenon also poses a challenge to scale up photosynthetic cultures in photobioreactors. There was a lot of optimisation required at every step of each protocol which was time consuming and it is possible that it is still not in the optimal condition, leading to inaccuracies and waste of resources. E.g. The protocol to extract the whole proteome of cyanobacteria is more difficult because of the abundant membrane components.

References

Ananyev, Gennady, Colin Gates, Aaron Kaplan, and G. Charles Dismukes. 2017. “Photosystem II-Cyclic Electron Flow Powers Exceptional Photoprotection and Record Growth in the Microalga *Chlorella Ohadii*.” *Biochimica et Biophysica Acta (BBA) - Bioenergetics* 1858(11): 873–83.

Atkinson, Nicky, Doreen Feike, Luke C. M. Mackinder, Moritz T. Meyer, Howard Griffiths, Martin C. Jonikas, Alison M. Smith, and Alistair J. McCormick. 2016. “Introducing an Algal Carbon-Concentrating Mechanism into Higher Plants: Location and Incorporation of Key Components.” *Plant Biotechnology Journal* 14(5): 1302–15.

Bar-Even, Arren, Elad Noor, Yonatan Savir, Wolfram Liebermeister, Dan Davidi, Dan S. Tawfik, and Ron Milo. 2011. “The Moderately Efficient Enzyme: Evolutionary and Physicochemical Trends Shaping Enzyme Parameters.” *Biochemistry* 50(21): 4402–10.

Bekker, A., H. D. Holland, P.-L. Wang, D. Rumble, H. J. Stein, J. L. Hannah, L. L. Coetzee, and N. J. Beukes. 2004. “Dating the Rise of Atmospheric Oxygen.” *Nature* 427(6970): 117–20.

Blank, C. E., and P. Sánchez-Baracaldo. 2010. “Timing of Morphological and Ecological Innovations in the Cyanobacteria – a Key to Understanding the Rise in Atmospheric Oxygen.” *Geobiology* 8(1): 1–23.

Bocchi, Stefano, and Antonino Malgioglio. 2010. “Azolla-Anabaena as a Biofertilizer for Rice Paddy Fields in the Po Valley, a Temperate Rice Area in Northern Italy.” *International Journal of Agronomy* 2010(1): 152158.

Bonacci, Walter, Poh K. Teng, Bruno Afonso, Henrike Niederholtmeyer, Patricia Grob, Pamela A. Silver, and David F. Savage. 2012. “Modularity of a Carbon-Fixing Protein Organelle.” *Proceedings of the National Academy of Sciences* 109(2): 478–83.

Bracher, Andreas, Amanda Starling-Windhof, F. Ulrich Hartl, and Manajit Hayer-Hartl. 2011. “Crystal Structure of a Chaperone-Bound Assembly Intermediate of Form I Rubisco.” *Nature Structural & Molecular Biology* 18(8): 875–80.

Brasier, Martin D., Owen R. Green, Andrew P. Jephcoat, Annette K. Kleppe, Martin J. Van Kranendonk, John F. Lindsay, Andrew Steele, and Nathalie V. Grassineau. 2002. “Questioning the Evidence for Earth’s Oldest Fossils.” *Nature* 416(6876): 76–81.

Brocks, Jochen J., Graham A. Logan, Roger Buick, and Roger E. Summons. 1999. “Archean Molecular Fossils and the Early Rise of Eukaryotes.” *Science* 285(5430): 1033–36.

Cardona, Tanai, James W. Murray, and A. William Rutherford. 2015. “Origin and Evolution of Water Oxidation before the Last Common Ancestor of the Cyanobacteria.” *Molecular Biology and Evolution* 32(5): 1310–28.

Chazaux, Marie, Christo Schiphorst, Gioele Lazzari, and Stefano Caffarri. 2022. “Precise Estimation of Chlorophyll a, b and Carotenoid Content by Deconvolution of the Absorption Spectrum and New Simultaneous Equations for Chl Determination.” *The Plant Journal* 109(6): 1630–48.

Chen, Guoxin, Yanni Li, Kaining Jin, Jiabei Gao, Suting Wu, Xuean Cui, Chuanzao Mao, et al. 2025. “Synthetic Photorespiratory Bypass Improves Rice Productivity by Enhancing Photosynthesis and Nitrogen Uptake.” *The Plant Cell* 37(1): koaf015.

Chen, Xi, Karoline Schreiber, Jens Appel, Alexander Makowka, Berit Fähnrich, Mayo Roettger, Mohammad R. Hajirezaei, et al. 2016. “The Entner–Doudoroff Pathway Is an Overlooked Glycolytic Route in Cyanobacteria and Plants.” *Proceedings of the National Academy of Sciences* 113(19): 5441–46.

Claassens, Nico J., Guillermo Bordanaba-Florit, Charles A. R. Cotton, Alberto De Maria, Max Finger-Bou, Lukas Friedeheim, Natalia Giner-Laguarda, et al. 2020. “Replacing the Calvin Cycle with the Reductive Glycine Pathway in *Cupriavidus Necator*.” *Metabolic Engineering* 62: 30–41.

Davidi, Dan, Melina Shamshoum, Zhijun Guo, Yinon M Bar‐On, Noam Prywes, Aia Oz, Jagoda Jablonska, et al. 2020. “Highly Active Rubiscos Discovered by Systematic Interrogation of Natural Sequence Diversity.” *The EMBO Journal* 39(18): e104081.

Demoulin, Catherine F., Yannick J. Lara, Luc Cornet, Camille François, Denis Baurain, Annick Wilmotte, and Emmanuelle J. Javaux. 2019. “Cyanobacteria

Evolution: Insight from the Fossil Record." *Free Radical Biology and Medicine* 140: 206–23.

Dienst, Dennis, Julian Wichmann, Oliver Mantovani, João S. Rodrigues, and Pia Lindberg. 2020. "High Density Cultivation for Efficient Sesquiterpenoid Biosynthesis in Synechocystis Sp. PCC 6803." *Scientific Reports* 10(1): 5932.

Du, Wei, Luna L. Meister, Tobias van Grinsven, and Filipe Branco dos Santos. 2025. "Efficient Multiplex Genome Editing of the Cyanobacterium Synechocystis Sp. PCC6803 via CRISPR-Cas12a." *Biotechnology and Bioengineering* 122(3): 736–43.

Falkowski, Paul. 2012. "Ocean Science: The Power of Plankton." *Nature* 483(7387): S17–20.

Falkowski, Paul G., Miriam E. Katz, Andrew H. Knoll, Antonietta Quigg, John A. Raven, Oscar Schofield, and F. J. R. Taylor. 2004. "The Evolution of Modern Eukaryotic Phytoplankton." *Science* 305(5682): 354–60.

Flamholz, Avi I, Eli Dugan, Cecilia Blikstad, Shmuel Gleizer, Roee Ben-Nissan, Shira Amram, Niv Antonovsky, et al. 2020. "Functional Reconstitution of a Bacterial CO2 Concentrating Mechanism in Escherichia Coli" eds. Manajit Hayer-Hartl, Christian S Hardtke, and Martin Casimir Jonikas. *eLife* 9: e59882.

Flamholz, Avi I., Noam Prywes, Uri Moran, Dan Davidi, Yinon M. Bar-On, Luke M. Oltrogge, Rui Alves, David Savage, and Ron Milo. 2019. "Revisiting Trade-Offs between Rubisco Kinetic Parameters." *Biochemistry* 58(31): 3365–76.

Flügel, Franziska, Stefan Timm, Stéphanie Arrivault, Alexandra Florian, Mark Stitt, Alisdair R. Fernie, and Hermann Bauwe. 2017. "The Photorespiratory Metabolite 2-Phosphoglycolate Regulates Photosynthesis and Starch Accumulation in Arabidopsis." *The Plant Cell* 29(10): 2537–51.

Holland, Heinrich D. 2006. "The Oxygenation of the Atmosphere and Oceans." *Philosophical Transactions of the Royal Society B: Biological Sciences* 361(1470): 903–15.

Hood, Rachel D., Sean A. Higgins, Avi Flamholz, Robert J. Nichols, and David F. Savage. 2016. "The Stringent Response Regulates Adaptation to Darkness

in the Cyanobacterium Synechococcus Elongatus." *Proceedings of the National Academy of Sciences* 113(33): E4867–76.

Hudson, Elton P. 2024. "The Calvin Benson Cycle in Bacteria: New Insights from Systems Biology." *Seminars in Cell & Developmental Biology* 155: 71–83.

Hunt, Andrew C., Blake J. Rasor, Kosuke Seki, Holly M. Ekas, Katherine F. Warfel, Ashty S. Karim, and Michael C. Jewett. 2025. "Cell-Free Gene Expression: Methods and Applications." *Chemical Reviews* 125(1): 91–149.

Jahn, Michael, Vital Vialas, Jan Karlsen, Gianluca Maddalo, Fredrik Edfors, Björn Forsström, Mathias Uhlén, Lukas Käll, and Elton P. Hudson. 2018. "Growth of Cyanobacteria Is Constrained by the Abundance of Light and Carbon Assimilation Proteins." *Cell Reports* 25(2): 478-486.e8.

Jester, Benjamin W., Hui Zhao, Mesfin Gewe, Thomas Adame, Lisa Perruzza, David T. Bolick, Jan Agosti, et al. 2022. "Development of Spirulina for the Manufacture and Oral Delivery of Protein Therapeutics." *Nature Biotechnology* 40(6): 956–64.

Kachel, Benjamin, and Matthias Mack. 2020. "Engineering of *Synechococcus* Sp. Strain PCC 7002 for the Photoautotrophic Production of Light-Sensitive Riboflavin (Vitamin B2)." *Metabolic Engineering* 62: 275–86.

Kaneko, Takakazu, Shusei Sato, Hirokazu Kotani, Ayako Tanaka, Erika Asamizu, Yasukazu Nakamura, Nobuyuki Miyajima, et al. 1996. "Sequence Analysis of the Genome of the Unicellular Cyanobacterium Synechocystis Sp. Strain PCC6803. II. Sequence Determination of the Entire Genome and Assignment of Potential Protein-Coding Regions." *DNA Research* 3(3): 109–36.

Kinney, James N., Seth D. Axen, and Cheryl A. Kerfeld. 2011. "Comparative Analysis of Carboxysome Shell Proteins." *Photosynthesis Research* 109(1): 21–32.

Knoop, Henning, Yvonne Zilliges, Wolfgang Lockau, and Ralf Steuer. 2010. "The Metabolic Network of Synechocystis Sp. PCC 6803: Systemic Properties of Autotrophic Growth." *Plant Physiology* 154(1): 410–22.

Küffner, A. M., B. Pommerenke, L. Kley, J. Z. Y. Ng, S. Prinz, M. Tinzl-Zechner, P. Claus, et al. 2024. "Bottom-up Reconstruction of Minimal Pyrenoids Provides Insights into the Evolution and Mechanisms of Carbon Concentration by EPYC1 Proteins." : 2024.06.28.601168.

Kugler, Amit, and Karin Stensjö. 2023. “Optimal Energy and Redox Metabolism in the Cyanobacterium Synechocystis Sp. PCC 6803.” *npj Systems Biology and Applications* 9(1): 1–13.

Li, Qiong, Yong-Liang Jiang, Ling-Yun Xia, Yuxing Chen, and Cong-Zhao Zhou. 2022. “Structural Insights into Cyanobacterial RuBisCO Assembly Coordinated by Two Chaperones Raf1 and RbcX.” *Cell Discovery* 8(1): 1–11.

Liu, Cuimin, Anna L. Young, Amanda Starling-Windhof, Andreas Bracher, Sandra Saschenbrecker, Bharathi Vasudeva Rao, Karnam Vasudeva Rao, et al. 2010. “Coupled Chaperone Action in Folding and Assembly of Hexadecameric Rubisco.” *Nature* 463(7278): 197–202.

Liu, Haijun, Hao Zhang, Dariusz M. Niedzwiedzki, Mindy Prado, Guannan He, Michael L. Gross, and Robert E. Blankenship. 2013. “Phycobilisomes Supply Excitations to Both Photosystems in a Megacomplex in Cyanobacteria.” *Science* 342(6162): 1104–7.

Lucius, Stefan, Alexander Makowka, Klaudia Michl, Kirstin Gutekunst, and Martin Hagemann. 2021. “The Entner-Doudoroff Pathway Contributes to Glycogen Breakdown During High to Low CO2 Shifts in the Cyanobacterium Synechocystis Sp. PCC 6803.” *Frontiers in Plant Science* 12.

Ludwig, Marcus, and Donald A. Bryant. 2011. “Transcription Profiling of the Model Cyanobacterium Synechococcus Sp. Strain PCC 7002 by Next-Gen (SOLiD™) Sequencing of cDNA.” *Frontiers in Microbiology* 2.

Ludwig, Marcus, and Donald A. Bryant. 2012. “Synechococcus Sp. Strain PCC 7002 Transcriptome: Acclimation to Temperature, Salinity, Oxidative Stress, and Mixotrophic Growth Conditions.” *Frontiers in Microbiology* 3.

Luo, Shanshan, David Adam, Simone Giaveri, Sebastian Barthel, Stefano Cestellos-Blanco, Dominik Hege, Nicole Paczia, et al. 2023. “ATP Production from Electricity with a New-to-Nature Electrobiological Module.” *Joule* 7(8): 1745–58.

Lyons, Timothy W., Christopher T. Reinhard, and Noah J. Planavsky. 2014. “The Rise of Oxygen in Earth’s Early Ocean and Atmosphere.” *Nature* 506(7488): 307–15.

Miller, Tarryn E., Thomas Beneyton, Thomas Schwander, Christoph Diehl, Mathias Girault, Richard McLean, Tanguy Chotel, et al. 2020.

“Light-Powered CO2 Fixation in a Chloroplast Mimic with Natural and Synthetic Parts.” *Science* 368(6491): 649–54.

Monshupanee, Tanakarn, Chayanee Chairattanawat, and Aran Incharoensakdi. 2019. “Disruption of Cyanobacterial γ-Aminobutyric Acid Shunt Pathway Reduces Metabolites Levels in Tricarboxylic Acid Cycle, but Enhances Pyruvate and Poly(3-Hydroxybutyrate) Accumulation.” *Scientific Reports* 9(1): 8184.

Mulkidjanian, Armen Y., Eugene V. Koonin, Kira S. Makarova, Sergey L. Mekhedov, Alexander Sorokin, Yuri I. Wolf, Alexis Dufresne, et al. 2006. “The Cyanobacterial Genome Core and the Origin of Photosynthesis.” *Proceedings of the National Academy of Sciences* 103(35): 13126–31.

Muro-Pastor, Alicia M., Ana Valladares, Enrique Flores, and Antonia Herrero. 1999. “The hetC Gene Is a Direct Target of the NtcA Transcriptional Regulator in Cyanobacterial Heterocyst Development.” *Journal of Bacteriology* 181(21): 6664–69.

Neidhardt, Frederick C., and Boris Magasanik. 1960. “Studies on the Role of Ribonucleic Acid in the Growth of Bacteria.” *Biochimica et Biophysica Acta* 42: 99–116.

Nikkanen, Lauri, Daniel Solymosi, Martina Jokel, and Yagut Allahverdiyeva. 2021. “Regulatory Electron Transport Pathways of Photosynthesis in Cyanobacteria and Microalgae: Recent Advances and Biotechnological Prospects.” *Physiologia Plantarum* 173(2): 514–25.

Och, Lawrence M., and Graham A. Shields-Zhou. 2012. “The Neoproterozoic Oxygenation Event: Environmental Perturbations and Biogeochemical Cycling.” *Earth-Science Reviews* 110(1): 26–57.

Pagels, Fernando, A. Catarina Guedes, Helena M. Amaro, Anake Kijjoa, and Vitor Vasconcelos. 2019. “Phycobiliproteins from Cyanobacteria: Chemistry and Biotechnological Applications.” *Biotechnology Advances* 37(3): 422–43.

Pan, Xiaowei, Duanfang Cao, Fen Xie, Fang Xu, Xiaodong Su, Hualing Mi, Xinzheng Zhang, and Mei Li. 2020. “Structural Basis for Electron Transport Mechanism of Complex I-like Photosynthetic NAD(P)H Dehydrogenase.” *Nature Communications* 11(1): 610.

Ponce-Toledo, Rafael I., Philippe Deschamps, Purificación López-García, Yvan Zivanovic, Karim Benzerara, and David Moreira. 2017. “An Early-Branching

Freshwater Cyanobacterium at the Origin of Plastids.” *Current Biology* 27(3): 386–91.

Porra, Robert J. 2002. “The Chequered History of the Development and Use of Simultaneous Equations for the Accurate Determination of Chlorophylls a and b.” *Photosynthesis Research* 73(1): 149–56.

Price, G. Dean, Murray R. Badger, Fiona J. Woodger, and Ben M. Long. 2008. “Advances in Understanding the Cyanobacterial CO2-Concentrating-Mechanism (CCM): Functional Components, Ci Transporters, Diversity, Genetic Regulation and Prospects for Engineering into Plants.” *Journal of Experimental Botany* 59(7): 1441–61.

Rasmussen, Birger, Ian R. Fletcher, Jochen J. Brocks, and Matt R. Kilburn. 2008. “Reassessing the First Appearance of Eukaryotes and Cyanobacteria.” *Nature* 455(7216): 1101–4.

Rippka, Rosmarie, Josette Deruelles, John B. Waterbury, Michael Herdman, and Roger Y. Stanier. 1979. “Generic Assignments, Strain Histories and Properties of Pure Cultures of Cyanobacteria.” *Microbiology* 111(1): 1–61.

Roell, Marc-Sven, Lennart Schada von Borzyskowski, Philipp Westhoff, Anastasija Plett, Nicole Paczia, Peter Claus, Urte Schlueter, Tobias J. Erb, and Andreas P.M. Weber. 2021. “A Synthetic C4 Shuttle via the β-Hydroxyaspartate Cycle in C3 Plants.” *Proceedings of the National Academy of Sciences* 118(21): e2022307118.

Sánchez-Baracaldo, Patricia, and Tanai Cardona. 2020. “On the Origin of Oxygenic Photosynthesis and Cyanobacteria.” *New Phytologist* 225(4): 1440–46.

Sánchez-Baracaldo, Patricia, John A. Raven, Davide Pisani, and Andrew H. Knoll. 2017. “Early Photosynthetic Eukaryotes Inhabited Low-Salinity Habitats.” *Proceedings of the National Academy of Sciences* 114(37): E7737–45.

Saschenbrecker, Sandra, Andreas Bracher, Karnam Vasudeva Rao, Bharathi Vasudeva Rao, F. Ulrich Hartl, and Manajit Hayer-Hartl. 2007. “Structure and Function of RbcX, an Assembly Chaperone for Hexadecameric Rubisco.” *Cell* 129(6): 1189–1200.

Sauer, Jörg, Ulrich Schreiber, Roland Schmid, Uwe Völker, and Karl Forchhammer. 2001. “Nitrogen Starvation-Induced Chlorosis

inSynechococcus PCC 7942. Low-Level Photosynthesis As a Mechanism of Long-Term Survival.” *Plant Physiology* 126(1): 233–43.

Schada von Borzyskowski, Lennart, Francesca Severi, Karen Krüger, Lucas Hermann, Alexandre Gilardet, Felix Sippel, Bianca Pommerenke, et al. 2019. “Marine Proteobacteria Metabolize Glycolate via the β-Hydroxyaspartate Cycle.” *Nature* 575(7783): 500–504.

Schirrmeister, Bettina E., Muriel Gugger, and Philip C. J. Donoghue. 2015. “Cyanobacteria and the Great Oxidation Event: Evidence from Genes and Fossils.” *Palaeontology* 58(5): 769–85.

Schirrmeister, Bettina E., Patricia Sanchez-Baracaldo, and David Wacey. 2016. “Cyanobacterial Evolution during the Precambrian.” *International Journal of Astrobiology* 15(3): 187–204.

Schmelling, Nicolas M., and Moritz Bross. 2024. “What Is Holding Back Cyanobacterial Research and Applications? A Survey of the Cyanobacterial Research Community.” *Nature Communications* 15(1): 6758.

Schwarz, Doreen, Anke Nodop, Jan Hüge, Stephanie Purfürst, Karl Forchhammer, Klaus-Peter Michel, Hermann Bauwe, Joachim Kopka, and Martin Hagemann. 2011. “Metabolic and Transcriptomic Phenotyping of Inorganic Carbon Acclimation in the Cyanobacterium Synechococcus Elongatus PCC 79421[W].” *Plant Physiology* 155(4): 1640–55.

Shih, Patrick M., Dongying Wu, Amel Latifi, Seth D. Axen, David P. Fewer, Emmanuel Talla, Alexandra Calteau, et al. 2013. “Improving the Coverage of the Cyanobacterial Phylum Using Diversity-Driven Genome Sequencing.” *Proceedings of the National Academy of Sciences* 110(3): 1053–58.

Shih, Patrick M., Jan Zarzycki, Krishna K. Niyogi, and Cheryl A. Kerfeld. 2014. “Introduction of a Synthetic CO2-Fixing Photorespiratory Bypass into a Cyanobacterium.” *Journal of Biological Chemistry* 289(14): 9493–9500.

So, Anthony K.-C., George S. Espie, Eric B. Williams, Jessup M. Shively, Sabine Heinhorst, and Gordon C. Cannon. 2004. “A Novel Evolutionary Lineage of Carbonic Anhydrase (ε Class) Is a Component of the Carboxysome Shell.” *Journal of Bacteriology* 186(3): 623–30.

Sun, Yaqi, Victoria M. Harman, James R. Johnson, Philip J. Brownridge, Taiyu Chen, Gregory F. Dykes, Yongjun Lin, Robert J. Beynon, and Lu-Ning Liu.

2022. “Decoding the Absolute Stoichiometric Composition and Structural Plasticity of α-Carboxysomes.” *mBio* 13(2): e03629-21.

Sun, Yaqi, Yuewen Sheng, Tao Ni, Xingwu Ge, Joscelyn Sarsby, Philip J Brownridge, Kang Li, et al. 2025. “Rubisco Packaging and Stoichiometric Composition of the Native β-Carboxysome in Synechococcus Elongatus PCC7942.” *Plant Physiology* 197(1): kiae665.

Tabita, F. Robert, Sriram Satagopan, Thomas E. Hanson, Nathan E. Kreel, and Stephanie S. Scott. 2008. “Distinct Form I, II, III, and IV Rubisco Proteins from the Three Kingdoms of Life Provide Clues about Rubisco Evolution and Structure/Function Relationships.” *Journal of Experimental Botany* 59(7): 1515–24.

Tan, Xiaoming, Shengwei Hou, Kuo Song, Jens Georg, Stephan Klähn, Xuefeng Lu, and Wolfgang R. Hess. 2018. “The Primary Transcriptome of the Fast-Growing Cyanobacterium Synechococcus Elongatus UTEX 2973.” *Biotechnology for Biofuels* 11(1): 218.

Tanaka, Shiho, Cheryl A. Kerfeld, Michael R. Sawaya, Fei Cai, Sabine Heinhorst, Gordon C. Cannon, and Todd O. Yeates. 2008. “Atomic-Level Models of the Bacterial Carboxysome Shell.” *Science* 319(5866): 1083–86.

Ungerer, Justin, Kristen E. Wendt, John I. Hendry, Costas D. Maranas, and Himadri B. Pakrasi. 2018. “Comparative Genomics Reveals the Molecular Determinants of Rapid Growth of the Cyanobacterium Synechococcus Elongatus UTEX 2973.” *Proceedings of the National Academy of Sciences* 115(50): E11761–70.

Wang, Peng, Jianxun Li, Tianpei Li, Kang Li, Pei Cing Ng, Saimeng Wang, Vincent Chriscoli, et al. 2024. “Molecular Principles of the Assembly and Construction of a Carboxysome Shell.” *Science Advances* 10(48): eadr4227.

Whitehead, Lynne, Benedict M. Long, G. Dean Price, and Murray R. Badger. 2014. “Comparing the in Vivo Function of α-Carboxysomes and β-Carboxysomes in Two Model Cyanobacteria1.” *Plant Physiology* 165(1): 398–411.

Włodarczyk, Artur, Tiago Toscano Selão, Birgitta Norling, and Peter J. Nixon. 2020. “Newly Discovered Synechococcus Sp. PCC 11901 Is a Robust Cyanobacterial Strain for High Biomass Production.” *Communications Biology* 3(1): 1–14.

Zarzycki, Jan, Volker Brecht, Michael Müller, and Georg Fuchs. 2009. “Identifying the Missing Steps of the Autotrophic 3-Hydroxypropionate CO2 Fixation Cycle in Chloroflexus Aurantiacus.” *Proceedings of the National Academy of Sciences* 106(50): 21317–22.

Zhang, Shanshan, Jiahui Sun, Dandan Feng, Huili Sun, Jinyu Cui, Xuexia Zeng, Yannan Wu, Guodong Luan, and Xuefeng Lu. 2023. “Unlocking the Potentials of Cyanobacterial Photosynthesis for Directly Converting Carbon Dioxide into Glucose.” *Nature Communications* 14(1): 3425.

Appendix

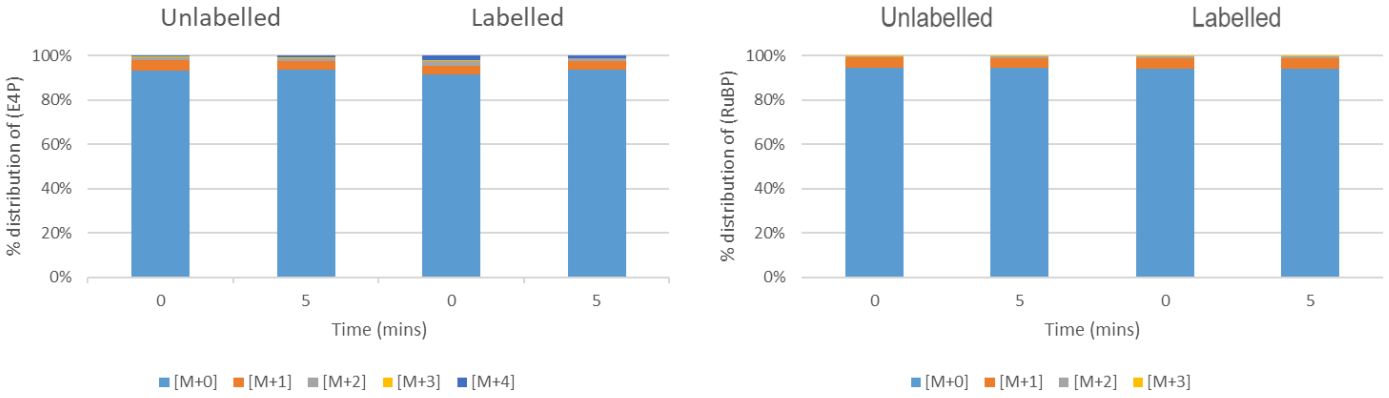

S1: ^{13}C labelling was done to check intermediates of CBB cycle. However, no incorporation of heavy carbon isotope was seen in any of the compounds (here erythrose-4-phosphate and ribulose-5-phosphate) in both 30 minute and 5 minute incubation.

Protein name	Source organism	Amino acid sequence	Molecular weight (kDa)	DNA length	Plasmid and selection marker	Insertion site
UDP-glucose transferase (UGT72E2)	*Escherichia coli*	MEKKIWSHPQFEKGGSGHITKPHAA MFSSPGMGHVIPVIELGKRLSANNG FHVTVFVLETDAASAQSKFLNSTGV DIVKLPSPDIYGLVDPDDHVVTKIGVI MRAAVPALRSKIAAMHQKPTALIVDL FGTDALCLAKEFNMLSYVFIPTNARF LGVSIYYPNLDKDIKEEHTVQRNPLAI PGCEPVRFEDTLDAYLVPDEPVYRD FVRHGLAYPKADGILVNTWEEMEPK SLKSLLNPKLLGRVARVPVYPIGPLC RPIQSSETDHPVLDWLNEQPNESVL YISFGSGGCLSAKQLTELAWGLEQS QQRFVWVVRPPVDGSCCSEYVSAN GGGTEDNTPEYLPEGFVSRTSDRG FVVPSWAPQAEILSHRAVGGFLTHC GWSSTLESVVGGVPMIAWPLFAEQN MNAALLSDELGIAVRLDDPKEDISRW KIEALVRKVMTEKEGEAMRRKVKKL RDSAEMSLSIDGGGLAHESLCRVTK ECQRFLERVVDLSRGA*	54.79	1494	pET29b with Kanamycin resistance	NdeI-XhoI
UTP-glucose-1-phosphate uridylyltransferase (UGPase)	*Arabidopsis thaliana*	MEKKIWSHPQFEKGGSGHITKPHAA MFSSPGMGHVIPVIELGKRLSANNG FHVTVFVLETDAASAQSKFLNSTGV DIVKLPSPDIYGLVDPDDHVVTKIGVI MRAAVPALRSKIAAMHQKPTALIVDL FGTDALCLAKEFNMLSYVFIPTNARF LGVSIYYPNLDKDIKEEHTVQRNPLAI PGCEPVRFEDTLDAYLVPDEPVYRD FVRHGLAYPKADGILVNTWEEMEPK SLKSLLNPKLLGRVARVPVYPIGPLC RPIQSSETDHPVLDWLNEQPNESVL YISFGSGGCLSAKQLTELAWGLEQS	34.47	957	pET29b with Kanamycin resistance	NdeI-XhoI

		QQRFVWVVRPPVDGSCCSEYVSAN GGGTEDNTPEYLPEGFVSRTSDRG FVVPSWAPQAEILSHRAVGGFLTHC GWSSTLESVVGGVPMIAWPLFAEQN MNAALLSDELGIAVRLDDPKEDISRW KIEALVRKVMTEKEGEAMRRKVKKL RDSAEMSLSIDGGGLAHESLCRVTK ECQRFLERVVDLSRGA*				
Phosphoglucomutase (PGM)	*Escherichia coli*	MEKKIWSHPQFEKGGSGKLQGVIFD LDGVITDTAHLHFQAWQQIAAEIGISI DAQFNESLKGISRDESLRRILQHGG KEGDFNSQERAQLAYRKNLLYVHSL RELTVNAVLPGIRSLLADLRAQQISV GLASVSLNAPTILAALELREFFTFCA DASQLKNSKPDPEIFLAACAGLGVP PQACIGIEDAQAGIDAINASGMRSVG IGAGLTGAQLLLPSTESLTWPRLSAF WQNV*	25.36	708	pET29b with Kanamycin resistance	NdeI-XhoI
Glucosyl-3-phosphoglycerate synthase (GPS1)	*Synechococcus elongatus PCC 7002*	MEKKIWSHPQFEKGGSGDFCQEFIT TIHDLDADLDYLEKRLMNLREICPMA LLIPSLYEELQRPALTRIKEHLKGCAYI QTINVCLHAETVEQYHHAVTFFRELP QKVNVIWTNGARIRGILEKLAQQNLN LLDYMGKGWAVWLGLGLASLDARAI ALHDADIVTFDRSLVAKLFYPIVEPEF GIAYNKAYYTRLGLETRAMNGRVVR LFVAPLLATLEDVLGRNAYLHYLKSY RYPLAGEFAMTADLALNLRVPCDWG IEVGLLAEVYRNVAPKRVAQVDLGFF DHKHKAVGNNPQEGLQKMCTEILSS ILRTLTETESIVFSEGHQIALQVKFRR VAQDMIRQYFVDATCNGIPYDRHRE EMTVESFEQIIPLAFDKYMHEPAVYRI PDWTRALAVMPDLREQLMAAVEAD MAEVQLEATMQRSEIPPLEMV*	49.69	1305	pET29b with Kanamycin resistance	NdeI-XhoI
Glucosyl-3-phosphoglycerate synthase (GPS2)	*Prochlorococcus marinus SS120*	MEKKIWSHPQFEKGGSGDFKQGLIT TIHEYGVTKDSLIDLRQGLKKRPTAILI PCLYEEFKRPALTQTRDVLSNLEGLN ELIIALSAQSADEVEEAKKFFSSMPF PVHVQWTNSPAVIELLQDQRKNGLD LIGTPGKGWAVWQGIGLATRESEVV ALFDADIRTFSTSYPARMLQPLLDQS HGISYVKAFYSRLSLESNALQGRATR LFVGPLLASLEQIFGQGAFLKYLEAF RYPLAGEFAFTRDLGMNLRIPCDWG LEIGLLSEVYRNVRLSRIAQVDLGIFD HKHKEVGKNPKEGLQRMCTEILSSV LRGLMEHQAETLTNSQISTLEVLYKR VGQDRVKQFGLDSAVNNIPYDRHEE ELSVQKFASILRPSIIQFLESPVTKQL PCWARVLSCENTLQNELAKAGLKKI P*	46.6	1245	pET29b with Kanamycin resistance	NdeI-XhoI

S2: Enzymes for sugar assay with their amino acid sequence, molecular weight in kDa, source organism, length of DNA fragment and vector

Spectrum Plot Report

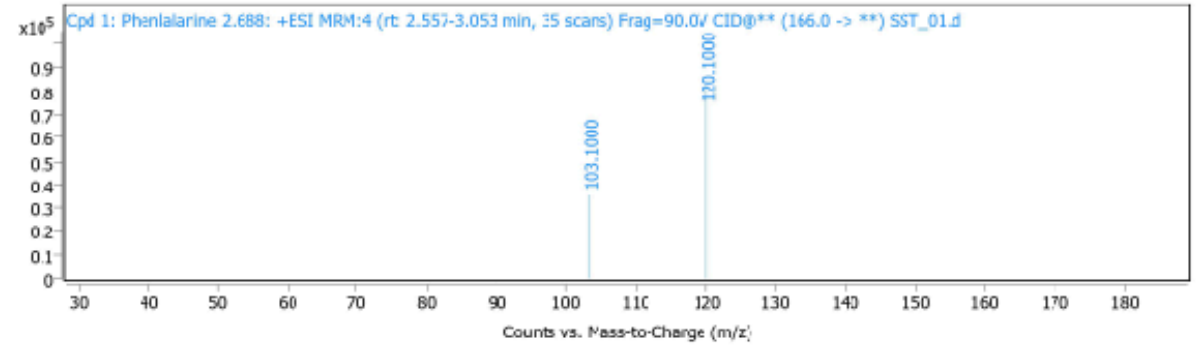

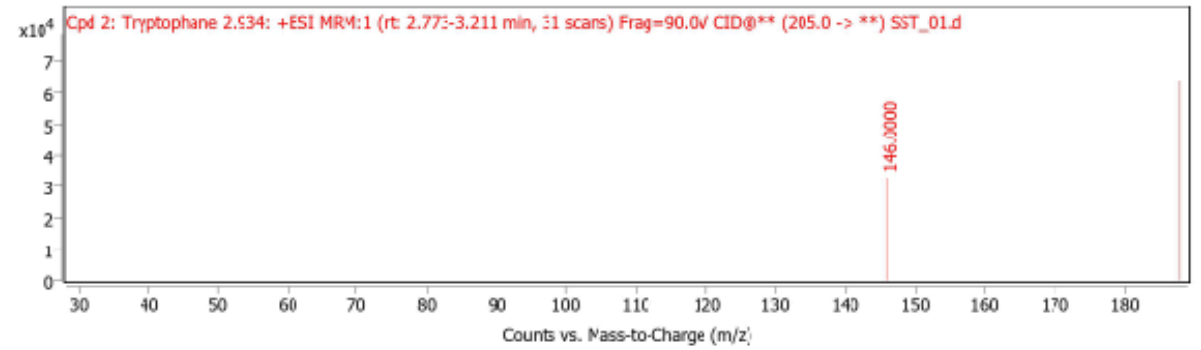

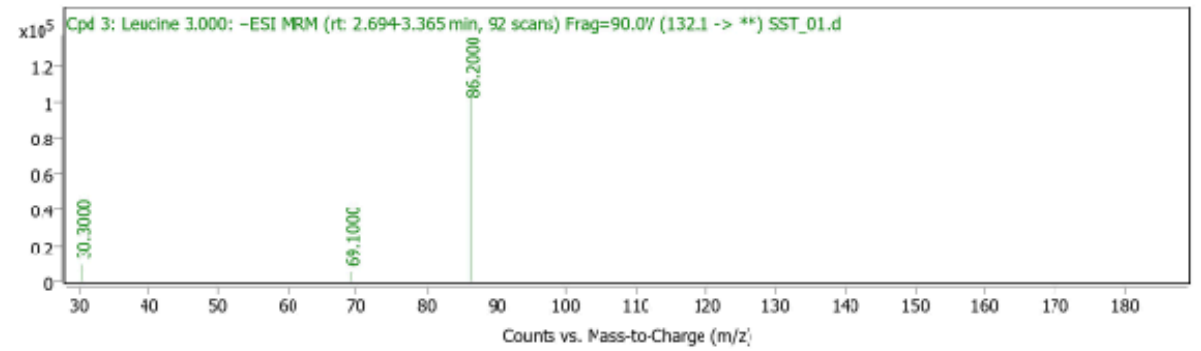

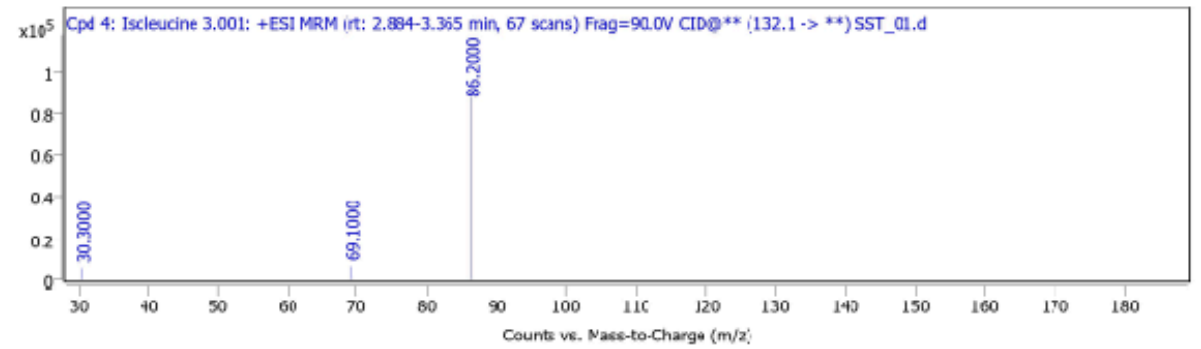

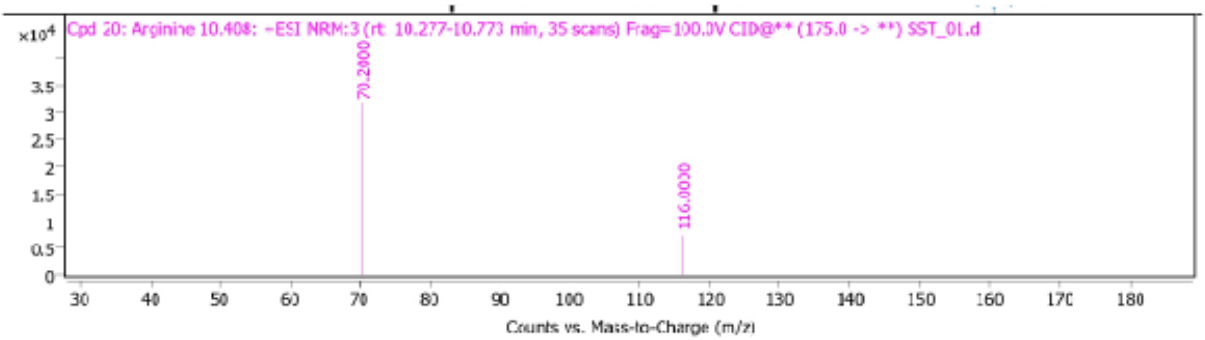

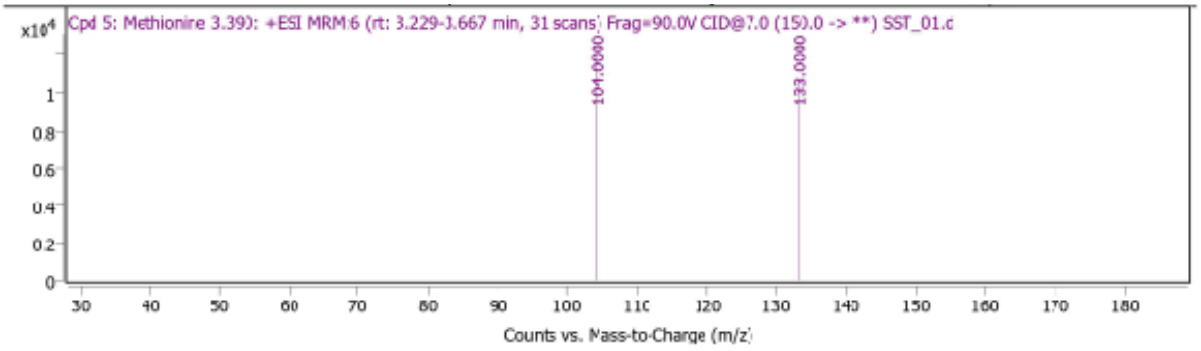
Cpd 5: Methionine 3.390: +ESI MRM:6 (rt: 3.229-3.667 min, 31 scans) Frag=90.0V CID@?.0 (150.0 -> **) SST_01.d
x10^4
104.0000
133.0000
Counts vs. Mass-to-Charge (m/z)

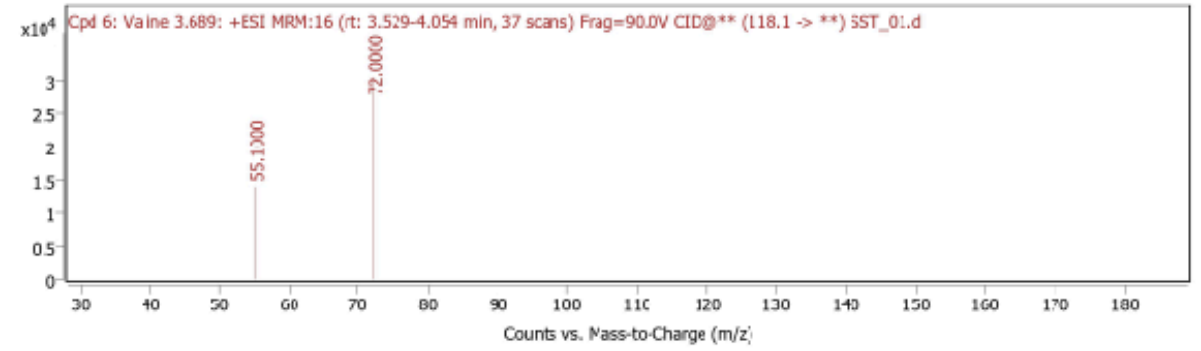
Cpd 6: Valine 3.689: +ESI MRM:16 (rt: 3.529-4.054 min, 37 scans) Frag=90.0V CID@** (118.1 -> **) SST_01.d
x10^4
72.0000
55.1000
Counts vs. Mass-to-Charge (m/z)

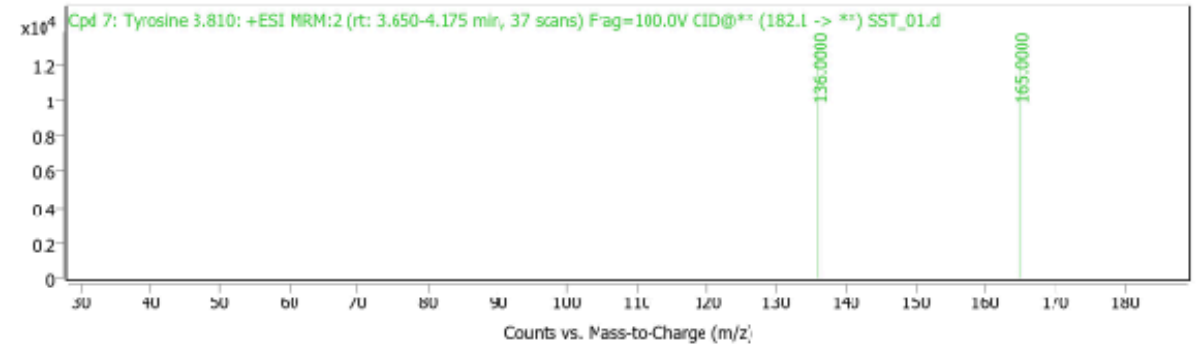
Cpd 7: Tyrosine 3.810: +ESI MRM:2 (rt: 3.650-4.175 min, 37 scans) Frag=100.0V CID@** (182.1 -> **) SST_01.d
x10^4
136.0000
165.0000
Counts vs. Mass-to-Charge (m/z)

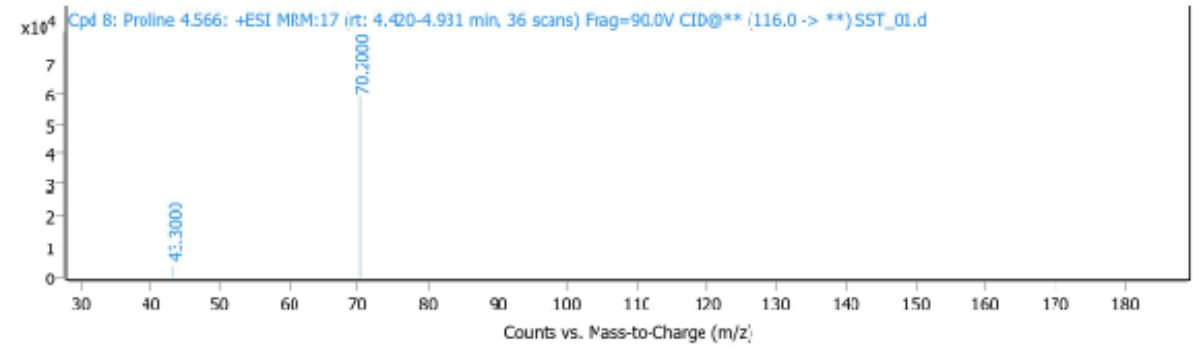
Cpd 8: Proline 4.566: +ESI MRM:17 (rt: 4.420-4.931 min, 36 scans) Frag=90.0V CID@** (116.0 -> **) SST_01.d
x10^4
70.2000
41.3000
Counts vs. Mass-to-Charge (m/z)

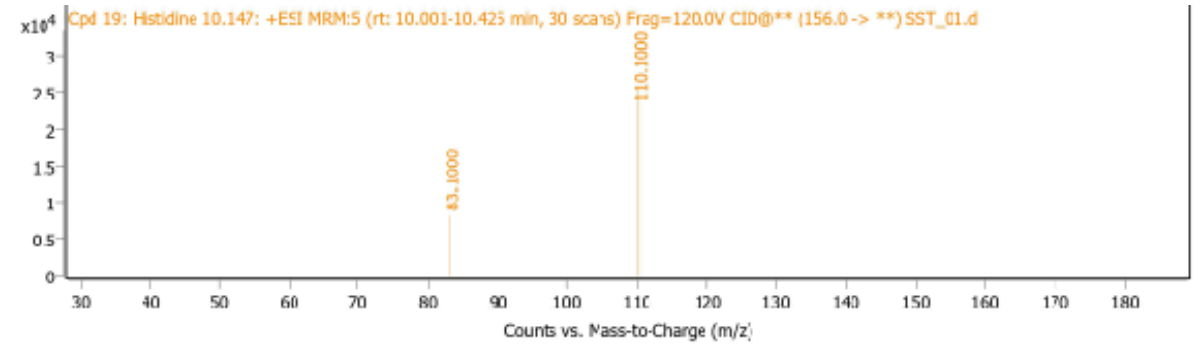
Cpd 19: Histidine 10.147: +ESI MRM:5 (rt: 10.001-10.425 min, 30 scans) Frag=120.0V CID@** (156.0 -> **) SST_01.d
x10^4
110.1000
83.1000
Counts vs. Mass-to-Charge (m/z)

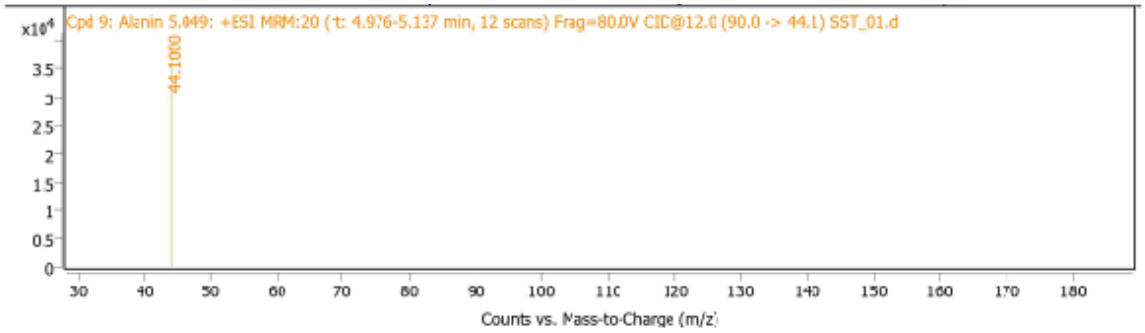
Cpd 9: Alanin 5.049: +ESI MRM:20 (rt: 4.976-5.137 min, 12 scans) Frag=80.0V CID@12.0 (90.0 -> 44.1) SST_01.d
x10^4
44.1000
Counts vs. Mass-to-Charge (m/z)

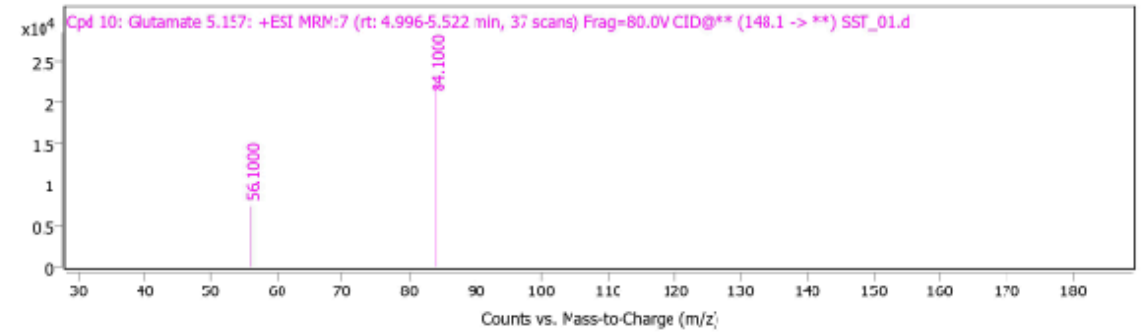
Cpd 10: Glutamate 5.157: +ESI MRM:7 (rt: 4.996-5.522 min, 37 scans) Frag=80.0V CID@** (148.1 -> **) SST_01.d
x10^4
84.1000
56.1000
Counts vs. Mass-to-Charge (m/z)

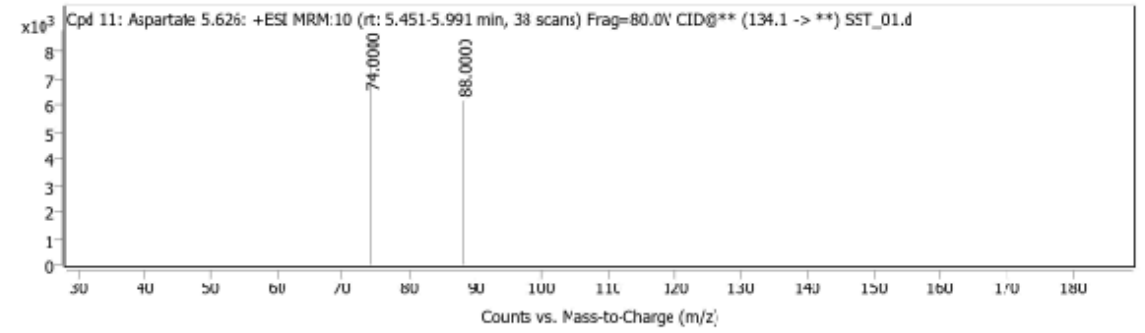
Cpd 11: Aspartate 5.626: +ESI MRM:10 (rt: 5.451-5.991 min, 38 scans) Frag=80.0V CID@** (134.1 -> **) SST_01.d
x10^3
74.0000
88.0000
Counts vs. Mass-to-Charge (m/z)

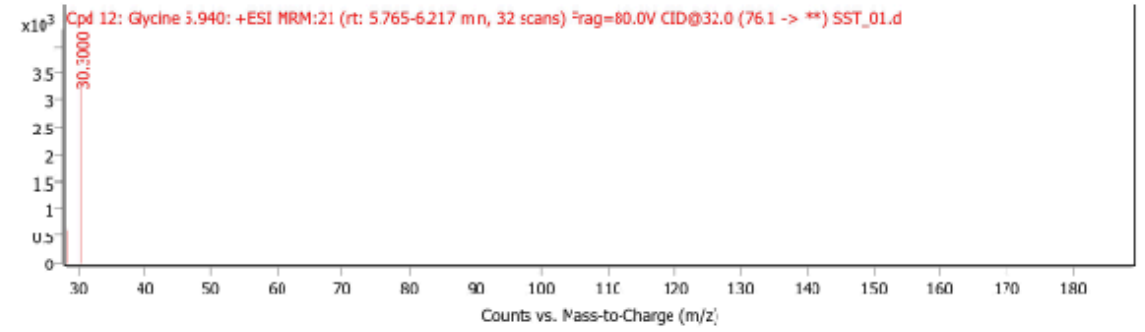
Cpd 12: Glycine 3.940: +ESI MRM:21 (rt: 3.765-4.217 min, 32 scans) Frag=80.0V CID@32.0 (76.1 -> **) SST_01.d
x10^3
30.3000
Counts vs. Mass-to-Charge (m/z)

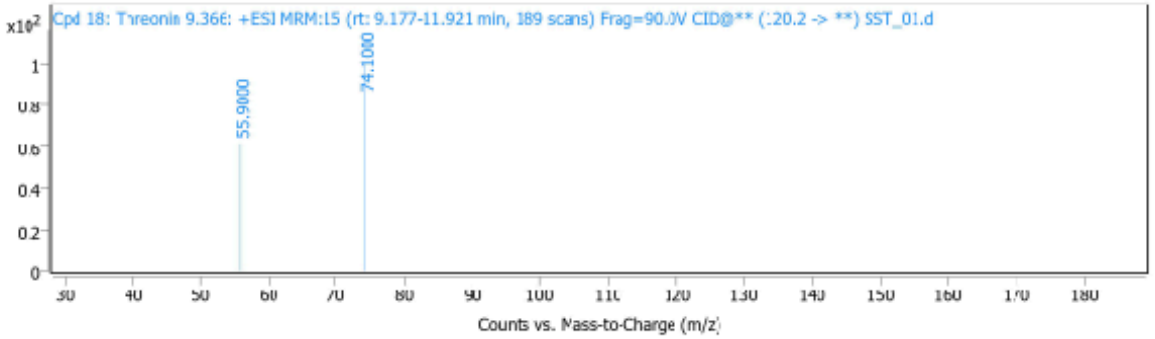
Cpd 18: Threonin 9.366: +ESI MRM:15 (rt: 9.177-11.921 min, 189 scans) Frag=90.0V CID@** (120.2 -> **) SST_01.d
x10^2
55.9000
74.1000
Counts vs. Mass-to-Charge (m/z)

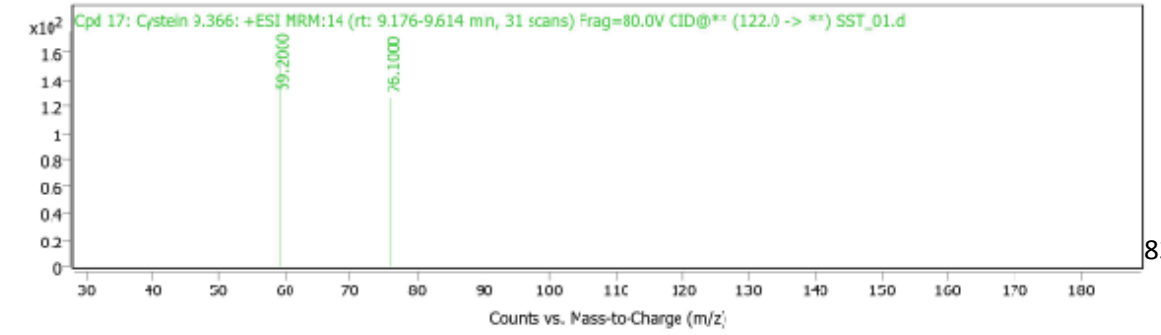
Cpd 17: Cystein 9.366: +ESI MRM:14 (rt: 9.176-9.614 min, 31 scans) Frag=80.0V CID@** (122.0 -> **) SST_01.d
x10^2
59.2000
76.1000
Counts vs. Mass-to-Charge (m/z)

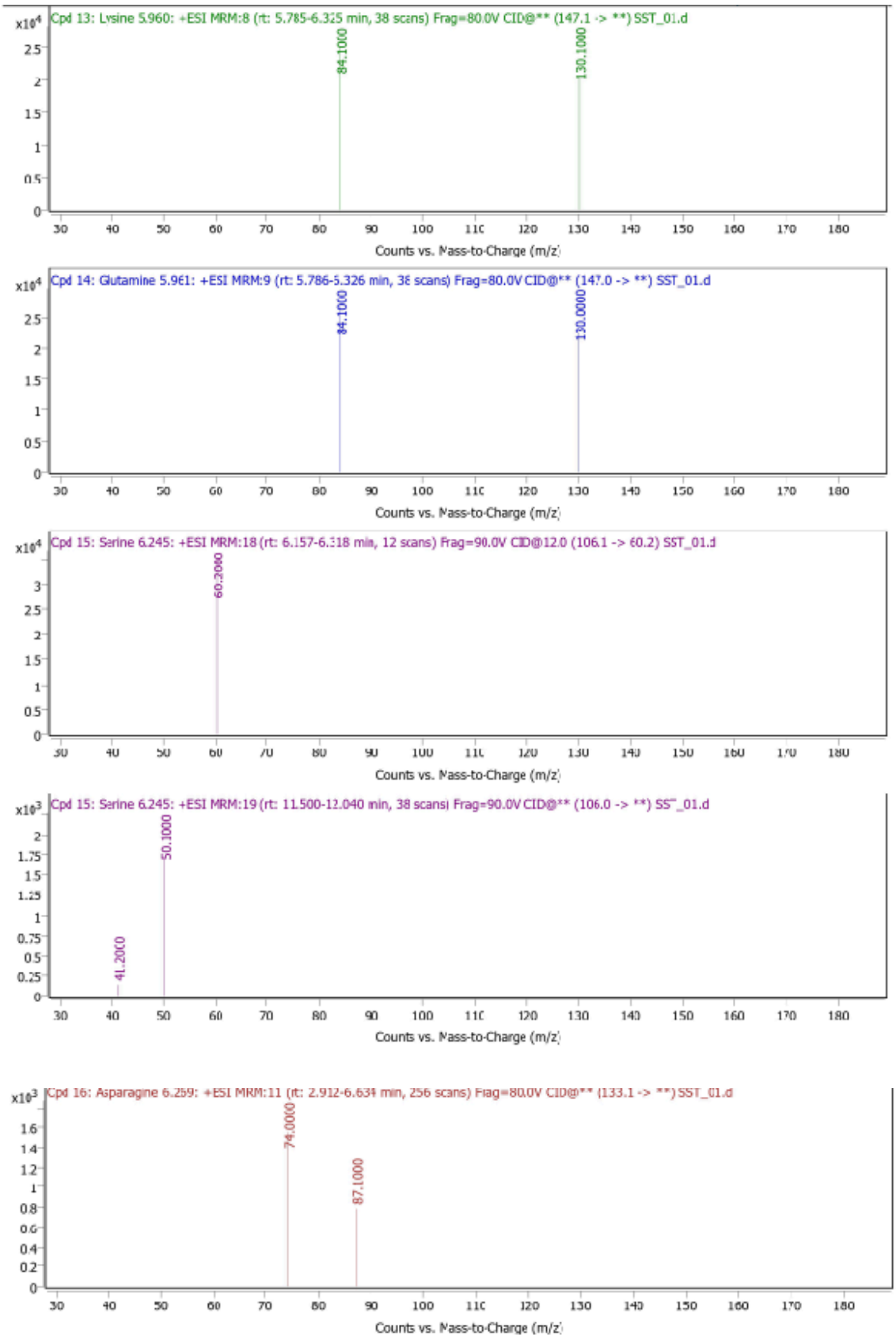

S3: m/z spectrum for all 20 amino acids- glycine, valine, leucine, isoleucine, proline, cysteine, threonine, lysine, arginine, aspargine, serine, glutamine, aspartate, glutamate, tryptophan, histidine, phenylalanine, alanine, tyrosine and methionine.

Spectrum Plot Report

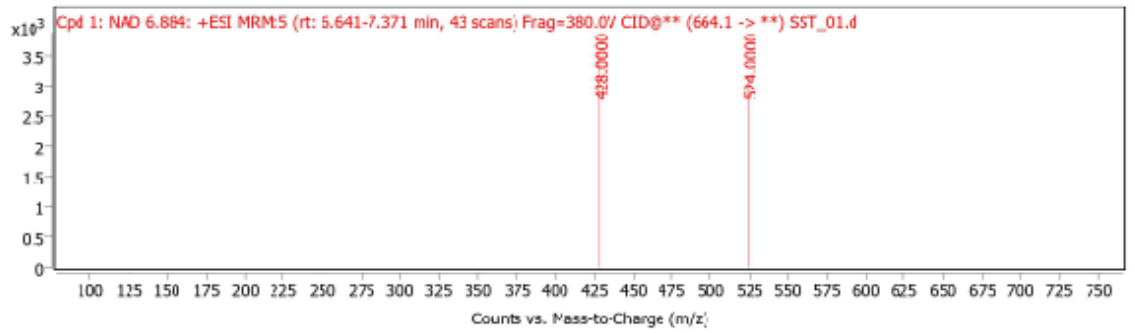

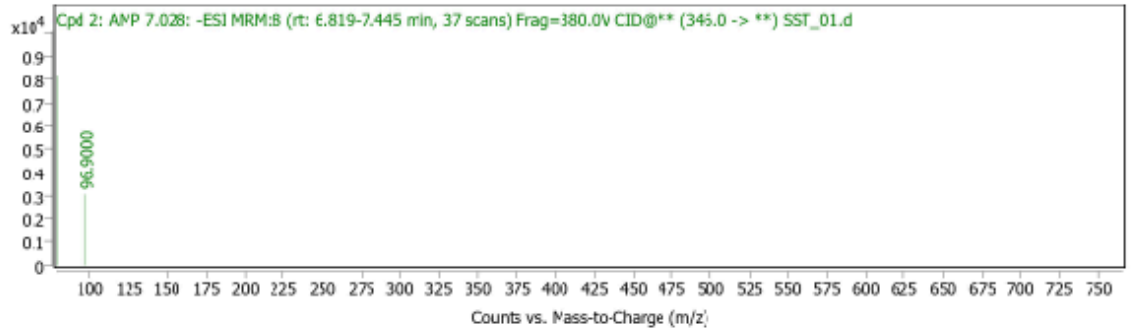

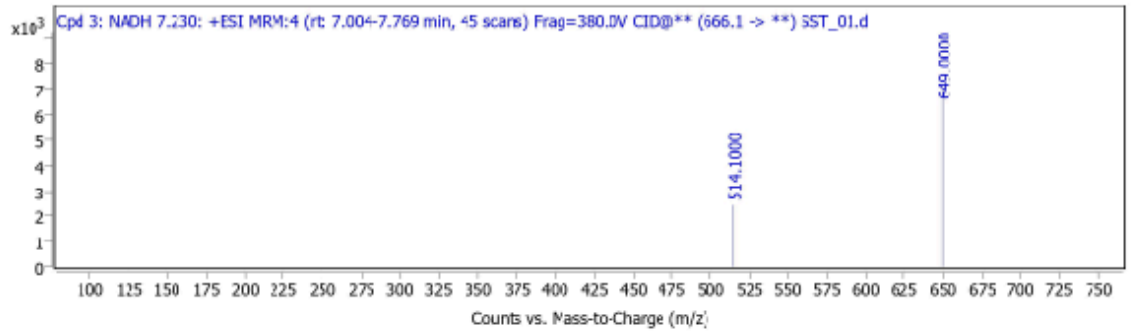

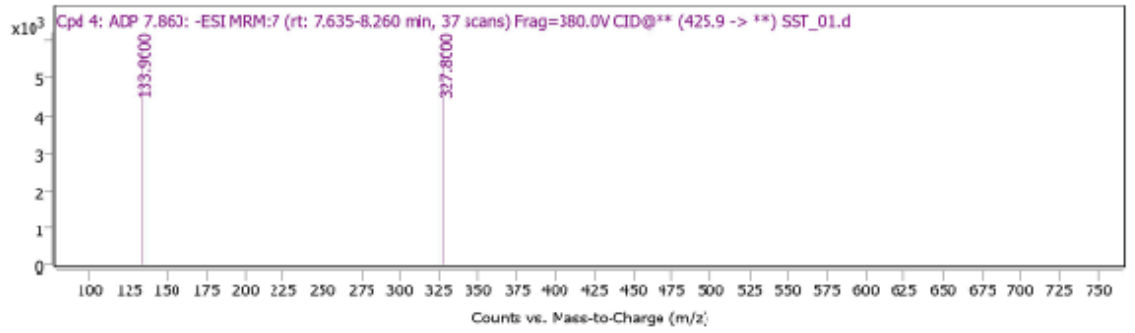

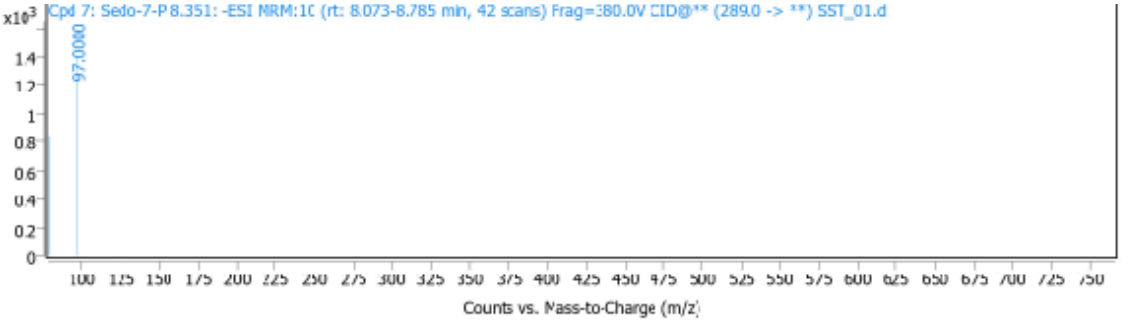

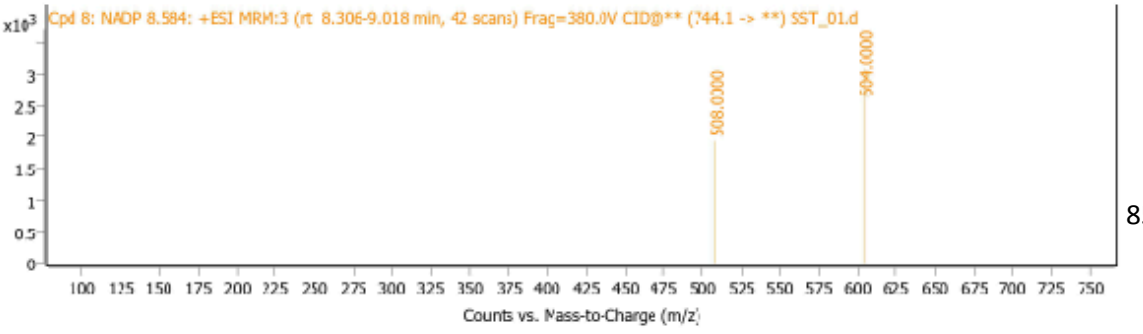

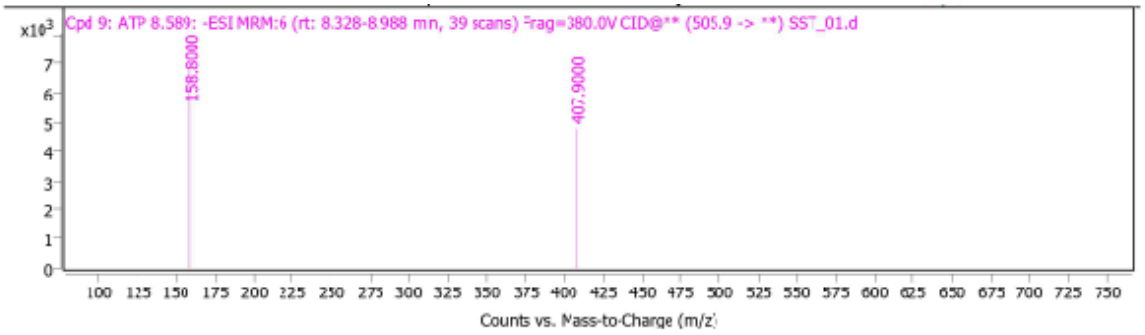
Cpd 9: ATP 8.589: -ESI MRM:6 (rt: 8.328-8.988 mn, 39 scans) Frag=380.0V CID@** (505.9 -> **) SST_01.d
158.6000
407.9000
Counts vs. Mass-to-Charge (m/z)

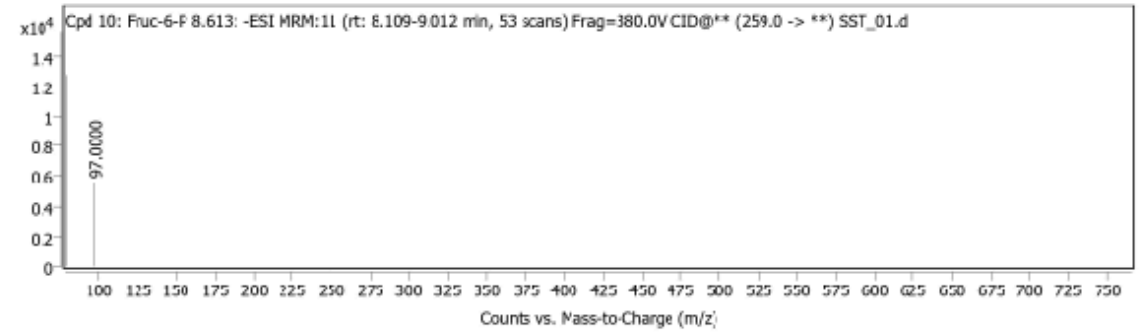
Cpd 10: Fruc-6-P 8.613: -ESI MRM:11 (rt: 8.109-9.012 min, 53 scans) Frag=380.0V CID@** (259.0 -> **) SST_01.d
97.0000
Counts vs. Mass-to-Charge (m/z)

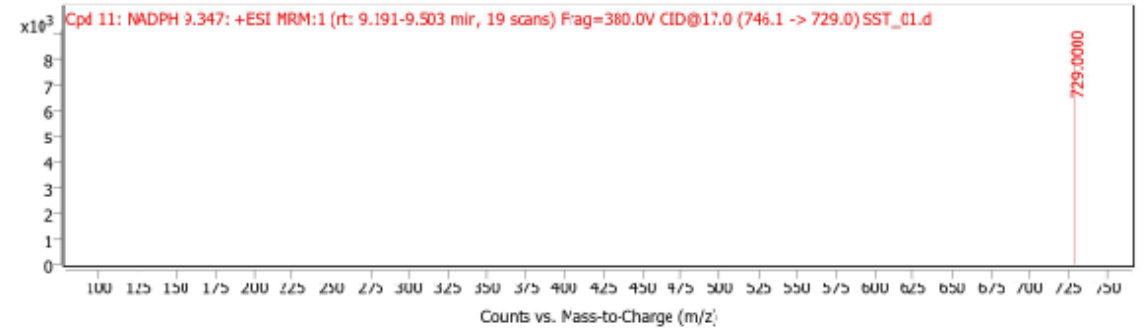
Cpd 11: NADPH 9.347: +ESI MRM:1 (rt: 9.191-9.503 min, 19 scans) Frag=380.0V CID@17.0 (746.1 -> 729.0) SST_01.d
729.0000
Counts vs. Mass-to-Charge (m/z)

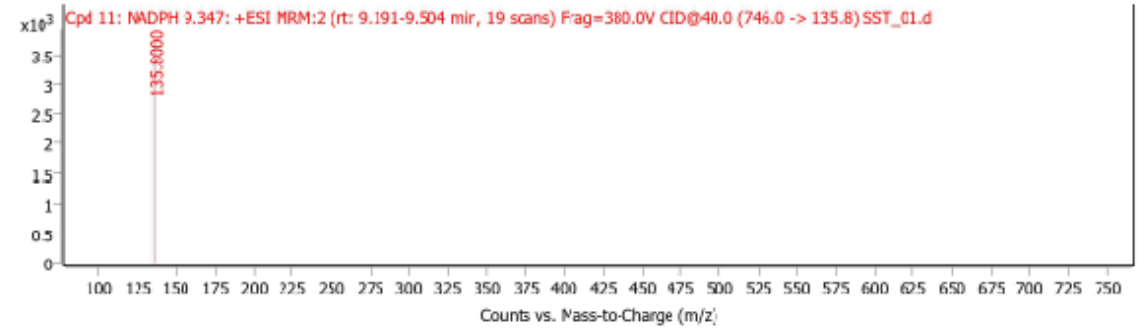
Cpd 11: NADPH 9.347: +ESI MRM:2 (rt: 9.191-9.504 min, 19 scans) Frag=380.0V CID@40.0 (746.0 -> 135.8) SST_01.d
135.6000
Counts vs. Mass-to-Charge (m/z)

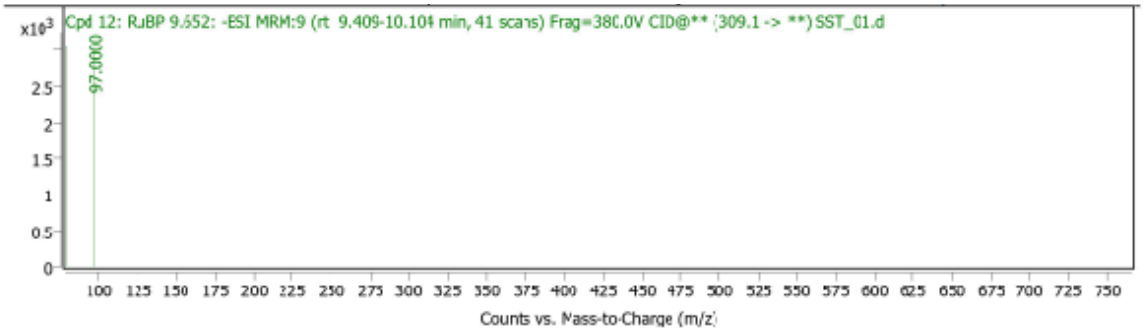
Cpd 12: RuBP 9.652: -ESI MRM:9 (rt: 9.409-10.104 min, 41 scans) Frag=380.0V CID@** (309.1 -> **) SST_01.d
97.0000
Counts vs. Mass-to-Charge (m/z)

S4: m/z spectrum for sugar phosphates- Sedoheptulose-7-phoshate, Ribose-5-phosphate, Fructose-6-phosphate, Glucose-6-phosphate, Fructose-1,5-bisphosphate and Ribulose-1,5,bisphosphate, AMP, ADP, ATP, NAD, NADH, NADP, NADPH

Spectrum Plot Report

Agilent | Trusted Answers

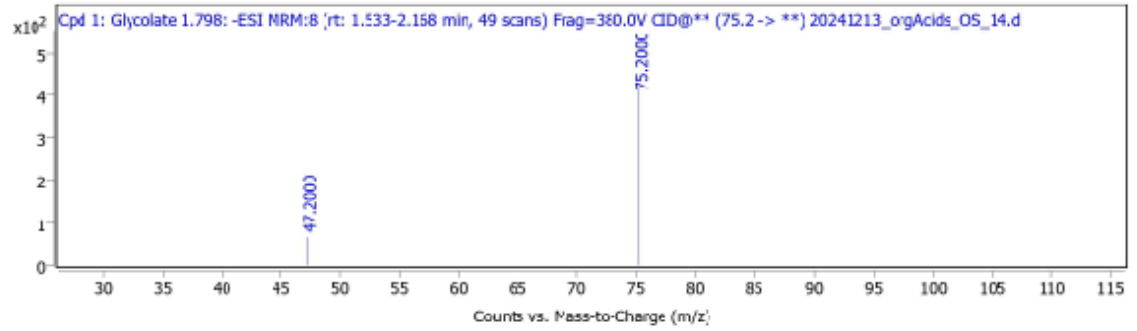

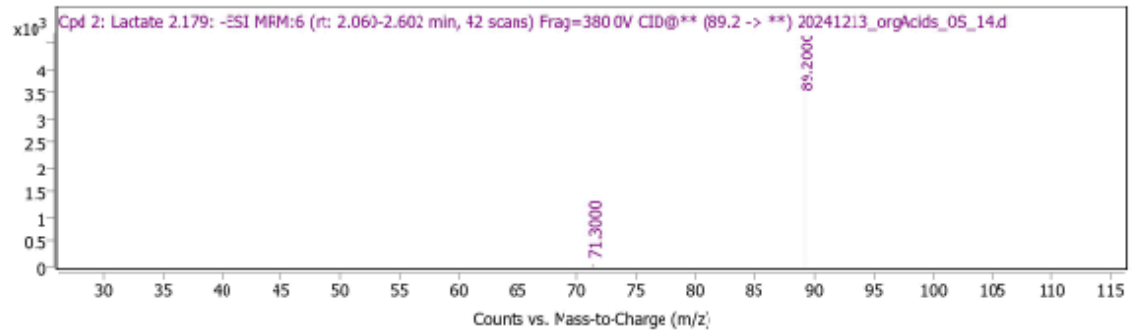

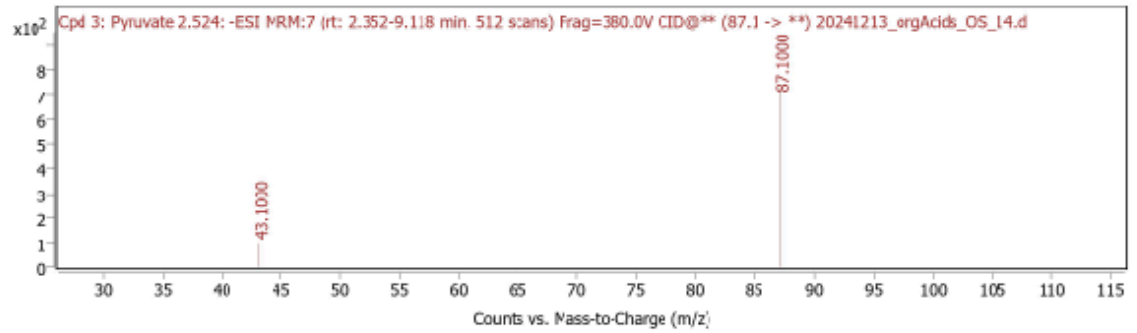

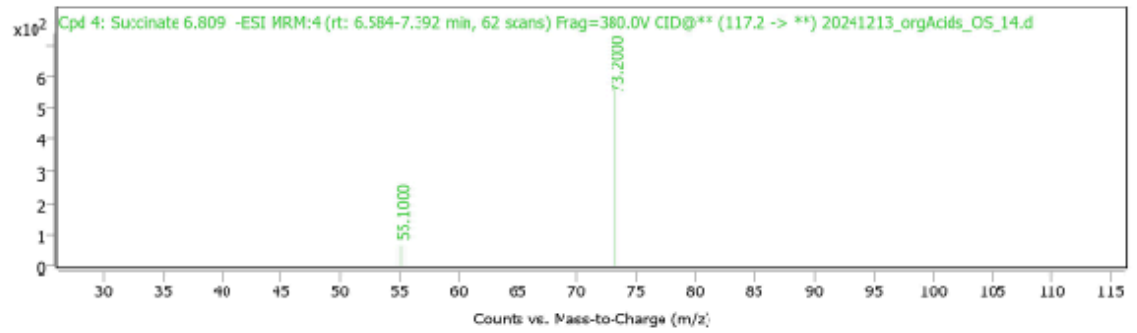

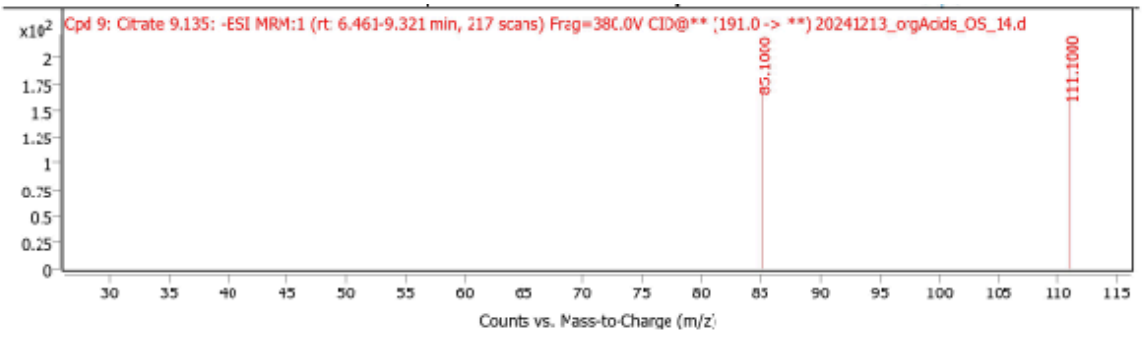

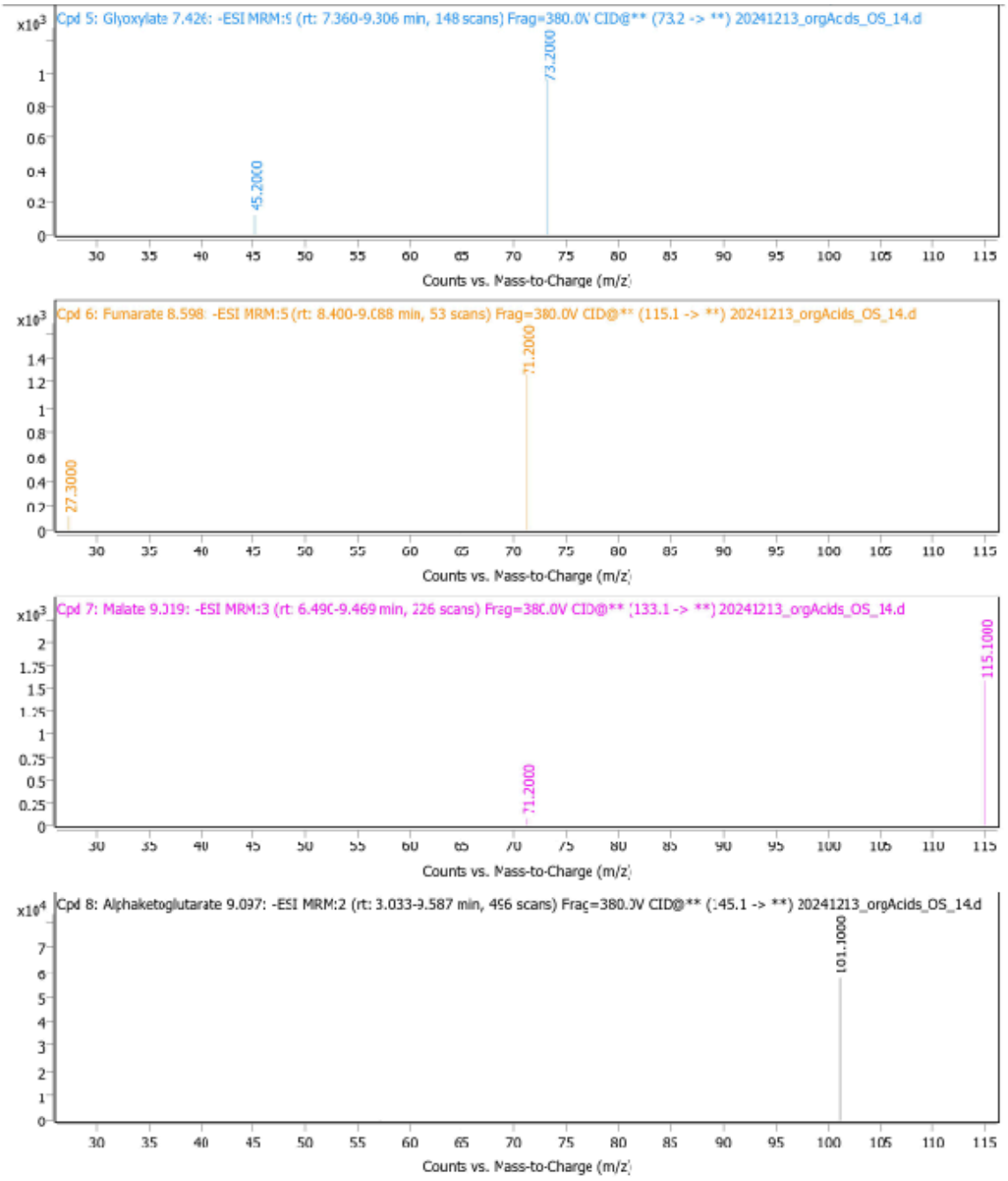

S5: m/z spectrum for organic acids namely- glycolate, lactate, succinate, pyruvate, citrate, alpha ketoglutarate, malate, fumarate and glyoxylate